Concentration Polarization and the Polarographic Current-Time Curve. I. Rate of the Consecutive Reaction Consisting of the Linear Diffusion Process and the Electrode Reaction

By Tomihito KAMBARA and Isamu TACHI

(Received October 2, 1951)

Introductory Remarks on the Consecutive Reaction

As the simplest consecutive reaction, let us suppose the reaction:

$$A \xrightarrow{k_1} B \xrightarrow{k_2} C, \qquad \text{(i)}$$

where k_1 and k_2 are the rate constants. Let C_A, C_B and C_C represent the respective concentrations, and if the initial condition is given by

$$C_A = a, \quad C_B = C_C = 0 \text{ when } t = 0, \qquad \text{(ii)}$$

it can be demonstrated that,[1],[2]

$$C_C = a\left\{1 - \frac{k_2}{k_2 - k_1}\exp(-k_1 t) + \frac{k_1}{k_2 - k_1}\exp(-k_2 t)\right\}, \qquad \text{(iii)}$$

where it is assumed that $k_1 \neq k_2$. It is clear that the condition

$$k_1 \gg k_2 \qquad \text{(a)}$$

reduces the Eq. (iii) to the form:

$$C_C = a\{1 - \exp(-k_2 t)\}. \qquad \text{(iii-a)}$$

And it is seen that this is equivalent to the supposition that the overall reaction is controlled by the process

$$A \xrightarrow{k_2} C. \qquad \text{(i-a)}$$

Similarly the condition

$$k_2 \gg k_1 \qquad \text{(b)}$$

reduces Eq. (iii) to the form:

$$C_C = a\{1 - \exp(-k_1 t)\}. \qquad \text{(iii-b)}$$

This result can be readily obtained, if we assume that the whole reaction is equivalent to the process

$$A \xrightarrow{k_1} C. \qquad \text{(i-b)}$$

From the above-stated deductions, it can be readily seen that the velocity of the overall reaction is approximately equal to the velocity of the slowest process, *i.e.* of the rate-determining step; but comparison of Eq. (iii) with Eqs. (iii-a) and (iii-b) clearly shows that this simplification is not always legitimate.

We have been hitherto accustomed to the conception that the velocity of the heterogeneous reaction in liquid phase, *e.g.* the electrode reaction, is governed by the rate of the slower one of the two processes, *i.e.* the rate of diffusion of the depolarizer transported from the bulk of the solution to the electrode surface and the rate of the electrode reaction of depolarizer at the surface. In this article, the author will discuss a rigorous mathematical treatment for the rate of heterogeneous reaction, in which neither of the rates of these two elementary processes can be neglected.

Basic Theory for the Overall Velocity of the Electrode Reaction Including the Diffusion Process

Electrolysis by means of the polarographic method gives one of the most convenient methods for the theoretical consideration; *viz.* the applied E. M. F. shows the potential of the dropping electrode relative to the constant potential of the impolarizable bottom electrode, and the depolarizer is obliged to reach to the dropping electrode surface only by diffusion. In this way the depolarizer diffuses towards the electrode surface and then the electrode reaction takes place; the reaction product thus produced also moves by thermal agitation. (When the product is soluble in the electrolytic solution, it diffuses away into the solution,

(1) S. Glasstone, "Textbook of Phys. Chemistry" (1940) p. 1055.
(2) E.A. Moelwyn-Hughes, "Phys. Chemistry" (1940) p. 526, 639.

CHEMISTRY HALL LIBRARY

and when the product forms an amalgam with the electrode mercury, it diffuses into the electrode.) In general we must consider the movements of two matters, *i. e.*, the depolarizer (denoted by the suffix 1) and the product (denoted by the suffix 2); and neglecting the curvature of the electrode surface, the following two equations hold:

$$\frac{\partial C_1}{\partial t}=D_1\frac{\partial^2 C_1}{\partial x^2} \quad \text{and} \quad \frac{\partial C_2}{\partial t}=D_2\frac{\partial^2 C_2}{\partial x^2} \ . \tag{1}$$

In these equations D_1 and D_2 are the diffusion coefficients and x_1 is the distance from the interface to the solution, and x_2 is also the distance from the interface, the sign of which depends on the nature of the reaction product. In our case we will suppose that

$$x=x_1=-x_2. \tag{2}$$

This simplification does not lose the generality of the mathematical procedure given below (This corresponds to the case that the cadmium ion in solution deposits on the mercury cathode).
The initial condition is given by

$$C_1={}^*C_1,\ C_2={}^*C_2 \text{ when } t=0,\ x>0, \tag{3}$$

where ${}^*C_1$ and ${}^*C_2$ are the concentrations in the body of solution. The boundary condition is controlled by the electrode reaction and is manifested by

$$D_1\frac{\partial C_1}{\partial x}=k_1{}^\circ C_1-k_2{}^\circ C_2=-D_2\frac{\partial C_2}{\partial x} \quad \text{when } x=0,\ t>0, \tag{4}$$

where k_1 and k_2 are the specific rates of the forward and reverse reactions, respectively, and ${}^\circ C_1$ and ${}^\circ C_2$ represent the concentrations of the depolarizer and the reaction product at the electrode surface ($x=0$), and are the functions of time t. In some cases, k_1 or k_2 includes the product of the concentrations of the chemical species which take part in the reaction. This boundary condition results from the conception that the rate of depolarization process is given by

$$v_1=k_1\cdot{}^\circ C_1$$

and that the rate of reverse process is given by

$$v_2=k_2\cdot{}^\circ C_2.$$

In general this condition depends on the mechanism of the electrode reaction and is written in the form:

$$D_1\frac{\partial C_1}{\partial x}=k_1'\cdot{}^\circ C_1^{n_1}-k_2'\cdot{}^\circ C_2^{n_2}=-D_2\frac{\partial C_2}{\partial x} \quad \text{when } x=0,\ t>0. \tag{4 a}$$

The physical meaning of Eqs. (1) and (4) can be readily seen, *i. e.*, the depolarizer and the reaction product move according to the law of diffusion, but their amount which penetrate the plane $x=0$, *i. e.* the velocity of the electrode reaction is governed by the law of chemical kinetics, and the flow of materials must be continuous even at the plane $x=0$.

In order to integrate the system of differential equations (1), we will employ the Laplace transformation[3] defined by

$$\mathfrak{L}\,C_i(x,\ t)=p\int_0^\infty e^{-pt}\cdot C_i(x,\ t)\cdot dt=u_i(x,\ p). \quad (\text{for } i=1,\ 2.)$$

Then it is found that

$$\mathfrak{L}\frac{\partial C_i}{\partial t}=\left[p\cdot C_i\cdot e^{-pt}\right]_0^\infty+p^2\int_0^\infty e^{-pt}\cdot C_i\cdot dt =-p{}^*C_i+pu_i. \quad (\text{for } i=1,\ 2.)$$

Hence we obtain the following system of ordinary differential equations

$$\left.\begin{aligned}\frac{p}{D_1}(u_1-{}^*C_1)&=\frac{\partial^2 u_1}{\partial x^2}\ ;\\ \frac{p}{D_2}(u_2-{}^*C_2)&=\frac{\partial^2 u_2}{\partial x^2}\ .\end{aligned}\right\} \tag{5}$$

The general integral of these two equations are:

$$\left.\begin{aligned}u_1&={}^*C_1+A_1\cdot\exp\left(\sqrt{\frac{p}{D_1}}x\right)\\ &\quad+B_1\cdot\exp\left(-\sqrt{\frac{p}{D_1}}x\right)\ ;\\ u_2&={}^*C_2+A_2\cdot\exp\left(\sqrt{\frac{p}{D_2}}x\right)\\ &\quad+B_2\cdot\exp\left(-\sqrt{\frac{p}{D_2}}x\right)\ .\end{aligned}\right\} \tag{6}$$

Since u_1 and u_2 must be finite even at $x\to\infty$, two constants A_1 and A_2 must be zero; *i. e.*,

$$A_1=A_2=0 \tag{7}$$

and

$$\left.\begin{aligned}u_1&={}^*C_1+B_1\cdot\exp\left(-\sqrt{\frac{p}{D_1}}x\right)\ ;\\ u_2&={}^*C_2+B_2\cdot\exp\left(-\sqrt{\frac{p}{D_2}}x\right)\end{aligned}\right\} \tag{8}$$

(3) K. W. Wagner, "Operatorenrechnung nebst Anwendungen in Physik und Technik." (1940); Japanese Translation by H. Tahara (1943) Kagaku-Shinko-Sha.

Differentiation of these equations gives

$$\left.\begin{aligned}\frac{\partial u_1}{\partial x}&=-B_1\sqrt{\frac{p}{D_1}}\exp\left(-\sqrt{\frac{p}{D_1}}x\right);\\ \frac{\partial u_2}{\partial x}&=-B_2\sqrt{\frac{p}{D_2}}\exp\left(-\sqrt{\frac{p}{D_2}}x\right).\end{aligned}\right\}\quad(9)$$

Hence from the Eqs. (4) and (9), it is found that

$$\begin{aligned}-B_1\sqrt{pD_1}&=k_1({}^*C_1+B_1)\\ -k_2({}^*C_2+B_2)&=B_2\sqrt{pD_2}.\end{aligned}\quad(10)$$

Thus the two integral constants B_1 and B_2 are found to be

$$\left.\begin{aligned}B_1&=-\frac{k_1{}^*C_1-k_2{}^*C_2}{\sqrt{pD_1}+k_1+k_2\sqrt{\frac{D_1}{D_2}}};\\ B_2&=\frac{k_1{}^*C_1-k_2{}^*C_2}{\sqrt{pD_2}+k_2+k_1\sqrt{\frac{D_2}{D_1}}}.\end{aligned}\right\}\quad(11)$$

Accordingly it is shown that

$$\left.\begin{aligned}u_1&={}^*C_1-\frac{\alpha\sqrt{D_2}}{\lambda}\cdot\frac{\lambda}{\lambda+\sqrt{lp}}\cdot\exp(-a_1\sqrt{lp});\\ u_2&={}^*C_2+\frac{\alpha\sqrt{D_1}}{\lambda}\cdot\frac{\lambda}{\lambda+\sqrt{lp}}\cdot\exp(-a_2\sqrt{lp});\end{aligned}\right\}\quad(12)$$

where

$$\left.\begin{aligned}&l=D_1D_2;\quad \alpha=k_1{}^*C_1-k_2{}^*C_2;\\ &\lambda=k_1\sqrt{D_2}+k_2\sqrt{D_1};\\ &a_1=\frac{x}{D_1\sqrt{D_2}};\quad a_2=\frac{x}{D_2\sqrt{D_1}}.\end{aligned}\right\}\quad(13)$$

Now let us perform the inverse transformation of Eq. (12) in order to evaluate the quantity C_1 and C_2; for this purpose, the following theorem is valid[3]:

If $$\mathfrak{L}^{-1}f(p)=A(t),$$

it is found that

$$\mathfrak{L}^{-1}f(lp)=A(t/l),\quad(14)$$

where l is a coefficient. Further it is known that

$$\left.\begin{aligned}&\mathfrak{L}^{-1}\frac{\lambda}{\lambda+\sqrt{p}}\cdot\exp(-a\sqrt{p})\\ &\quad=1-\operatorname{erf}\frac{a}{2\sqrt{t}}-\Psi(t);\end{aligned}\right\}\quad(15)$$

$$\Psi(t)\equiv\exp(a\lambda+\lambda_2 t)\times\left\{1-\operatorname{erf}\left(\frac{a}{2\sqrt{t}}+\lambda\sqrt{t}\right)\right\},$$

where $\operatorname{erf}\xi$ is the Gauss' error function defined by

$$\operatorname{erf}\xi\equiv\frac{2}{\sqrt{\pi}}\int_0^{\xi}\exp(-z^2)\cdot dz.$$

Accordingly it is found finally that

$$\left.\begin{aligned}\mathfrak{L}^{-1}u_1&=C_1={}^*C_1-\frac{k_1{}^*C_1-k_2{}^*C_2}{s\sqrt{D_1}}\\ &\quad\times\left[1-\operatorname{erf}\frac{x}{2\sqrt{D_1t}}-\exp\left(\frac{sx}{\sqrt{D_1}}+s^2t\right)\right.\\ &\quad\left.\times\left\{1-\operatorname{erf}\left(\frac{x}{2\sqrt{D_1t}}+s\sqrt{t}\right)\right\}\right];\\ \mathfrak{L}^{-1}u_2&=C_2={}^*C_2+\frac{k_1{}^*C_1-k_2{}^*C_2}{s\sqrt{D_2}}\\ &\quad\times\left[1-\operatorname{erf}\frac{x}{2\sqrt{D_2t}}-\exp\left(\frac{sx}{\sqrt{D_2}}+s^2t\right)\right.\\ &\quad\left.\times\left\{1-\operatorname{erf}\left(\frac{x}{2\sqrt{D_2t}}+s\sqrt{t}\right)\right\}\right];\end{aligned}\right\}\quad(16)$$

where s is given by

$$s=\frac{k_1}{\sqrt{D_1}}+\frac{k_2}{\sqrt{D_2}}.\quad(17)$$

Hence it is obvious that the concentrations at the interface ($x=0$) are shown by

$$\left.\begin{aligned}{}^\circ C_1&={}^*C_1-\frac{k_1{}^*C_1-k_2{}^*C_2}{s\sqrt{D_1}}\\ &\quad\times\{1-\exp s^2t\cdot(1-\operatorname{erf}s\sqrt{t})\};\\ {}^\circ C_2&={}^*C_2+\frac{k_1{}^*C_1-k_2{}^*C_2}{s\sqrt{D_2}}\\ &\quad\times\{1-\exp s^2t\cdot(1-\operatorname{erf}s\sqrt{t})\}.\end{aligned}\right\}\quad(18)$$

Applications of the Theory

(1) In the case that the Reverse Reaction dose not Take Place.—In this case k_2 equals zero, and from Eqs. (16) and (18) it is seen that

$$\begin{aligned}\lim_{k_2\to 0}C_1&={}^*C_1\left[\operatorname{erf}\left(\frac{x}{2\sqrt{D_1t}}\right)\right.\\ &\quad+\exp\left(\frac{k_1^2}{D_1}t+\frac{k_1}{D_1}x\right)\\ &\quad\left.\times\left\{1-\operatorname{erf}\frac{x}{2\sqrt{D_1t}}+\frac{k_1\sqrt{t}}{\sqrt{D_1}}\right)\right\}\right];\quad(19)\end{aligned}$$

$$\lim_{k_2\to 0} {}^{\circ}C_1 = {}^{*}C_1 \cdot \exp\left(\frac{k_1^2}{D_1}t\right) \times \left\{1-\mathrm{erf}\left(\frac{k_1}{\sqrt{D_1}}\sqrt{t}\right)\right\} . \quad (20)$$

This result can be obtained when we solve the equation

$$\partial C_1/\partial t = D_1 \cdot \partial^2 C_1/\partial x^2 \quad (1)$$

with the conditions

$$C_1 = {}^{*}C_1 \quad \text{when} \quad t=0, \quad x>0;$$

$$D_1 \frac{\partial C_1}{\partial x} = k_1 \cdot C_1 \quad \text{when} \quad t>0, \quad x=0.$$

I. e., it can be readily found that the solution given by Fürth[4] is quite in harmony with Eq. (19).

(2) The final Concentrations at the Electrode Surface.—For large value of ξ, it can be shown that

$$\sqrt{\pi}\,(1-\mathrm{erf}\,\xi) = 2\left(\int_0^{\infty} - \int_0^{\xi}\right) \sim \exp(-\xi^2) \times \left(\frac{1}{\xi} - \frac{1}{2\xi^3} + \frac{3}{4\xi^5} - \cdots\right), \quad (21)$$

i. e.,

$$\exp\xi^2 \cdot (1-\mathrm{erf}\,\xi) \sim \frac{1}{\sqrt{\pi}} \times \left(\frac{1}{\xi} - \frac{1}{2\xi^3} + \frac{3}{4\xi^5} - \cdots\right). \quad (22)$$

Hence it follows that

$$\lim_{t\to\infty} {}^{\circ}C_1 = \frac{k_2({}^{*}C_1\sqrt{D_1} + {}^{*}C_2\sqrt{D_2})}{k_1\sqrt{D_2} + k_2\sqrt{D_1}} = {}^{\circ}C_1(\text{fin.}), \quad (23)$$

$$\lim_{t\to\infty} {}^{\circ}C_2 = \frac{k_1({}^{*}C_1\sqrt{D_1} + {}^{*}C_2\sqrt{D_2})}{k_1\sqrt{D_2} + k_2\sqrt{D_1}} = {}^{\circ}C_2(\text{fin.}), \quad (24)$$

and accordingly it is found that

$$\lim_{t\to\infty} \frac{{}^{\circ}C_1}{{}^{\circ}C_2} = \frac{{}^{\circ}C_1(\text{fin.})}{{}^{\circ}C_2(\text{fin.})} = \frac{k_2}{k_1} = K, \quad (25)$$

where k_1, k_2, and the equilibrium constant K depend on the electrode potential. Thus it is found that the depolarizer and the reaction product finally reach to their equilibrium concentrations.

(3) Electro-deposition of Solid Metal or Alloy on a Solid Cathode.—In this case the concentration of the deposited material is considered to show a constant value ${}^{\circ}C_s$. Hence we must solve the equation

$$\partial C_1/\partial t = D_1 \cdot \partial^2 C_1/\partial x^2 \quad (1)$$

with the initial condition given by Eq. (3) and with the boundary condition given by

$$D_1 \frac{\partial C_1}{\partial x} = k_1 \cdot C_1 - k_2 \cdot {}^{\circ}C_s \quad \text{when} \quad t>0, \ x=0. \quad (4b)$$

And it is found finally that

$$C_1 = {}^{*}C_1 - \frac{k_1{}^{*}C_1 - k_2{}^{\circ}C_s}{k_1}\left[1-\mathrm{erf}\frac{x}{2\sqrt{D_1 t}} - \exp\left(\frac{k_1 x}{D_1} + \frac{k_1^2 t}{D_1}\right) \times \left\{1-\mathrm{erf}\left(\frac{x}{2\sqrt{D_1 t}} + \frac{k_1}{\sqrt{D_1}}\sqrt{t}\right)\right\}\right]. \quad (26)$$

Hence it follows that

$$\lim_{t\to\infty} {}^{\circ}C_1 = \frac{k_2}{k_1}\,{}^{\circ}C_s, \quad (27)$$

i. e., when the considerable time has elapsed after the beginning of electrolysis, the equilibrium concentration is established at the interface.

(4) Current-Time Curves.—

(a) Stationary Electrode.—Ilkovic etc.[5~11] have solved the differential equation

$$\partial C_1/\partial t = D_1 \cdot \partial^2 C_1/\partial x^2 \quad (1)$$

with the condition

$$\left.\begin{aligned} C_1 &= {}^{*}C_1 \quad \text{when} \quad t=0, \quad x>0; \\ C_1 &= {}^{\circ}C_1\ (\text{fin.}) \quad \text{when} \quad t>0, \quad x=0, \end{aligned}\right\} \quad (28)$$

and the result is

$$C_1 = {}^{\circ}C_1\,(\text{fin.}) + \{{}^{*}C_1 - {}^{\circ}C_1\,(\text{fin.})\} \cdot \mathrm{erf}\frac{x}{2\sqrt{D_1 t}}. \quad (29)$$

(4) R. Fürth, "Wärmeleitung und Diffusion" in "Die Differential und Integralgleichungen der Mechanik und Physik." Bd. II. Herausgegeben von Ph. Frank und R. v. Mises. (1927) S. 234.

(5) D. Ilkovic, *Collection Czech. Chem. Communs.*, **6**, 498 (1934).

(6) D. Ilkovic, *Jour. chim. physique*, **35**, 129 (1938).

(7) D. MacGillavry and E. K. Rideal, *Rec. trav. chim. Pays-Bas*, **56**, 1013 (1937).

(8) M. v. Stackelberg, *Z. Elektrochem.*, **45**, 466 (1939).

(9) H. Strehlow und M. v. Stackelberg, *Ibid.*, **54**, 51 (1950).

(10) T. Kambara, M. Suzuki and I. Tachi, *This Bulletin*, **23**, 219 (1950).

(11) T. Kambara and I. Tachi, *This Bulletin*, **23**, 225 (1950).

where it is supposed that the concentration of the depolarizer at the electrode surface shows a constant value ${}^{\circ}C_1$ (fin.) according to the electrode potential immediately after the commencement of the electrolysis. From Eq. (29), it follows that

$$\left(\frac{\partial C_1}{\partial x}\right)_{x=0} = \frac{{}^{*}C_1 - {}^{\circ}C_1\,(\text{fin.})}{\sqrt{\pi D_1 t}}, \qquad (30)$$

and therefore if q is the surface area of the electrode, and nF (F: Faraday) is the electricity required for the electrolysis of one mol of the depolarizer, it can be seen that the instantaneous current intensity i is given by

$$i = nFqD_1\left(\frac{\partial C_1}{\partial x}\right)_{x=0} = nFqD_1\frac{{}^{*}C_1 - {}^{\circ}C_1(\text{fin.})}{\sqrt{\pi D_1 t}}, \qquad (31)$$

i.e., it is shown that

$$i \propto t^{-1/2} \qquad (32)$$

Hence just at the beginning of the electrolysis the current intensity is given by

$$i_{t=0} = \infty, \qquad (33)$$

which is clearly an inadequate result.

According to the above-developed theory it is seen that

$$i/nFq = k_1{}^{\circ}C_1 - k_2{}^{\circ}C_2 = (k_1{}^{*}C_1 - k_2{}^{*}C_2) \times \exp s^2 t \cdot (1 - \operatorname{erf} s\sqrt{t}), \qquad (34)$$

and therefore it follows that

$$i_{t=0} \simeq nFq(k_1{}^{*}C_1 - k_2{}^{*}C_2), \qquad (35)$$

which is a quite rational conclusion. On the other hand, when the long time has elapsed after the commencement of electrolysis, it is shown from Eq. (22) that

$$i \simeq nFq\left({}^{*}C_1 - \frac{k_2}{k_1}{}^{*}C_2\right)\cdot\frac{D_1}{\sqrt{\pi D_1 t}} \times \frac{1}{1 + \dfrac{k_2}{k_1}\sqrt{\dfrac{D_1}{D_2}}}.$$

Further, it is seen from Eq. (23) that

$${}^{*}C_1 - {}^{\circ}C_1\,(\text{fin.}) = \frac{k_1{}^{*}C_1\sqrt{D_2} - k_2{}^{*}C_2\sqrt{D_2}}{k_1\sqrt{D_2} + k_2\sqrt{D_1}} = \left({}^{*}C_1 - \frac{k_2}{k_1}{}^{*}C_2\right)\Big/\left(1 + \frac{k_2}{k_1}\sqrt{\frac{D_1}{D_2}}\right),$$

and hence it can be found that

$$i \simeq nFqD_1\{{}^{*}C_1 - {}^{\circ}C_1\,(\text{fin.})\}/\sqrt{\pi D_1 t}, \qquad (36)$$

which perfectly coincides with Eq. (31). Analogously it can be readily found that

$$i \simeq nFqD_2\{{}^{\circ}C_2\,(\text{fin.}) - {}^{*}C_2\}/\sqrt{\pi D_2 t}. \qquad (36a)$$

It may be concluded that the boundary condition given by Eq. (28), and also the expessions shown by Eqs. (30) and (31) are merely approximate formulae representing the limiting case of our general theory.

On the contrary, when the electrode process is the rate-determining step, it is seen that k_1 and k_2 are much smaller than $\sqrt{D_1}$ and $\sqrt{D_2}$ and so the quantity s given by Eq. (17) is vanishingly small, *i.e.*

$$s \fallingdotseq 0. \qquad (37)$$

Then it can be seen from Eq. (34) that

$$i \simeq nFq(k_1{}^{*}C_1 - k_2{}^{*}C_2). \qquad (38)$$

This equation indicates that the overall reaction rate is nearly equal to the rate of electrode reaction.

In Fig. 1 (a) is shown the change of concentrations of the depolarizer and the product with time according to the conditions given by

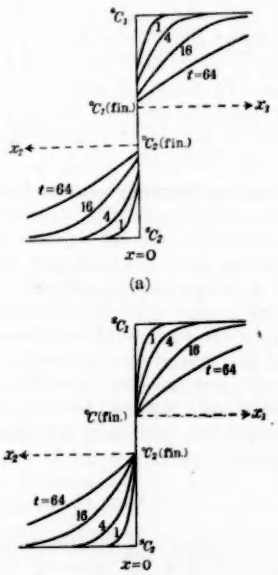

Fig. 1.—Schematic representation of the structure of diffusion layer. Variation of C–x curves with time.
Curve (a): The present theory. Curve (b): Ilkovic theory.

Eqs. (3) and (4), and in Fig. 1 (b) is illustrated the change which is controlled by the conditions given by Eq. (28). The change of the diffusion current with time is illustrated in Fig. 2; curve (a) represents the current intensity given by Eq. (34) and the curve (b) shows that given by Eq. (36). In the Table are given the numerical values employed therefor.

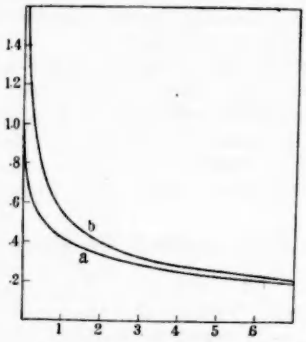

Fig. 2.—Current-time curve at the stationary electrode.

There is no doubt that the general formula for the linear diffusion current, *i.e.* Eq. (34), is reduced to the hitherto employed old formulae shown by Eq. (36) or Eq. (38) according to the simplification that the overall reaction rate is equal to either the rate of diffusion or the rate of electrode process; this is reasonably comparable to the relation between Eq. (iii) and the Eqs. (iii-a) and (iii-b).

(b) Dropping Mercury electrode.—Investigations by MacNevin with Balis[12] and by Smith[13] show that at the instant when the growth of the new drop has just begun, the new drop exposes a residual surface. Ilkovic[14] describes in his paper on the theory of polarographic maxima that at the beginning of the growth of the new drop, its radius would be equal to the internal radius of the capillary. Taking these opinions into account, it may be supposed that the volume of the mercury drop V is given by

$$V = V_0 + vt, \qquad (39)$$

where V_0 is the residual volume at $t=0$ and v is the rate of flow of mercury out of the capillary in ccm/sec. Accordingly the radius of drop at any instant t is shown by

$$r = \{3(V_0+vt)/4\pi\}^{1/3},$$

and therefore the surface area q of drop is seen to be

Table

Numerical Values of Functions Appearing in Eqs. (34), (36), (42) and (47)

s^2t	$s\sqrt{t}$	$f_1(t)$*	$f_2(t)$*	$f_3(t)$*	$f_4(t)$*
0	0	1.000,0	∞	1.000,0	0
0.000,001	0.001	0.998,9	564.19	0.999,6	5.642
0.000,004	0.002	0.997,7	282.10	1.000,4	7.106
0.000,009	0.003	0.996,6	188.06	1.002,6	8.135
0.000,016	0.004	0.995,5	141.05	1.006,1	8.955
0.000,1	0.01	0.988,8	56.419	1.053,7	12.15
0.000,4	0.02	0.977,8	28.210	1.223,7	15.31
0.000,9	0.03	0.967,0	18.806	1.483,4	17.53
0.001,6	0.04	0.956,4	14.105	1.808,4	19.30
0.002,5	0.05	0.946,0	11.284	2.180,5	20.79
0.003,6	0.06	0.935,8	9.403	2.588,3	22.11
0.004,9	0.07	0.925,7	8.060	3.022,3	23.25
0.006,4	0.08	0.915,8	7.052	3.477,1	24.32
0.008,1	0.09	0.906,0	6.268	3.950,3	25.28
0.01	0.1	0.896,5	5.641,9	4.434	26.18
0.04	0.2	0.809,0	2.821,0	9.617	32.99
0.09	0.3	0.734,6	1.880,6	14.861	37.77
0.16	0.4	0.670,8	1.410,5	19.846	41.57
0.25	0.5	0.615,7	1.128,4	24.499	44.78
0.36	0.6	0.567,8	0.940,3	28.763	47.63
0.49	0.7	0.525,9	0.806,0	32.729	50.09
0.64	0.8	0.489,1	0.705,2	36.365	52.39
0.81	0.9	0.456,5	0.626,8	39.708	54.46
1.00	1.0	0.427,6	0.564,2	42.759	56.42
1.21	1.1	0.401,7	0.512,9	45.573	58.19
1.44	1.2	0.378,9	0.470,2	48.284	59.92
1.69	1.3	0.357,6	0.434,0	50.762	61.60
1.96	1.4	0.338,7	0.403,0	53.039	63.11
2.25	1.5	0.321,5	0.376,1	55.202	64.57
2.56	1.6	0.305,9	0.352,6	57.241	65.97
2.89	1.7	0.291,7	0.331,9	59.171	67.33
3.24	1.8	0.278,6	0.313,4	60.998	68.63
3.61	1.9	0.266,5	0.296,9	62.667	69.82
4.00	2.0	0.255,5	0.282,1	64.386	71.08
4.84	2.2	0.235,2	0.256,5	67.282	73.35
5.76	2.4	0.219,0	0.235,1	70.377	75.55
6.76	2.6	0.207,0	0.217,0	74.018	77.58

* $f_1(t) = \exp s^2t \cdot (1-\mathrm{erf}\, s\sqrt{t})$;
$f_2(t) = \dfrac{1}{\sqrt{\pi s^2 t}}$;
$f_3(t) = \left(1+\dfrac{v}{V_0}t\right)^{2/3} \cdot \exp s^2t \cdot (1-\mathrm{erf}\, s\sqrt{t})$;
$f_4(t) = \left(\dfrac{v}{V_0}t\right)^{2/3} \cdot \dfrac{1}{\sqrt{\pi s^2 t}}$;
$v/V_0 = 10^3$.

(12) W. M. MacNevin and E. W. Balis, *J. Am. Chem. Soc.*, **65**. 660 (1943).
(13) G. S. Smith, *Trans. Faraday Soc.*, **47**, 63 (1951).
(14) D. Ilkovic, *Collection Czech. Chem. Communs.*, **8**, 13 (1936).

$$q=4\pi\cdot(3/4\pi)^{2/3}\cdot(V_0+vt)^{2/3}, \qquad (40)$$

and the residual surface area q_0 is demonstrated by

$$q_0=4\pi(3V_0/4\pi)^{2/3}. \qquad (41)$$

Hence the instantaneous current intensity at the dropping electrode is manifested by

$$i=nF\cdot q_0\cdot\left(1+\frac{v}{V_0}t\right)^{2/3}\cdot(k_1{}^*C_1-k_2{}^*C_2)$$
$$\times\exp s^2t\cdot(1-\mathrm{erf}\, s\sqrt{t}). \qquad (42)$$

From this equation, the current which flows at the instant when the preceding drop has just fallen off is given by

$$i_{t=0}\simeq nFq_0(k_1{}^*C_1-k_2{}^*C_2). \qquad (43)$$

According to the Ilkovic theory, it is known that

$$i\propto t^{1/6},$$

and hence it follows that

$$i_{t=0}=0. \qquad (44)$$

Many oscillographic observations,[10] however, indicate that the current intensity at $t=0$ does not diminish away to zero, but shows a finite, although small, value. Differentiating Eq. (42) with respect to the time and putting $t=0$ gives

$$(\mathrm{d}i/\mathrm{d}t)_{t=0}=-\infty. \qquad (45)$$

It is required by the Ilkovic theory that

$$(\mathrm{d}i/\mathrm{d}t)_{t=0}=+\infty, \qquad (46)$$

which does not agree with the oscillogaphic findings. For the large value of t, since vt is much greater than V_0, it follows from Eqs. (22) and (42) that

$$i\simeq nF\cdot 4\pi(3/4\pi)^{2/3}\cdot(vt)^{2/3}\cdot D_1$$
$$\{{}^*C_1-{}^\circ C_1\,(\text{fin.})\}/\sqrt{\pi D_1 t}, \qquad (47)$$

which is completely in accordance with the old theory of Ilkovic,[5] neglecting the effect of compressions of the diffusion layer by the expansion of mercury drop.

It may be concluded that the instantaneous current at the dropping electrode starts from a certain small value given by Eq. (43) and at first decreases rapidly but soon it begins to increase as indicated by Eq. (42) and finally becomes asymptotically identical with that predicted by the Ilkovic theory. Such a course of current change as is reported by McKenzie[15] and by us[10] is first comprehensible from our theory which takes the diffusion process and the electrode reaction into consideration at the same time.

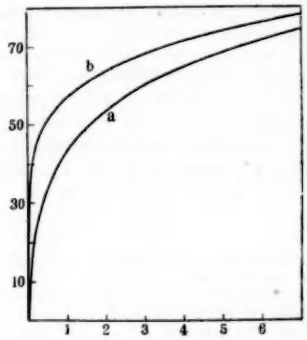

Fig. 3.—Current-time curve at the dropping electrode.

In the Table are given the numerical values of the functions appearing in Eqs. (42) and (47). For the sake of simplicity, it is assumed that $s=1$ and $v/V_0=10^5$. Randles[16] gives the value 6×10^{-3} for the electrode reaction constant of zinc ion in potassium chloride solution. The internal radius of capillary electrode is said to be about $20\sim30\ \mu$, and v under the ordinary condition is about 10^{-4} cc./sec. Curve (a) in Fig. 3 shows the theoretical current-time curve plotted according to Eq. (42) and curve (b) is drawn by Eq. (47). In the above considerations the effects produced by the convection of solution due to the expansion[5~8] of drop and by the curvature[9~11] of mercury drop are ignored; it may be said, however, that the reason why the current intensity increases very slowly in the infancy of drop-life is cleared up.

Randles[16] states that the rate constant k decreases remarkably with the addition of gelatine. On the other hand, it is well known that the mobility of an ion, and hence the diffusion coefficient, are hardly effected thereby.[17] It is noteworthy that the polarographic current-time curve is much effected by the addition of gelatine, as observed by us[10]; this will be elucidated by the above theory which regards the electrode reaction as an ensemble of the diffusion and electrode process.

(15) H. A. McKenzie, *J. Am. Chem. Soc.*, **70**, 3147 (1948).
(16) J. E. B. Randles, *Discuss. Faraday Soc.*, No. 1., 11 (1947).
(17) H. Ulich, "Elektrische Leitfähigkeit. Flüssigkeiten und Lösungen" in "Hand- und Jahrbuch der chemischen Physik" herausgegeben von A. Eucken und K. L. Wolf. Bd. 6/Abschnitt II. (1933) S. 150.

Note:—(1) The investigation by Koutecky and Brdicka[18] on the reaction current is the direct motive for the present paper. In their communication the numerical value of the integral defined by

$$f(y_1)=\int_0^{y_1} y^{2/3}\cdot\exp y\cdot(1-\mathrm{erf}\sqrt{y})\cdot dy$$

is tabulated, and this tabulation may be convenient for the study of the polarographic mean diffusion current; but it is pointed out that this table contains some miscalculations.[19]

(2) In the monograph by Frank and v. Mises,[20] the special case that is shown by

$$k_1=k_2=D^*;\ D_1=D_2=D;\ {}^*C_2=0:$$

is discussed. This condition corresponds to the problem of diffusion through a diaphragm, and its conclusion is immediately obtainable from Eq. (18).

(18) J. Koutecky and R. Brdicka, *Collection Czech. Chem. Communs.*, **12**, 337 (1947).
(19) J. Koryta, *Proceedings of the I. Intern. Polarographic Congress in Prague*, Part 1., p. 794, 798. (1951)
(20) Reference 4, p. 237.

Summary

The differential equation of linear diffusion was solved with the boundary condition controlled by the chemical kinetics. The result obtained gives the rate of the consecutive reaction consisting of the diffusion process and the electrode process. This theory can explain the course of the polarographic current-time curve very well.

Agricultural Chemical Laboratory
Faculty of Agriculture, Kyoto
University, Kyoto

Amperometric Titrations. IV. The Use of Metal Electrode of High Negative Potential and its Application to the Determination of Sulfur in Pyrite

By Masayoshi Ishibashi and Taitiro Fujinaga

(Received November 28, 1951)

In the previous paper,[1] the authors reported on the use of reference electrodes having high negative potential, *e. g.* the mercuric sulfide electrode (E = −0.8 volt *v. s.* S. C. E.) in the short-circuited amperometric titration of some organic reagents with copper sulfate.

In the present paper, some fundamental experiments on the short-circuited amperometric titration by the use of metal electrode of high negative potential, especially of metallic zinc-potassium chloride electrode, are presented and their application to the determination of sulfur in pyrite after its oxidation to sulfate is reported.

Experimental.

In amperometric titrations, different from the polarographic method where the electrolytic current is a function of the electrode potential, the current is a function of the concentration of the reducible ion in question, and the potential of the indicator electrode is invariant, so in spite of the change in the composition of the titrating solution, the potential of the opposite electrode (anode) must be kept constant while the titration is carried out. In the polarographic method, the mercury pool is generally used as anode of the constant electrode potential, and the potential of dropping electrode is proportional to the applied voltage. In amperometric method, however, if the naked mercury pool is used as the opposite electrode, a very indefinite result is apt to occur. The example is shown in the argentometric titration of cyanide (see Fig. 1). From curve 1 in Fig. 1, where the mercury pool is used as the opposite electrode, the end point is difficult to be determined. The reason is clearly shown by tracing the change of the electrode potential of mercury pool electrode, which is shown by curve 2 in the Fig. 1. As is shown in the curve, the mercury pool electrode has a highly negative potential in the original cyanide solution, but it comes to have a highly positive potential in excess of silver ion against the saturated calomel

(1) M. Ishibashi, T. Fujinaga, this bulletin, **23**, 229 (1950).

electrode and so the amperometric titration curve comes to show irregularity. These effects are thought to occur more or less in all titration reactions. In this case, however, when the separated metallic silver-potassium chloride electrode is used, the titration curve becomes a straight line as is shown in curve 3 in the Fig. 1 and the end point is clearly shown by the cross point of two straight lines (see also Fig. 2)

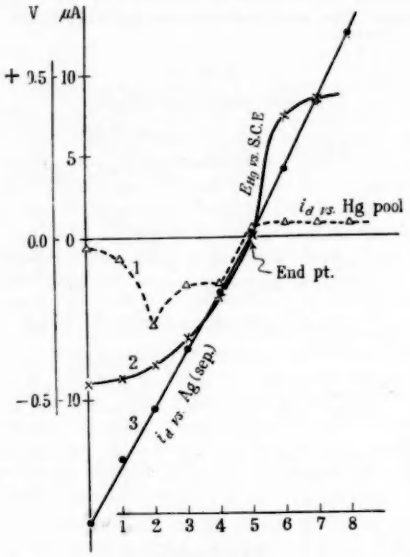

Fig. 1.—Argentometric titration curves of cyanide: curve 1, amperometry using mercury pool as opposite electrode; curve 2, potential change of mercury pool electrode; curve 3, amperometry using separated silver electrode.

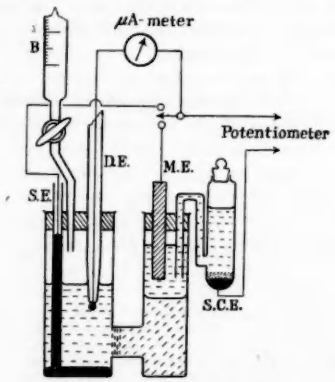

Fig. 2.—Titration cell for the measurement of diffusion current and electrode potential: B, burette; D. E., dropping electrode; M. E., separated metal electrode, S. C. E., saturated calomel electrode; S. E., stationary mercury pool electrode.

These metal electrodes are supposed to be unstable, but from the authors' experiments, an even baser metal like zinc can be used as a stable reference electrode for the amperometric purpose. Table 1 shows the change in the electrode potential of metallic zinc (surface amalgamated) inserted in the anodic solution of potassium chloride,

Table 1

Potential of Zinc Electrode

Discharge time, min.	Electrode potential, volts *vs.* S. C. E.	Discharge current, μA
0 (not connected)	−1.120	0
5	−1.122	21.1
60	−1.118	21.1
150	−1.122	20.0

while the cathodic solution containing 10^{-2} M. lead ion is discharged on the dropping mercury electrode for 2.5 hours by short-circuiting both electrodes. In these experiments, 21.1 microamperes flowed continuously, but the electrode potential was kept constant at $E_e = -1.1$ volts *v. s.* S. C. E. So it appears that such natural electrodes are stable and usable for the amperometric titration at E_e of up to −1.1 volts *v. s.* S. C. E. instead of those produced by the battery-potentiometer method. The examples of other metal electrodes and thereby reducible ions are shown in Table 2.

Table 2

Electrode Potential of Some Metal Electrodes

Electrode	Electrode potential, volts *vs.* S. C. E.	Reducible ion
Ag/sat. KCl	−0.08	Ag^+, Hg^+, Fe^{+++}, CrO_4^{--} etc.
Cu/sat. KCl	−0.325	Bi^{+++}
Sb/buffer soln.	−0.1∼−0.6	
Cd/sat. KCl	−0.820	Cu^{++}, $Cu(NH_3)_4^{++}$
Zn/sat. KCl	−1.120	Cd^{++}, Pb^{++}

Determination of Sulfur in Pyrite.

Sulfate can be determined by the amperometric titration with lead nitrate standard solution.[2] In this titration, the potential of −1.2 volts *v. s.* S. C. E. was applied to the dropping mercury electrode; therefore this outside e. m. f. can be replaced by the zinc-potassium chloride electrode. The apparatus is the same as that shown in Fig. 2 (the calomel electrode and the mercury pool electrode are unnecessary).

(2) I. M. Kolthoff, Y. D. Pan, *J. Am. Chem. Soc.*, **62**, 3332 (1940).

Reagents Used: Pure sodium sulfate was accurately weighed out and 0.1N-sodium sulfate solution was prepared as the standard of sulfate. The titre was again determined as barium sulfate by the gravimetric method. 0.1N-lead nitrate solution (1 ml. of 0.1N-nitric acid is added per litre of the solution to prevent the hydrolysis of lead nitrate) was prepared and also the concentration was determined as lead sulfate. Other reagents such as nitric acid, sodium hydroxide and alcohol were all c. p. grade.

Procedure: The fundamental experiment was carried out using the standard sodium sulfate and lead nitrate solution. To 10 ml. of 0.1N-sodium sulfate solution is added 10 ml. ethyl alcohol and 10 ml. of water and one drop of 0.1% methyl red, and titration is worked out with 0.1N-lead nitrate standard solution using the same electrode and the titration cell as mentioned above. The procedure is the same as reported in the previous paper.[1]

By the experiments, it is observed that the presence of less than 1N-sodium nitrate does not interfere in this titration. However, the acidity of the titrating solution gives much influence on the results of titration because of the amphotericity of lead ion. So in strong alkaline or acidic medium, the current increases from the beginning of the addition of lead ion, and lead sulfate does not precipitate. Near the *p*H of 9, owing to the coprecipitation of lead oxide with lead sulfate, a larger result is obtained. So, before the titration is carried out, it is preferred to regulate the *p*H of the solution to be about 3 to 5 using nitric acid or sodium hydroxide, and to titrate in 30% alcoholic medium. The recommended procedure for the determination of sulfur in pyrite is, therefore, as follows.

Sample (*ca.* 1 g.) is dissolved in 20 ml. of aqua regia and heated to boiling point and then evaporated to a syrupy state. Nitric acid is then added to the solution and is again concentrated to the same state. After the oxidation of sulfur to sulfate is completed, 20 ml. of water are added to it to dissolve the residue and 10 ml. of sodium hydroxide are added, heated to boiling point, filtered and washed with hot water. The precipitate is dissolved with hot 3N-nitric acid and reprecipitated with sodium hydroxide at boiling state and filtered and washed again. Both filtrates are transferred to a 100 ml. measuring flask and diluted with water to the mark. The aliquot portion is transferred to the cell and neutralized with 3N-nitric acid using phenolephtalein as an indicator. The same volume of alcohol is added to it and the solution is titrated with 0.1N-lead nitrate. The results are shown in Table 3.

Table 3

Determination of Sulfate

No.	0.1N-Na_2SO_4, ml.	Kind of indifferent Salt	0.1N-$PbSO_4$ used (f:1.058), ml.	Error or Result
1	10	None	9.45, 9.45, 9.45	0
2	10	*p*H=3	9.25, 9.30	−2.2%, −1.5%
3	10	1N-$NaNO_3$	9.45	0
4	10	*p*H=9	10.20	+8.0%
5	10	*p*H $\begin{matrix}>12\\<1\end{matrix}$	not found	.....
6	Pyrite (0.05 g.) (S=25.71%)		7.48 7.54 7.50	S=25.71% 25.58% 25.44%
7	Pyrite (0.10 g.) (S=3.56%)		2.14 2.14 2.16	S= 3.63% 3.63% 3.66%

Conclusion

The amperometric titration of sulfate with lead nitrate standard solution by the use of metallic zinc-potassium chloride electrode as an anode was examined and this method was applied to the determination of sulfur in pyrite. A satisfactory result was obtained. These natural electrodes are sufficiently stable and reproducible for the use in short-circuited amperometric titrations.

Laboratory of Analytical Chemistry
Faculty of Science, Kyoto University, Kyoto.

The Spatial Configurations and the Ultraviolet Absorption Spectra of the Stilbene Derivatives[1]

Hiroshi SUZUKI

(Received December 1, 1951)

The ultraviolet absorption spectrum of *trans*-stilbene has a maximum at λ 2940 A., which is shifted progressively toward shorter wave lengths as one, and then two methyl groups are introduced into the α- and α′-positions of the molecule.[2] These hypsochromic shifts have been explained as being due to the steric interferences of the substituents which prevent the molecule from assuming a planar configuration.

On the other hand, *cis*-stilbene has an absorption maximum at shorter wave lengths than the trans isomer. This has been also explained by the inference that in this compound the two phenyl groups can not be simultaneously coplanar with the central ethylenic linkage owing to the steric necessities. For the same reason, it is inferred that the resonance energy is less in the cis isomer than in the trans isomer. This provides a reasonable explanation for the fact the cis isomer is more labile and is easily converted to the trans isomer by the action of heat or of various reagents.[3]

Similar hypsochromic effects have been observed also in other cases; for examples, *ortho*-substituted biphenyls,[4] *N*, *N*-dimethylanilines,[5] and acetophenones,[4,a] and have been explained in a similar manner by the steric interferences by the substituents.

These prevailing explanations are based on the rather vague assumption that the spectrum is related to resonance and hence to the planar configuration of the molecule, and that the destruction of the planar configuration may cause a change in the spectrum. But how the spectrum changes when the planar configuration is prevented to any extent is not satisfactorily accounted for by these explanations.

Jones[6] has divided several stilbene derivatives into three groups: compounds which have spectra similar to that of styrene, compounds which have spectra similar to that of *trans*-stilbene, and compounds which have spectra intermediate between these two extremes. In triphenylethylene and tetraphenylethylene, all the phenyl groups cannot be accommodated in a strainless planar structure, so that one, or two, phenyl groups are turned out from the plane, leaving the two remaining *trans*-related phenyl groups in the plane of the central ethylenic linkage, hence these compounds have the spectra similar to that of *trans*-stilbene; that is, these compounds have the structures containing a "stilbene chromophore". Also, a close similarity of the spectra between 1,1-diphenylethylene and styrene has been explained by assuming a rotation of one of the phenyl groups of the former compound out of the plane of the ethylenic linkage, giving rise to a molecule containing a "styrene chromophore". In a similar manner, the fact that *trans*-α, α′-dimethylstilbene has a spectrum similar to that of styrene has been explained by the assumption that only one phenyl group is turned out, leaving a structure containing a "styrene chromophore".

But such considerations can not explain the "intermediate" spectra of *cis*-stilbene and α-methylstilbene. Further, the two phenyl groups in α, α′-dimethylstilbene are in equivalent positions with regard to the molecular structure, so that, even when one of these is turned out from the plane, the steric strain cannot be relieved. Rather, both should be considered as turned out to the same extent from the plane of the central ethylenic linkage. According to this assumption, the so-called "stilbene chromophore" or "styrene chromophore" must be absent in α, α′-dimethylstilbene. But it may be rather reasonable to think that the deviation of both phenyl groups to some extent from the plane of the ethylenic linkage does result not in the notable deformation or the simple destruction of the

(1) Presented at the Symposium on the π-electron held under the auspices of the Chemical Society of Japan in Tokyo, June 24th, 1951.

(2) (a) H. Ley and F. Rinke, *Ber.*, **56**, 771 (1923).
(b) B. Arends, *Ber.*, **64**, 1936 (1931).

(3) G. Egloff, G. Hulla, and V. I. Komarewsky, "Isomerization of Pure Hydrocarbons" Reinhold, 1942, p. 164-167.

(4) (a) W. H. Rodebush, *et al.*, *J. Am. Chem. Soc.*, **62**, 2906 (1940); **63**, 3018 (1941); **68**, 896 (1946).
(b) D. W. Sherwood and M. Calvin, *J. Am. Chem. Soc.*, **64**, 1350 (1942).

(5) Remington, *J. Am. Chem. Soc.* **67**, 1838 (1945).

(6) R. N. Jones, *J. Am. Chem. Soc.*, **65**, 1818 (1943).

spectrum characteristic of stilbene, but only in the shift of the absorption maximum toward shorter wave lengths, with the result that the spectrum of α, α'-dimethylstilbene happens to resemble that of styrene. This assumption implies that the perfect coplanarity is not prerequisite to the appearance of a spectrum characteristic of such a conjugated system as stilbene or biphenyl but that the necessity of coplanarity is a question of degree.

From such a view point, and generally, in order to obtain a clearer understanding of the relationship between the resonance and the absorption spectrum which is frequently apt to be misunderstood, the present author has carried out new measurements of the absorption spectra of several stilbene derivatives and has performed calculations to assess the quantitative relations between the degree of the deviation from the coplanarity and the absorption spectrum as well as the resonance energy for the stilbene derivatives.

Calculations

The calculations have been performed according to the usual molecular orbital method[7] and therefore require no detailed description. Since, for this treatment, the stilbene molecule can be considered as belonging to the symmetry group D_2, the secular equation for the determination of the fourteen approximate molecular orbitals as linear combinations of $2p\pi$ atomic orbitals is factorized into the following four equations:

$$A_1,\ x^5+\gamma x^4-(5+\alpha^2)x^3-5\gamma x^2+(4+3\alpha^2)x+4\gamma=0,$$
$$B_2,\ x^5-\gamma x^4-(5+\alpha^2)x^3+5\gamma x^2+(4+3\alpha^2)x-4\gamma=0,$$
$$B_1,\ x^2-1=0,$$
$$B_3,\ x^2-1=0,$$

where $x=W/\beta=(Q-E)/\beta$, Q, E, and β having their usual meanings. By parameters α and γ allowances are made for the situation that the $1-2$, $1'-2'$ and $1-1'$ bonds have lengths different from those in the phenyl group, $\alpha\beta$ and $\gamma\beta$ denoting the exchange integral for the $1-2$ or $1'-2'$ and the $1-1'$ bond respectively. (See Fig. 1.)

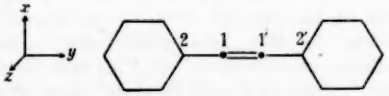

Fig. 1.—Stilbene molecule skeleton.

Now, since the exchange integral can be taken to be approximately proportional to the overlap integral S,[6] the overlap integal for some $\pi-\pi$ bond divided by that for the $\pi-\pi$ bond in benzene whose length is 1.39 A., namely S/S (1.39 A.), represents the coefficient of β in the exchange integral for this $\pi-\pi$ bond. The relation between the $\pi-\pi$ bond length and the corresponding overlap integral can be obtained from Mullikens' Tables.[9] Thus, using the value of 1.34 A. for the length of the $1-1'$ bond which is assumed to be not varied to any important extent by resonance,[10] γ is estimated to be 1.08.

According to the results of X-ray diffraction measurement reported by Robertson and Woodward,[10] stilbene has a planar configuration and the length of the bonds joining the phenyl groups to ethylenic carbon atoms, namely the $1-2$ and $1'-2'$ bonds, is 1.45 A.. With this value, α is estimated to be 0.900 for stilbene. This value of α must become smaller as the phenyl groups are turned out from the plane of the central ethylenic linkage. Thus we can see how the energy levels change as the phenyl groups are twisted gradually from the plane, by taking decreasing values such as 0.9, 0.8, 0.7,....., 0.1, 0, in turn for α in the above equations and solving them.

The results of such calculations are shown in Fig. 2, where the values of W are plotted against α. The solid lines represent the energy levels belonging to A_1 and the broken lines the energy levels belonging to B_2. In addition to these levels, there are two two-fold degenerate levels at $-\beta g$ and $+\beta$ belonging to B_1 and B_3, whose energies do not vary with the value of α. In the lower part of Fig. 2, the calculated extra-resonance energy, R. E., is plotted against α.

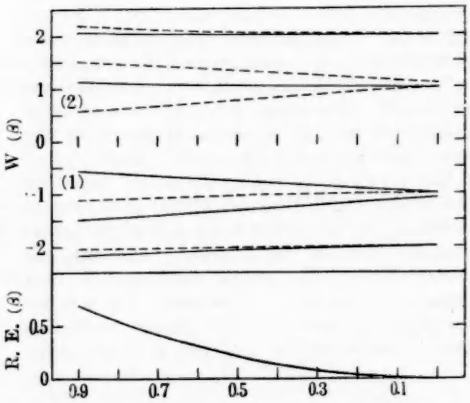

Fig. 2.—The energy levels and the resonance energy as functions of α for stilbenes.

(7) H. Eyring, J. Walter, and G. E. Kimball, "Quantum Chemistry", John Wiley & Sons, Inc., 1944, p. 255.

(8) (a) R. S. Mulliken, C. A. Rieke, and W. G. Brown, *J. Am. Chem. Soc.*, **63**, 41 (1941).
(b) J. Van Dranen and J. A. A. Ketelaar, *J. Chem. Phys.*, **17**, 1338 (1949).

(9) R. S. Mulliken, C. A. Rieke, D. Orloff, and H. Orloff, *J. Chem. Phys.*, **17**, 1248 (1949).

(10) J. M. Robertson and I. Woodward, *Proc. Roy. Soc.* (London), **A 162**, 568 (1937).

In the ground state, the levels lower than zero are all occupied by pairs of electrons, and the levels higher than zero are all vacant. According to the group theory, the transition from A_1 to B_2 is allowed by the absorption of the light polarized in the y-direction. Therefore, since the present calculations apply to vertical excitation, that is, to electron jumps without change in nuclear configuration, the absorption band characteristic of stilbene derivatives is assumed to correspond to the energy difference between the (1)- and (2)-levels in Fig. 2, which is denoted by ΔE. From Fig. 2, it can be seen that the value of ΔE, which is $1.150\,\beta$ when $\alpha=0.900$, that is, for stilbene itself, increases with the decrease of the value of α, and simultaneously, the resonance energy decreases. Thus, the present calculations indicate clearly that the absorption maximum is shifted progressively toward shorter wave lengths, and simultaneously, the resonance energy decreases, as the departure from the planar configuration becomes gradually larger. When $\alpha=0$, the energy levels reduce to those of benzene and ethylene, and the value of ΔE becomes 2β. In Table 1, the values of ΔE and R. E. for various values of α are recorded.

Table 1

α	0.9	0.8	0.7	0.6	0.5
$\Delta E(\beta)$	1.150	1.236	1.326	1.422	1.522
R. E. (β)	0.690	0.548	0.418	0.312	0.216
α	0.4	0.3	0.2	0.1	0
$\Delta E(\beta)$	1.624	1.730	1.838	1.940	2
R. E. (β)	0.134	0.076	0.032	0.009	0

According to Platt,[11] in the absorption spectrum of benzene, the "center-of-gravity of singlets", 48,000 cm.$^{-1}$ in wave number, *i.e.* the average of the energies of the three singlet levels measured in solution, corresponds to the energy difference of 2β calculated by the molecular orbital method of the same order of approximation as the present treatment. On the other hand, the wave number 34,014 cm.$^{-1}$ of the observed absorption maximum of stilbene corresponds to the calculated energy difference ΔE of $1.150\,\beta$. Therefore, in order to correlate the position of the absorption maximum with the calculated energy difference ΔE, it is assumed that the former expressed in wave number changes linearly with respect to the change in the latter from 34,014 cm.$^{-1}$ corresponding to $\Delta E=1.150\,\beta$ to 48,000 cm.$^{-1}$ corresponding to $\Delta E=2\beta$.

The next problem to be settled is in what manner the value of α varies as the phenyl groups are gradually turned out. Denoting by θ the angle through which the axis of the $2p\pi$-orbital on C atom 2 or 2′ is twisted about the 1–2 or 1′–2′ bond axis against the axis of the $2p\pi$-orbital on C atom 1 or 1′ which lies perpendicular to the plane of ethylenic linkage, it is easily verified that the overlap integral $S(\theta)$ in the case where the angle of twist is θ is equal to the overlap integral $S(0)$ when θ is zero, multiplied by $\cos\theta$. If it is assumed that the exchange integral is approximately proportional to the overlap integral in such a case also, and further that the bond length R is maintained constant even when the phenyl groups are turned out to any extent, α would be $S(R)\cos\theta/S(1.39\text{ A.})$. But any deviation from the planar configuration must inevitably inhibit the $\pi-\pi$ interaction to the corresponding extent, and consequently must be accompanied by change in the bond length. Therefore, we need to take into consideration the variation of α due to the change in the bond length resulting from the twist. This problem may be very complicated, but we can proceed approximately as follows.

The length R of the 1–2 bond was tentatively assumed to vary with θ according to the relation

$$\{S(R)-S(1.54\text{ A.})\}/\{S(1.45\text{ A.})-S(1.54\text{ A.})\} = S(\theta)/S(0)=\cos\theta,$$

since R will vary from 1.45 A. for stilbene to 1.54 A., the length of the normal $C-C$ single bond, as θ varies from 0° to 90°. When the angle of twist θ is given, the corresponding value of $S(R)$ is easily obtained, and then the value of α is given by $S(R)\cos\theta/S(1.39\text{ A.})$. Thus the position of absorption maximum for a stilbene derivative in which the phenyl groups are twisted from the coplanar position to any extent is inferred by estimating the ΔE by means of Fig. 2 for an appropriate value of α and then the corresponding wave number by means of the linear relationship assumed above between the absorption maximum and ΔE.

Conversely, when the position of the absorption maximum is known experimentally for some stilbene derivative, the values of ΔE, α, θ, R, and R. E. can be successively estimated by reversing the above procedure.

A few examples of the results of such estimations are shown in Table 2. In the calculations of the extra-resonance energies, the value of 21.74 kcal. was used for β, which was deduced from the calculated value $0.690\,\beta$ and the observed value 15 Kcal.[12] for the extra-resonance energy for stilbene itself. In α-methylstilbene, the positions of the two phenyl groups are not equivalent, and therefore, their angles of twist may not be equal. But they were assumed to be so in deducing the above values.

The difference in resonance energy between the trans and the cis isomers of stilbene as calculated above is 3.9 kcal./mol in satisfactory agreement with the experimental value of 3 kcal./mol estimated from the results of the thermal isomerization by Kistiakowsky and Smith[13] and by Taylor

(11) J. R. Platt, *J. Chem. Phys.*, **18**, 1168 (1950).

(12) L. Pauling and J. Sherman, *J. Chem. Phys.*, **1**, 606 (1933).

(13) G. B. Kistiakowsky and W. R. Smith, *J. Am. Chem. Soc.*, **56**, 638 (1934).

Table 2

	λ(A.)obs.	$\Delta E(\beta)$	α	R. E.		θ	R(A.)
cis-Stilbene	2780	1.268	0.765	0.51 β	11.1 kcal.	29°	1.462
trans-α-Methylstibene	2720	1.318	0.709	0.43	9.3	36°	1.467
trans-α, α'-Dimethylstilbene	2435	1.578	0.445	0.17	3.7	58°	1.492
trans-α, α'-Diethylstilbene	2400	1.616	0.408	0.14	3.0	60°	1.496

Table 3

The Absorption Maxima of the Stilbene Derivatives

	Trans	λ(A)	$\varepsilon\times10^{-4}$	*Cis*	λ(A.)	$\varepsilon\times10^{-4}$
Stilbene	(1) m. p. 123–4°	2940	2.76	(1') b. p. 136–7°/10 mm.	2780	0.98
α-Methylstilbene	(2) m. p. 83.0–83.5°	2720	2.10	(2') b. p. 151–5°/14 mm.	2670	0.934
α, α'-Dimethylstilbene	(3) m. p. 107°	2435	1.226	(3') m. p. 67°	2520	0.878
α-Methyl-α'-ethylstilbene	(4) m. p. 47–8°	2400	1.195			
α, α'-Diethylstilbene	(5) m. p. 77–8°	2375	1.102	(5') b. p. 177–8°/22 mm.	2440	0.774
Methyltriphenylethylene	m. p. 88–9°	2750 2260	0.986 1.372			

and Murray.[14]

Regarding the angle of twist, there is no available experimental evidence such as X-ray diffraction measurement. But these values may be guessed from purely geometrical considerations. Thus, according as we assume a twisted structure for *trans*-α, α'-dimethylstilbene in which the ortho hydrogen atom of a phenyl group just touches the methyl group attached to the same ethylenic carbon atom as the phenyl group or a structure in which that hydrogen atom just touches the other methyl group, the angle of twist is calculated to be 60° or 56°, the following values for distances and angles being used: C=C, 1.34A.; C–CH_3, 1.54 A.; C_6H_5–C, 1.49 A.; C–C in C_6H_5, 1.39 A.; C_6H_5–H, 1.08 A.; angles C=C–CH_3 and C=C–C_6H_5, 124°20'[15]; CH_3-radius, 2.0 A.; H-radius, 0.9 A. (the "Wirkungsradius" of Stuart[6]) (Fig. 3.).

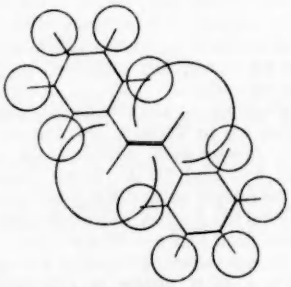

Fig. 3.—Scale drawing of *trans*-α, α'-dimethylstilbene.

For *cis*-stilbene, using the same values except for C_6H_5-C, for which the length is assumed to be 1.46 A., the angle of twist of both phenyl groups out of the plane of the ethylenic linkage is calculated to be about 25°. These values for the angles of twist are in fair agreement with the values calculated above from the absorption spectra. Although to these agreements too much significance should, perhaps, not be attached mainly because of uncertainties in the values for bond lengths, bond angles, and interference radii, it may be supposed that the quantitative relation between the angle of twist and the absorption spectrum has been satisfactorily assessed here.

Results of Measurements of Spectra

The results of the measurements of the absorption spectra are shown in Fig. 4 and in Table 3.

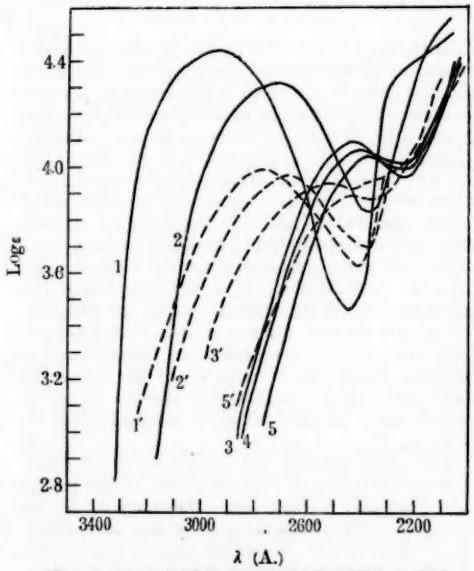

Fig. 4.—Absorption spectra of stilbene derivatives. The solid lines are those for *trans* compounds and the broken-lines those for *cis* compounds listed in Table 3.

(14) T. W. J. Taylor and A. R. Murray, *J. Chem. Soc.*, 2078 (1938).

(15) L. Zechmeister and A. L. LeRosen, *J. Am. Chem. Soc.* **64**, 2755 (1942).

It can be seen that the absorption maximum is shifted progressively toward shorter wave lengths and decreases in intensity gradually, as a larger substituent is introduced into the α- and α'-positions of *trans*- or *cis*-stilbene. In addition it may be noticed that the absorption spectra for the trans and those for the cis isomers form two groups quite distinct from each other in that the former shows a larger molecular extinction coefficient than the latter. This fact may be explained on the basis of the theory advanced by Mulliken[16] and applied to the interpretation of the spectra of carotenoids[17] that the longer the conjugated system in the direction of the electric vector of the light wave responsible for an absorption band, the greater is the intensity of the absorption maximum. On account of this fact, it is believed that the present measurements make it possible to make assignment of trans or cis configuration to these compounds, even when the difference in the position of the absorption maximum between the trans and the cis isomers is very small as compared with that between the two isomers of stilbene, or even when the maximum of a trans isomer is at shorter wave lengths than that of the corresponding cis isomer as in the case of dimethylstilbene. Thus, the geometrical configuration has now been determined as shown in Table 3 for diethylstilbene, methylstilbene and methylethylstilbene for which either only one of the possible geometrical isomers is known or, when both isomers are known, the geometrical configuration has not been unambiguously established.

The cis isomer of α,α'-dimethylstilbene has the absorption maximum at longer wave lengths than the trans isomer. Therefore, it would be anticipated from the above arguments that the former is more stable than the latter. Actually, it was reported by Lamart-Lucas and coworker[18] that the isomerization of the trans isomer to the cis isomer took place by heat whereas the reverse isomerization did not. But the results of the experiments by the present author were contrary to this theory. The isomerization by heat at 210°C. in the presence of traces of sulfuric acid gave an equilibrium mixture, in which the ratio of the amounts of the cis and the trans isomers was about 45:55, whether the starting material was the trans or the cis isomer. From this result, the difference in the stability between the two isomers of dimetylstilbene is concluded to be very small, the trans isomer to be slightly more stable. This conclusion is contrary to the anticipation from the absorption spectra alone. But a more careful examination of the stereochemistry of dimethylstilbenes shows that such may actually be the case, because, while in the trans isomer the steric repulsion between the large substituents may be almost completely relieved by the rotation of the two phenyl groups out of the plane of the molecule, in the cis isomer on the other hand, the steric repulsion between the two methyl groups can not be reduced by the rotation of the phenyl groups, the steric strain still remaining causing the cis isomer to be the less stable one.

Methyltriphenylethylene has the two absorption maxima at 2750 A. and 2260 A., and the absorption curve near the maximum at longer wave lengths coincides almost perfectly with that of *cis*-stilbene. On the other hand, the absorption spectrum of tetraphenylethylene resembles that of *trans*-stilbene. These facts may be thought to indicate that the two *trans*-related phenyl groups in tetraphenylethylene, if rotated out of the plane, permit the other *trans*-related phenyl groups to assume the configuration coplanar with the othylenic linkage, and that, if one of the rotated phenyl groups is replaced by a methyl groud, even the *trans*-related phenyl groups cannot assume the coplanar configuration.

A similar relation may be found on comparison of the spectrum of *trans*-α-methylstilbene with that of triphenylethylene.

Experimental

The measurements of the spectra.—The absorption spectra were determined with a Beckman Quartz Spectrophotometer Model DU. 95% Ethanol was used as the solvent. The concentrations of the solutions were approximately 10^{-4} mole per liter in all the cases.

Materials.—α, α'-Dimethylstilbene was prepared by dehydration of 2,2-diphenylbutanol-(3), which was obtained by the action of methylmagnesium iodide on methyldiphenylcarbinal.[19] The trans and the cis isomers were separated by fractionational crystallization from petroleum ether.

Other compounds were prepared by analogous methods.

Isomerization of α,α'-dimethylstilbene.—About 0.8 g. of *cis*-or *trans*-α,α'-dimethylstibene and pumice impregnated with concentrated sulfuric acid were placed in a sealed tube, and heated in boiling nitrobenzene for about 20 hours. The composition of the products were determined by comparing the melting-points with those of the standard mixtures prepared from known amounts of the two isomers.

Summary

(1) With certain simple assumptions, calculations based on the molecular orbital method have been performed to assess the quantitative relations between the degree of the deviation from the coplanarity of the molecular configuration and the ultraviolet absorption spectrum as well as the resonance energy for the stilbene derivatives.

(16) R. S. Mulliken, *J. Chem. Phys.*, **7**, 364 (1939).
(17) L. Zechmeister, *Chem. Rev.*, **34**, 207 (1944).
(18) Ramart-Lucas and M. E. Salmon-Legagneur, *Bull. soc. chim. France*, [4] **45**, 718 (1929).
(19) E. Ott, *Ber.*, **61**, 2135 (1928).

(2) New measurements of the spectra of the several stilbene derivatives have been carried out.

(3) By these calculations and the measurements of the spectra, it has been clarified that the absorption maximum is shifted progressively toward shorter wave lengths with the increasing angle of twist of the phenyl groups out of the plane of the ethylenic linkage.

(4) Further, from the results of these calculations and the observed position of the absorption maximum, it is possible to deduce the adequate values of the angle of twist and the resonance energy for any stilbene derivative.

(5) It has been shown that the absorption spectra for the trans isomers and those for the cis isomers of the stilbene derivatives form two groups quite distinct from each other in hat the former shows a larger molecular t extinction coefficient than the latter. On the basis of this fact, the assignments of the geometrical configurations have been determined for some stilbene derivatives.

(6) The experiments on the geometrical isomerization of α, α'-dimethylstilbene by heat have been carried out and the results have been interpreted, based on a consideration of the spatial configurations of the two isomers.

The author expresses his sincere thanks to Prof. Osamu Simamura, Drs. Saburo Nagakura and Makoto Takahashi for their kind guidance and encouragement throughout this study. Thanks are also due to the Ministry of Education for a Grant-in-Aid for Scientific Research.

The College of General Education (Kyoyo-Gakubu), Tokyo, University Tokyo

---

The Near Ultraviolet Absorption Spectra of Acetophenone and Benzophenone Vapors and the Long Wave-lengths Absorption System of Benzaldehyde Vapor

By Sunao IMANISHI, Kimio SEMBA, Mitsuo ITO and Toshinobu ANNO

(Received January 9, 1952)

Introduction

Recently, one of the authors[1] analyzed the near ultraviolet absorption band system lying in the 2480-2970 A. region and arising from the electronic transition of the type $^1A_1 - {}^1B_1$, which is allowed in C_{2v} symmetry, of the benzaldehyde molecule. The present paper is concerned with similar attempts for the acetophenone and benzophenone spectra, together with some accounts on another, wave absorption region in the benzaldehyde spectrum which has longer wave-lengths than that mentioned above.

Absorption measurements for acetophenone and benzophenone in alcohol or hexane solutions have been reported, but their vapor spectra have not been studied in detail.[2] There are two absorption regions in each of these spectra, just as in the case of benzaldehyde. The long wave-lengths absorption region fo acetophenone, and both the short and long wave-lengths regions of benzophenone are continuous. Only the short wave-lengths absorption region of acetophenone has a discrete band structure, which, however, is much more diffuse than that of the benzaldehyde referred to above. The general diffuseness of these spectra are attributable to the introduction of heavier and more complicated substituents into the molecule.

Experimental

The spectra of acetophenone and benzophenone were photographed with a Hilger *E*—2 medium quartz spectrograph having a linear dispersion of about 10 A. per mm. at 2700 A. The absorption cell was a quartz tube 40 cm. in length and 3 cm. in diameter, to which a side recess was attached for placing the substance to be investigated in liquid form and sealed in a small thin-walled glass ampoule. The cell was evacuated and the liquid was vaporized by raising the temperature of the cell in an electrically heated mantle, after

(1) S. Imanishi, *J. Chem. Phys.*, **19**, 389 (1951).
(2) Y. Hukumoto, *Sci. Rep. Tohoku Univ.*, **28**, 1162(1936). S. Kato and F. Someno, *Sci. Pap. Inst. Phys. Chem. Res.*, **12**, 329 (1944)

breaking the ampoule containing the liquid. The continuous background was supplied by a water-cooled hydrogen discharge lamp consuming about 2.5 kW. at 5,000 volts terminal voltage. To cover the great change in absorbance of the vapors with wave-length it was necessary to make many exposures, each of 40 min. duration on Fuji panchromatic plates, at different temperatures of the vapor and liquid, ranging from 20 to 100°C for acetophenone, and from 70 to 170°C for benzophenone. Iron arc was used to supply the comparison spectrum for the calibration of wave-lengths. Wave-lengths were determined from dispersion curves for each set of measurements of a spectrogram negative.

Acetophenone used was supplied by Takeda-Seiyaku Co. Ltd., and was redistilled before use, and benzophenone was synthesized from benzene and benzoyl chloride which had been prepared by the chlorination of benzoic acid in the presence of phosphorus pentachloride in carbon disulfide solution. The sample thus obtained was purified and distilled several times in vacuum.

Table 1

Wave-lengths Regions of Absorption (A.)

Substance	Long wave-lengths region		Short wave-lengths region	
	Vapor	Liquid	Vapor	Liquid
Acetophenone	3060 ~3500	3204 (alc. sol.)[3]	2480 ~2610	2785 (alc. sol.)[3]
Benzophenone	3270 ~3510	3389 (hexane sol.)[4]	2500 ~2910	2550 (hexane sol.)[4]

Analysis and Interpretation of Spectra

Short Wave-lengths Absorption Regions of Acetophenone and Benzophenone

The symmetry of the carbon-oxygen skeleton of the acetophenone molecule belongs to the point group C_s, in which the electronic transition derivable from the forbidden transition ${}^1A_{1g}-{}^1B_{2u}$ of the benzene molecule (D_{6h} symmetry) is of the type $A'-A'$, and is allowed in this symmetry having the transition moment in the plane of symmetry, *i. e.* the molecular plane. The electronic terms of representations A_{1g} and B_{2u} in D_{6h} symmetry go over into the A_1 and B_1 terms in molecules of C_{2v} symmetry, and the transition between these two terms is allowed having the transition moment in the molecular plane and perpendicular to the C_2 axis. The vibrational structures in the strong absorption systems lying in the 2500~2800 A. region of mono-substituted benzenes, *e. g.* mono-chlorobenzene[5] and benzaldehyde,[1] have been analyzed from this viewpoint. In these substituted benzene spectra the "forbidden" character of the benzene 2650 A. system still remains in that non-totally symmetric vibrations of proper symmetries, excited to an odd quantum state, can interact with the electronic transition to make bands bearing their frequencies to be observed.

Now, the B_1 term in C_{2v} is symmetric with respect to the molecular plane and anti-symmetric with respect to the plane perpendicular to it, so that by dropping the latter symmetry element both A_1 and B_1 terms go over into A' type terms in C_s.[6]

Wave-numbers of the observed band heads in the acetophenone short wave absorption are given in Table 2.

The strong and sharp head at 35375 cm^{-1} is taken to be the 0,0 vibrational transition.

Table 2

The Short Wave-lengths Absorption Bands of Acetophenone Vapor

Wave-length A.	Wave-number $cm.^{-1}$	Intensity	Distance from the 0,0 band $cm.^{-1}$	Combination
2826	35375	s.	0	0,0
2797	35742	v. w.	367	0,367
2783	35922	v. w.	547	0,547
2752	36326	s.	951	0,954
2724	36700	w.	1325	0,367+954
2711	36876	w.	1501	0,547+954
2681	37288	m. w.	1913	0,2×954
2645	37796	v. w.	2421	0,547+2×954
2615	38230	v. w.	2855	0,3×954

In the intensity column: s. strong; w. weak; m. medium.

Table 3

Fundamental Vibration Frequencies of the Acetophenone Molecule found in U. V. Absorption

Raman effect (ground state)[7]			U. V. Absorption (excited state)	Symmetry	
$\Delta\nu$ $cm.^{-1}$	Intensity	Depolarization Factor ρ		C_{2v}	C_s
368	3b	p?	367	α_1	α'
406	1/2	—			
617	6s	0.78	547	β_1	α'
999	15s	0.10	954	α_1	α'

(3) J. Bielecki and V. Henri, *Ber.*, **47**, 1690 (1914).
(4) International Critical Tables, Vol. V.
(5) H. Sponer and S. H. Wollman, *J. Chem. Phys.*, **9**, 816 (1941).
(6) H. Sponer and E. Teller, *Rev. Mod. Phys.*, **13**, 75 (1941).

This band and the three bands at 36326, 37288, and 38230 cm.$^{-1}$ form the main progression, giving a frequency interval of 954 cm.$^{-1}$, which is the mean value obtained from these four bands and other bands containing multiples of this frequency in combination with other fundamentals. This 954 cm.$^{-1}$ must be the excited state value of the 999 cm.$^{-1}$ frequency found in the Raman effect for this substance. The intensity decreases regularly along this progression in accordance with the Boltzmann law. Two weak bands with wave-numbers 35742 and 35922 cm.$^{-1}$ are separated from the 0,0 band by 367 and 547 cm.$^{-1}$, respectively, on its violet side. These distances probably represent the upper state values of the 368 and 617 cm.$^{-1}$ ground state frequencies observed in Raman effect, and are analogues of the 404 and 549 cm.$^{-1}$ excited state frequencies of the benzaldehyde molecule observed in ultraviolet absorption,[1] whose ground state values are 439 and 623 cm.$^{-1}$, respectively. We may apply to these bands the same interpretation as done for benzaldehyde, and say that they arise from the splitting of the degenerate 606 cm.$^{-1}$ (ground state value) ε_g^+ vibration of the benzene molecule into one of the β_1 type non-totally symmetric vibration of a frequency nearly of the unchanged magnitude, and another of the α_1 type totally symmetric vibration of a much lower frequency in going over into mono-substituted benzenes having C_{2v} symmetry. In such cases usually the α_1 type vibration appears with a much higher intensity than the β_1 type. In acetophenone, however, these bands are observed with almost the same intensity. This may be understood if we assume that the symmetry of the molecule is still lowered to C_s, and, by the same reason as stated above for the electronic states (which applies as well to the symmetry properties of molecular vibrations), the two types of vibration have become indistinguishable. On the other hand, polarization measurements of Raman lines clearly indicate the C_{2v} characters of these vibrations as seen in Table 3, so that we may consider there still remains a pronounced two-fold axis in the acetophenone molecule.

Other bands on the shorter wave-length side are all very diffuse, but several peaks can be measured and assigned to combinations of the fundamental frequencies found above as given in Table 2.

The short wave-lengths absorption of benzophenone vapor (2910-2500 A.) is continuous as stated earlier. This is to be expected because chances of the occurrence of predissociation increase as the molecule becomes more complex, and although this absorption region arises from electronic transition of the same type as the acetophenone short wave region, it has lost the discrete vibrational structure possessed by the latter.

Long Wave-lengths Absorption Regions of Acetophenone, Benzophenone and Benzaldehyde

The absorption region between 3060 and 3500 A. of acetophenone and that between 3270 and 3510 A. of benzophenone are both very weak and continuous. In connection with these weak absorptions, we may consider the corresponding long wave absorption bands of benzaldehyde vapor previously reported by Almasy.[8] This system (Almasy's première région) extends from 3160 to 3747 A., and contains a large number (159 measured by Almasy) of narrow weak bands, showing a pronounced group appearance. We have re-examined this region using the 1st. order of a 3 meter focus concave grating spectrograph,

Table 4

Long-wave Absorption System in Benzaldehyde Vapor

Wave-number cm.$^{-1}$	Relative intensity	Wave-number distance from band 26915 cm.$^{-1}$	Vibrational assignment
26892	s.	−23	
26915 } 28	v. s.	0	0
26943 }	v. s.		
26973	s.		
27636	s.	721	721
28005	s.	1090	1090
28098	s.		
28156	s.		
28229 } 24	v. s.	1314	1310
28253 }	s.		
28280	s.		
28357	m.	1442	2×721
28386	s.		
28949	m.	2031	721+1310
29319	s.	2404	1090+1310
29340	s.		
29404	s.		
29440	s.		
29528 } 31	v. s.	2613	2×1310
29559 }	v. s.		
30259	s.	3344	721+2×1310
30627	s.	3713	1090+2×1310
30842	m.	3927	3×1310

(7) K. W. F. Kohlrausch, "Ramanspektren", Akademische Verlagsges. Leipzig, 1943.

(8) F. Almasy, *J. Chim. Phys.*, **30**, 528, 634, 713 (1933).

and an absorption path of 1 meter at saturation pressures of benzaldehyde corresponding to 180°C at the highest (over 1 atmosphere). The total absorption intensity of this system appears to be of the order of 10^{-3} or smaller compared with that of the short wave system. Stronger bands in this system, according to our measurements, are listed in Table 4, together with probable vibrational assignments.

The three excited state frequencies 721, 1090 and 1310 cm.$^{-1}$ found in the above analysis may be identified in mode with the ground state frequencies of the benzaldehyde molecule 799, 1208 and 1434 cm.$^{-1}$, respectively, found in the analysis of the short wave absorption system.[1] All of these are of the α_1 type, and the ratio of the excited state value to the ground state value is 0.90 in all cases. The completely different appearances of the vibrational structures of the short and the long wave systems are due to the fact that no common vibrational modes are excited in the respective upper electronic states. This may be understood by considering the difference in nature of the two upper electronic states as stated below, but the fact that the carrier molecule is the same for the two systems is established unambiguously by the relations found above.

McMurry[9] has discussed, using mainly liquid phase data, the elctronic transition of the long wave-lengths absorption near 3500 A. invariably appearing in spectra of aliphatic and aromatic aldehydes and ketones, and has concluded that the upper state of this transition is the one which arises from the excitation of one of the non-bonding electrons localyzed on the oxygen atom of the C=O group, while the short wave system corresponds to the excitation of the ring π electron. The weakness of the long wave absorption is attributed to the fact that its upper state is one of the ^{1}E states theoretically predicted by Mulliken, to which the electronic transition from the ground state ^{1}N is forbidden.

Assuming this interpretation to be true, and if the forbiddenness is due to the symmetries of the electronic eigenfunctions, the band 26915 cm.$^{-1}$, the strongest first member of the progression with the 1310 cm.$^{-1}$ interval which is arbitrarily chosen as the origin in the above analysis (Table 4), may not be the 0,0 band of the system, and the 0,0 frequency may lie, just as in th case of the benzene 2650 A. forbidden transition, at a still longer wave-length shifted by the frequency of a certain non-totally symmetrical vibration which makes this system to be observed on the spectrum.

The authors express their thanks to the financial aids given them by the Scientific Research Funds of the Board of Education.

Chmical Laboratory, Faculty of Science, Kyushu University, Fukuoka.

(9) H. L. McMurry, *J. Chem. Phys.*, **9**, 231, 241 (1941).

The Near Ultraviolet Absorption Spectrum of *p*-Cresol Vapor

By Sunao IMANISHI and Mitsuo ITO

(Received January 23, 1952)

Introduction

The near ultraviolet absorption by *p*-cresol in the vapor phase, extending in the spectral region between 2480 and 2950 A., and having the strongest band corresponding to the 0,0 vibrational transition at 2829 A., was studied by Purvis and McCleland,[1] and by Savard.[2] Savard's photograph of this absorption system is reproduced in Sponer and Teller's surveying article on "The Electronic Spectra of Polyatomic Molecules".[3] Robertson and his coworkers[4] utilized the spectra of *p*-, *o*-, and *m*-cresol vapors for their quantitative chemical analysis of synthetic cresol mixtures, and also reproduced their spectrograms in their paper.

As to the more modern interpretation of the origin of the *p*-cresol spectrum, Sponer,[5] and Cave and Thompson,[6] both on re-examining

(1) J. Purvis and N. McCleland, *J. Chem. Soc.*, **103**, 1088 (1913).

(2) J. Savard, *Ann. de chim.*, **11**, 287 (1929); *Compt. rend.* **188**, 762 (1929).

(3) H. Sponer and E. Teller, *Rev. Mod. Phys.*, **13**, 75 (1941), on page 120.

(4) W. W. Robertson, N. Ginsburg, and F. A. Matsen, *Ind. Eng. Chem.*, **18**, 743 (1946).

(5) H. Sponer, *J. Chem. Phys.*, **10**, 672 (1942).

(6) W. T. Cave and H. W. Thompson, Farad. Soc. Discussions, 1950, p. 35.

Savard's published data, found out several conclusive features completely in line with results obtained recently for many of closely related molecules, *i. e.* mono- and di-substituted benzenes.

Savard's work, while appearing to contain the most reliable experimental informations on this spectrum so far published, gives us only three or four fundamental vibrational frequencies of the molecule, all of them belonging to the excited electronic state involved in the absorption transition. In order to complete the observational data for this band system, and also for the corresponding systems of *o*- and *m*-cresols appearing in the same wave-lengths region, at least to the extent achieved for their parent substance toluene,[7] we have photographed them anew, varying the concentration of the absorbing molecules in much wider range than by the previous workers. In this paper results of analysis for the *p*-cresol spectrum will be reported.

Experimental

For photographing the cresol vapor spectra a laboratory-built quartz spectrograph having a 120 cm. focus (for visible light) camera lens and a mean linear dispersion of 6 A. per mm. in this region was employed. The light source, absorption cell, and procedures of photography etc. are the same as described in our previous paper published in this journal on the near ultraviolet absorption spectra of acetophenone and other vapors.[8]

Commercial *p*-cresol sample supplied by Kanto-Kagaku Chemcals Mfg. Co. was used after several careful distillations in air. Unfortunately a very small trace of *o*-cresol could not be completely removed by such ordinary distillations, and a few of the strongest bands due to the latter isomer were recorded on some of our spectrograms. These could easily be identified and eliminated by comparing with our measurements of *o*-cresol bands, except perhaps in several cases where the close superposition might have affected the measured *p*-cresol wave-lengths slightly.

Exposures were made at the following temperatures of the liquid reservoir (Table 1), but the vapor filling the absorption cell (length 40 cm.) was always kept at a temperature 5 to 10 degrees higher than that of the liquid reservoir to prevent condensation on the windows and wall of the cell.

Table 1

Temperature of liquid (°C.)	20	30	40	50	60	70	80	90	100	110	120	130	140
Saturated Vapor pressure (mm.Hg)	.08	.18	.40	.83	1.7	3.3	6.1	11	18	30	47	71	108

The finer details of the structure on the shorter wave-length side of the 0,0 band are best observed on exposures made at temperatures below 60°C. At higher temperatures the absorption in this region becomes so intense that a complete continuum results, and as we elevate the temperature and pressure, bands corresponding to excitations of higher frequency vibrations in the ground electronic state of the molecule gradually appear on the red end of the continuum. All bands of this system are degraded towards the longer wave-length side. Wave-lengths of band heads measured on different spectrograms are averaged and the correspondingv acuum wave-numbers are listed in Table 2. Head wave-lengths observed at very different vapor densities and temperatures may differ slightly from each other, depending mainly on different photographic densities, and, to some extent, on different developments of the rotational structure. But in the majority of cases they agree within 0.1 A. which is about the limit of accuracy of our measurements for sharp heads. A few bands, especially those "satellites" accompanying closely on the longer wave side of very strong bands, show no heads, and for them positions of maximum intensity are measured and given in Table 2 with the letter m affixed in the intensity column. In the notation adopted in the last column of the table, numbers standing on the left of the comma refer to excitations of ground state vibrations, and those on the right, to electronically excited state vibrations.

Interpretation of Spectrum and Discussion

The electronic transition responsible for this absorption system is an "allowed" one as in all substituted benzenes, and the 0,0 band must be the strongest, as the one at 35338 cm.$^{-1}$ actually is. Fundamental vibrational frequencies of the molecule participating in this transition are listed in Table 3 against the published Raman and infrared data observed in the liquid

The difference frequency -23 cm.$^{-1}$ used in the above analysis occurs always with satellite bands mentioned in the preceding section, for which heads could not be measured. If examined under much higher resolution, these bands would be more satisfactorily explained as arising from the 1-1 transition of a certain low frequency fundamental, or superposition of 1-1 transitions of several different fundamentals, accompanying each strong main transition.

The *p*-cresol molecule has, strictly speaking, no

(7) N. Ginsburg and W. W. Robertson, *J. Chem. Phys.*, **14**, 511 (1946).

(8) S. Imanishi, K. Semba, M. Ito and T. Anno, *This Bulletin*, **25**, 150 (1952).

Table 2

Near Ultraviolet Absorption Bands of *p*-Cresol Vapor.

m: Intensity-maxima data.

*: Measurement probably affected by superposition of a strong *o*-cresol band.

Wave-Number ($cm.^{-1}$)	Intensity, °C												Interpretation
	140	130	120	110	100	90	80	70	60	50	40	30	
(33964)	00	00											1374, 0; 3×458, 0
34004	00	00											839+499, 0
042	0	0											1296, 0; 2×648, 0
079	0	0	00										1259, 0
107	00	00											1231, 0
147	0	0											458+734, 0
186	3	2	00	00									1152, 0
226	5	4	0	00									2×230+648, 0; 648+458, 0
264	8	8	1	0	00								230+839, 0
339			8	0	00								2×499, 0
385				3	0								458+499, 0
423				10	3								2×458, 0
460				10	4								230+648, 0; 734+839.694
499				10	7	0	00	00					839, 0
562				10	2								2×734, 694
604					5								734, 0
654					10	00							230+458, 0
690						00							648, 0
718						00	00						2×310, 0; 839, 217
764						0							230+310+458, 422
804						4	0	00					310+648, 422
839						8	2	1	.				499, 0
880						10	5	2	0				458, 0; 1152, 694; 2×230, 0
940							0	00					2×230, 217
993							1	0					1152, 808
35028							5	4	00				734, 422, ; 310, 0
069								3	0				230+734, 694
108							10	7	3	1	00		230, 0; 648, 422
179									2	0	00		159, 0: 230+734, 808
229									4	2	00		1259, 1153
261								10	10	7	3	1	499, 422
283												3	230+734, 217+694
298										10	7	5	734, 694
308										7m	4m	5m	839, 808
317											5m	4m	0, −*23*
338									10	10	10	8	0, 0
397							10	7	2	1	0	00	159, 217
469							5	3	00				458, 585
515								4	0				734, 217+694
536								3	0				499, 694
555							8	5	2	0	00		0, 217
650									2	00	00		839, 1153; 499, 808
686									3	0	00		458, 808
719									*3*	1	0		734, 422+694
725									1m	00m			839, 1226; 1152, 1536; 310, 694; 1231, 2×808
738									2m	0m			0, 422-*23*
760								10	5	2	1	1	0, 422; 734, 1153
(807)								3	0				1152, 2×808
879									0				
901									0	00			

Wave-Number (cm^{-1})	Intensity, °C												Interpretation
	140	130	120	110	100	90	80	70	60	50	40	30	
35923									2	0	00		0, 585
981									1	0	00		0, 217+422
36032										2	0	00	0, 694; 458, 1153
068									10	8	3	2	499, 422+808
103											8	2	734, 694+808; 458, 1226
109											3m	2m	458, 422+808
120											3m	2m	0, 808-*33*; 839, 2×808
146									10	10	10	8	0, 808
205*									4	3	1	0	159, 217+808
294									2	2	1	0	458, 217+1196
354*										7*	5*	4*	0, 217+808
454									4	1	0		499, 2×808
491									5	3	2		0, 1153; 458, 2×808
534									8	6	4	3	0, 1196; 939, 808+1226; 1231, 3×808
564									6	4	2	1	0, 1226; 310, 1536; 0, 422+808
610									5	4	2	2	0, 1272; 1152, 3×808
730									0	00	00		0, 585+808; 0, 2×694; 230, 2×808
830*									4	3	2	0	0, 217+1272
874									5	3	1	00	0, 1536; 499, 1226+808
918									7	5	3		458, 422+2×808; 734, 694 +2×208; 839, 3×808
955*									8	7	5	3	0, 2×808
37011*									1	0	0		159, 217+2×808
176*									0	00	00		0, 217+2×808
258*									0	00	00		499, 3×808;
305*									1	0			458, 3×808; 0, 1153+808; 0, 694+1272
318									3	1			0, 1196+808-*33*
341											1		0, 1196+808; 839, 1126 +2×808; 1231, 4×808
375									2	1			0, 422+2×808; 0, 1226+808
420								10	3	2	2	0	0, 3×694; 0, 1272+808; 1152, 4×808
476								3	1	00	00		499, 217+3×808
629								5	3	2	1	0	0, 217+1272+808
679*									2	0			0, 1536+808
723									2	1			734, 694+3×808; 839, 4×808
763								10	3	3	1	0	0, 3×808; 0, 1153+1272
807									4	2	0	00	0, 1196+1272
921*								3	1	0	00	00	648, 4×808
975								0	00	00			0, 217+3×808
38072*								8	3	1	1	0	499, 4×808; 0, 1196+1536
111								4	2	0	00		458, 4×808; 0, 4×694
148								5	2	0	00		0, 1196+2×808
197								2m	0m				1152+839, 6×808
227							5	5	2	0	0	00	0, 1272+2×808; 1152, 5×808
272							6	4	0				648, 1153+3×808
350							4	0					230, 4×808
410*							6	4	00				0, 2×1536
450							3	00					
469							3						
527							5	2	00				734, 694+4×808
567							6	5	1				0, 4×808
610							3	2	00				734+458, 422+5×808
(645)								0					734, 5×808

Wave-Number (cm^{-1})	Intensity, °C												Interpretation
	140	130	120	110	100	90	80	70	60	50	40	30	
38702							2	1					159+734, 217+5×808
786							1	00					0, 217+4×808
857							3	2					458+1296, 422+6×808
891							1	1					1296, 6×808
952							2	1					1231, 6×808; 0, 1196+3×808
39004							2	1					0, 2×1196+1272
042							00	00					0, 1272+3×808; 1152, 6×808
284							00	00					
346						7	1	1					839, 6×808
380						2	0	00					0, 5×808
362						3	0	0					458+734, 422+6×808
447						1	00	00					734, 6×808
494						2	00	00					
545						1							
(583)						1							(0, 217+5×808)
(647)						1							
(699)						1							(499, 6×808)
(795)							0						(0, 422+5×808)
(829)						0							(0, 1272+4×808; 1152, 7×808)
(887)						0							(310, 6×808)
(982)						00							(230, 6×808)
(40233)						00							(0, 6×808)

Table 3

Fundamental Vibrational Frequencies of *p*-Cresol Molecule.

Raman Effect (Liquid)				Ultraviolet Absorption (Vapor)				Infra-Red Abs. (Liquid) [11]
				Ground State	Excited State			
				Present Work			ref. 5,6	
$\Delta\nu$ (Intensity) [5]		Depolarization Factor [9], ρ	Assignment [10] (C_{2v})					Ground State
				159				
				230	β_1 or α_2	217		
338	(4)	1.00	ω_{16}, β_1	310	β_1			
465	(5)	0.52	ω_{11}, α_1	458	α_1	422	419	
507	(0)			499				
649	(5)	0.92	ω_2, β_1	648	β_1	585		
703	(0)	0.87						680~690 (w)
736	(1)			734	α_1	694		720~730 (w)
822	(3)	0.15						818 (st)
842	(10)	0.07	ω_1, α_1	839	α_1	808	808	860~870 (w)
1016	(00)							910~920 (m) 1000~1010 (w) 1080 (m)
1171	(2)	0.34	δ_3, α_1	1152				1170~1180 (st)
1214	(5)	0.09	ω_4, α_1	1231		1153		
1256	(3)	0.07	ω_3, α_1	1259		1196	1187	
1297	(0)	0.55		1296		1226		
1381	(3)	0.49		1374		1272	1268	
1450	(00)	0.92						
1615	(4)	0.74				1536		
2864	(1/2)	p						
2922	(2)	p						
3015	(1/2)	p						
3046	(3)	0.47						

(9) K. W. F. Kohlrausch u. A. Pongraz, *Monatsh. f. Chem.*, **63**, 427 (1933).

(10) O. Paulsen, *Monatsh. f. Chem.*, **72**, 244 (1939).

(11) J. Lecomte, *J. Phys. radium*, **9**, 13 (1938).

symmetry element, but as far as the ultraviolet absorption is concerned, skeleton vibrations involving only heavy-atom-containing bonds chiefly come into question. In this sense the molecule has approximately the C_s or even C_{2v} symmetry if we take the oxygen atom of the OH group as lying in the ring plane. Then its mass distribution is nearly the same as in the *p*-fluorotoluene molecule, the ultraviolet absorption of which was investigated by Cave and Thompson in the vapor phase.[6] They found the following fundamental frequencies in this molecule.

p-Fluorotoluene. 0,0 band at 36876 cm.$^{-1}$

Excited State	185,	—,	—,	398,	584,	794,
Ground State	217,	311,	377,	453,	641,	825,

Excited State	843,	1014,	1194,	1229 cm^{-1}.
Ground State	844,	1156,		cm^{-1}.

From the close parallelism between these and the *p*-cresol fundamentals given in Table 3, we may identify 230 (217) cm.$^{-1}$ in *p*-cresol with 217 (185) cm.$^{-1}$ in *p*-fluorotoluene in mode of vibration, even though no corresponding Raman shifts are reported. At the same time we notice the characteristic structure-sensitiveness of this low-frequency fundamental in that its values are approximately in the inverse ratio of the masses of the OH group and the F atom in both the electronic states. There is another set of frequencies 734 (694) cm.$^{-1}$ in *p*-cresol and 825 (794) cm.$^{-1}$ in *p*-fluorotoluene, which, apparently, is also structure-sensitive, but in comparing the respective Raman values the physical correspondence of these fundamentals in the two molecules seems doubtful. Now the structure-sensitive 230(217) cm.$^{-1}$ frequency of *p*-cresol must be of the mode in which the C–OH bond chiefly changes, and we suggest that it is the bending of this bond in the ring plane (β_1 type) or perpendicular to it (α_2 type), the single quantum excitation of either of which can produce a transition moment with the elec tronic transition under consideration (A_1–B_1). This is supported by the fact that the manner in which the 217 cm.$^{-1}$ excited state frequency combines with other α_1 type fundamentals clearly indicates its non-totally symmetric nature (see Table 2).

In mono-substituted benzenes we find the analogous behavior of a low frequency fundamental around 200 cm.$^{-1}$, so far judged from vapor ultraviolet absorption data. Thus in phenol,[12] monofluorobenzene,[13] aniline,[14] benzaldehyde,[15] benzonitrile,[16] and benzotrifluoride[17] fundamental frequencies 245, 240 (assigned to α_2), 231, 223 (α_2 or β_1), 170 and 141 (assigned to β_1) cm.$^{-1}$, respectively, are reported. These are again in the inverse order of the masses of the OH, F, NH_2, CHO, CN and CF_3 groups or atom, and their corresponding Raman lines are all depolarized, suggesting their belonging to the similar bendings of the substitution bonds in these mono-substituted benzene molecules.

Returning to *p*-cresol, we have taken another low frequency fundamental 159 cm.$^{-1}$ in the ground state from the appearance and intensity of the 35179 cm.$^{-1}$ band on the longer wave-length side of the 0,0 band, although an alternative interpretation can be given to this band as shown in Table 2. The weakly excited β_1 type 310 cm.$^{-1}$ ground state frequency has its analogue 311 cm.$^{-1}$ in *p*-fluorotoluene, while their closely coinciding Raman counterparts are not found. Another β_1 type frequency 648 (585) cm.$^{-1}$, which originated from the ε_g^+ type 606 cm.$^{-1}$ degenerated vibration in benzene is also weakly excited in both states. Correspondence between other structure-insensitive fundamentals and the Raman values is generally good as we see in Table 3.

The authors express their gratitude to the financial aids from the Scientific Grant of the Ministry of Education.

Chemical Laboratory, Faculty of Science, Kyushu University, Fukuoka

(12) F. A. Matsen, N. Ginsburg, and W. W. Robertson, *J. Chem. Phys.*, **13**, 309 (1945).
(13) S. H. Wollman, *J. Chem. Phys.*, **14**, 123 (1946).
(14) N. Ginsburg and F. A. matsen, *J. Chem. Phys.*, **13**, 167 (1945).
(15) S. Imanishi, *J. Chem. Phys.*, **19**, 389, (1951)
(16) H. C Hirt and J. P. Howe, *J. Chem. Phys.*, **16**, 480 (1948).
(17) H. Sponer, *J. Opt. Soc. Am.*, **39**, 840 (1949); also reference (6).

Dipole Moments of Some Hydroxyl Compounds

By Keniti HIGASI

(Received December 12, 1951)

In this note the present author wishes to report some unpublished values of dipole moments of phenol derivatives and also discuss the influence of solvent upon the moments of hydroxyl compounds in general.

In Table 1 the electric moments of three isomers of cresol, chlorophenol and nitrophenol are recorded with those of phenol and chlorobenzene. The values of the table were obtained by the dilute solution method, toluene being chosen as solvent; and the following equation was used in the calculation of moments: $\mu=0.127\sqrt{P_{2\infty}-MR_D}$, the symbols having the usual significance.

Table 1

Dipole Moments in Debye Unit

temp. (°C.)	ortho	meta	para
Cresols			
0	1.35	1.66	1.62
25	1.35	1.61	1.58
50	1.35	1.58	1.57
75	1.38	1.58	1.54
Chlorophenols			
0	1.23	2.06	2.26
25	1.24	2.08	2.24
50	1.24	2.10	2.25
75	1.24	2.12	2.23
Nitrophenols			
0	3.06	3.66	—
25	3.12	3.76	4.72
50	3.16	3.86	4.63
75	3.16	3.86	4.60

temp. (°C.)	Phenol	Chlorobenzene
Phenol and Chlorobenzene		
0	1.52	1.54
25	1.49	1.56
50	1.44	1.57
75	1.43	1.57

As toluene is seldom used as the solvent for dipole moment work, a comparison is made with the values in benzene[1] for the substances measured (see Table 2). In spite of the difference in polarity between the two solvents, no appreciable deviation* is found between the values of the second and third columns of the table.

Table 2

Dipole Moments and Solvents

Solute	Solvent: Benzene	Solvent: Toluene
o-Cresol	1.41	1.35
m- 〃	1.54	1.61
p- 〃	1.57	1.58
o-Chlorophenol	1.33	1.24
m- 〃	2.10	2.08
p- 〃	2.22	2.24
o-Nitrophenol	3.11	3.12
m- 〃	3.90	3.76
p- 〃	5.02	4.72
Phenol	1.56	1.49
Chlorobenzene	1.57	1.56

On inspection, it is seen in Table 1 that the moments of most of the ortho and meta disubstituted compounds increase with the increase in temperature. One might interpret this increase as the change of the equilibrium-ratio of the *cis-trans* isomers with temperature, or one might instead favor the hypothesis of inner-molecular rotation. Indeed, one could succeed in calculating the moments on any of these assumptions. However, such calculations are equally unreliable, since the moment of phenol itself is not independent of temperature. It is also to be noted that para derivatives of phenol show the same decrease with temperature in moment, which is certainly either due to association or to solute-solvent interaction.

Recently Nagakura and Baba[2] pointed out that the electron migration plays an important role in moments of aromatic molecules. It is not unlikely that such an effect is also included in the moments recorded here, but admittedly the observed temperature-variation should not be regarded as arising solely from this cause.

(1) "Table of Electric Dipole Moments" Massachusetts Institute of Technology, 1949.

* Exceptions to this rule occur in the cases of *m*- and *p*-nitrophenols.

(2) Nagakura, and Baba Shortly to be printed in J. Am. Chem. Soc., **74** (1952)

It is a well-known fact that hydroxyl compounds are apt to associate together into groups by the formation of hydrogen bonds. Further, it has often been pointed out that these molecules easily interact with hydrogen bonding solvents such as dioxane and ethers.[2][3] The present author once examined the use of ethyl ether as a solvent for dipole moment studies and found that it reduces the degree of association of alcohol to a remarkable extent, that there should be no peak in P_2-x curve in ether solution[4] (Fig. 1). This remarkable phenomenon can be explained by the hypothesis that on account of the strong interaction between the solute and the solvent there are scarcely any associated solute molecules in the diluted part of the ether solution. This explanation is in good accord with the higher moment of alcohols in ether, *viz.*, 1.8-1.9D., while further support may be found in the recent work of Nagakura and Baba.[2] Moreover, the high dielectric constant of ether is certainly able to reduce the degree of association, but it cannot possibly be the dominant cause of this phenomenon.

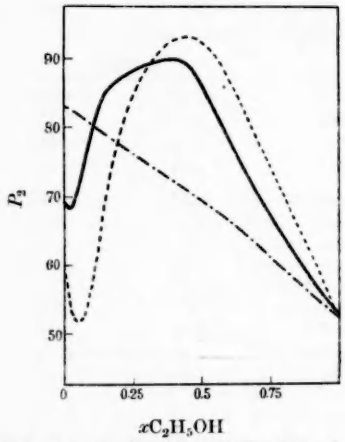

Fig. 1.—The molecular polarization of ethyl alcohol in various solvents. P_2 are plotted against the concentrations of alcohol: ——benzene; ····hexane; -·-· ethyl ether.

The formation of hydrogen bonds with benzene is not certain. But a very weak tendency to form such a solute-solvent interaction may be suspected, since benzene also gives a less pronounced maximum of polarization and a slightly higher moment for alcohols than any other normal solvents. Consequently, the result in toluene, which resembles benzene in many respects, may not be free from the possible errors arising from this sort of solute-solvent interaction.

Summary

Dipole moments of cresols, chlorophenols and nitrophenols were measured in toluene at 0°, 25°, 50° and 75°C. They are found to be in general agreement with the corresponding values measured in benzene. Further, factors which may affect the moment are considered in detail. As a connected topic it is shown that some anomalies of hydroxyl compound in ether are explainable by the hypothesis of hydrogen bond formation with the solvent.

Research Institute of Applied Electricity
Hokkaido University, Sapporo

(3) Curran and Estok, *J. Am. Chem. Soc.*, **72**, 4575(1950).
(4) Higasi, *Sc. Pap. I. P. C. R.* (Tokyo) **24**, 57 (1934).

On the Molecular State of Water Bound to the Peptide Linkage

By Masamichi TSUBOI

(Received February 8, 1952)

According to A. M. Buswell *et al*[1] and K. Kuratani[2] the water molecules bound to gelatin and other proteins cause infrared absorption bands which range from 2.85 μ to 3.03 μ. As Sponsler, Bath, and Ellis[3] have pointed out, these water molecules must be of

(1) A. M. Buswell, K. Krebs and W. H. Rodebush, *J. Am. Chem. Soc.*, **59**, 2603 (1937); *J. Phys. Chem.*, **44**, 1126 (1940).
(2) K. Kuratani, *Raports of the Radiation Chemistry Research Institute (Tokyo Univ.)*, Vol. III, 14 (1949).
(3) O. L. Sponsler, J. D. Bath and J. W. Ellis, *J. Phys. Chem.*, **44**, 996 (1940).

two kinds—(1) those bound to the peptide linkages in the backbone of protein and (2) those bound to the polar groups in the side chains. In order to obtain information about the molecular state of water bound exclusively to the peptide linkage, the present writer made 3μ region infrared absorption measurements of a film of "amilan" (Poly ε-capramide),[4]

$$\ldots\text{—}(CH_2)_5\text{—CONH—}(CH_2)_5\text{—CONH—}\ldots,$$

in dry as well as in wet state, and found that there exists a band at about $2.86\ \mu$ which is attributable to the water bound to the peptide linkage in this compound. The result obtained and its interpretation are given in this paper.

The dried specimen of amilan used here was prepared by keeping an amilan film for two weeks in a sealed tube specially made of silica glass with plane-parallel windows as shown in Fig. 1, which contained concentrated H_2SO_4

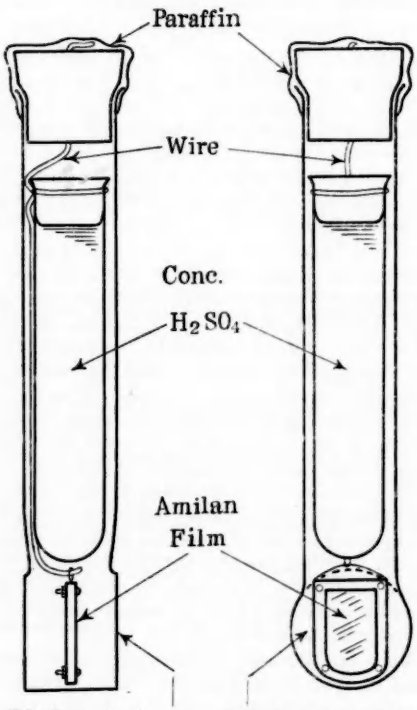

Windows of plane parallel silica glass plates
Fig. 1.

as is illustrated.[5] The dried film within the tube was subjected to the spectroscopic measurement without being taken out, by passing the infrared radiations through the film between the plane parallel windows. The result of this measurement is shown graphically by curve A in Fig. 2, where the infrared absorptions due to the silica glass plates of the windows have been eliminated. Curve B in Fig. 2 is obtained on the same amilan film, measured after it was taken out from the tube

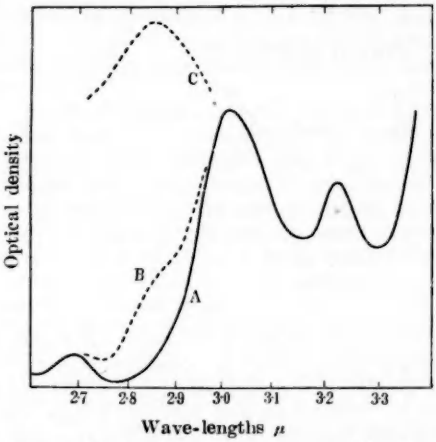

Fig. 2.—Infrared absorption curves for (A) conc. H_2SO_4-dried amilan film, (B) amilan film under water vapor of 0.01 atm., and (C) water bound to amilan.

and exposed to the air of 76% relative humidity at 11°C. (*i. e.* 0.01 atmospheric pressure of water vapor). According to the private communication of Mr. H. Yumoto, amilan contains in the air of this humidity about 0.3 mole of H_2O per $-(CH_2)_5-CONH-$ unit (=113 g.) in equilibrium. As is seen in the figure, deviation of the absorption spectrum of wet amilan from that of dry amilan is conspicuous in 2.8-2.9μ region. Curve C in Fig. 2 represents the absorption spectrum due to the water bound to amilan as obtained by subtraction of the data of curves A from B (B —A). It shows an absorption peak at about 2.86μ, which may be associated to the O—H stretching vibrations in the bound-water molecules. It is noteworthy that, while bound-water of gelatin and other proteins always shows absorptions not only in 2.85-2.90μ region but also in 2.90-3.03μ region, the amilan-bound-water shows an absorption only at 2.86μ and not in the 2.90-3.03μ region. This fact may be taken as indicating that the water molecules which cause the absorption in the 2.90-3.03μ region are those bound to side chains of the proteins, and those bound to the peptide linkages cause the absorption at about 2.86μ.

(4) Material of synthetic fibers made by the Toyo Rayon Co.

(5) The writer owes to Mr. H. Yumoto's suggestion in devising this drying apparatus.

Table 1

Molecules and their states	Number of perturbing hydrogen bonds versus maximum possible number of perturbing hydrogen bonds	Positions of O—H bands	Observers
		μ	
H_2O in CCl_4	0/4	2.70	Fox and Martin[7]
in amilan	2?/4	2.86	Tsuboi
pure water	4/4	2.95	Fox and Martin[7]
ice	4/4	3.08	Fox and Martin[7]
gelatin		2.85—3.03	Buswell, Krebs, and Rodebush[1]; Kuratani[2]
ROH in CCl_4 (dil.)	0/2	2.74	Fox and Martin[8] Smith and Creitz[9]
in 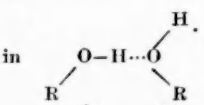 (b) (a)	1/2	(a) 2.76	Fox and Martin[8] Smith and Creitz[9]
		(b) 2.86	Smith and Creitz[9]
$ROH\cdots O(CH_3)C_6H_5$	1/2	2.80	Tsuboi[10]
$ROH\cdots O(C_2H_5)_2$	1/2	2.85	Tsuboi[10]
pure liquid	2/2	2.95	Smith and Creitz[9], and others
pyridine	1/2	3.00	Errera and Sack[11]

It is also noticed that the O—H band of amilan-bound-water or peptide-bound-water is situated at a wave-length much shorter than the O—H band of pure water (at 2.95μ). This indicates that the water molecule in peptide linkage is in a less distorted state than the water molecule in pure water.

Further details of the molecular state of the peptide-bound-water may be conjectured from the position of its O—H band in the following way.

The positions of the O—H bands of H_2O as well as of other hydroxy molecules (ROH) depend upon how far O—H vibrations in these molecules are perturbed through hydrogen bondings by other molecules. Each of these molecules has two possible types of perturbing hydrogen bonds—*i. e.* (I) hydrogen bonds through the hydrogens of the molecule under consideration and (II) hydrogen bonds through

(type I) O—H....X
X—H....O—H (type II)

the hydrogens of molecules other than the one under consideration.[6] In Table 1 are listed the positions of some of the O—H bands known for water and alcohol molecules perturbed in various ways. As may be seen from the table, the number of the perturbing hydrogen bonds of each type is a factor determining the degree of perturbation; and the strength of the proton-accepting or proton-donating powers of molecules with which the molecule under consideration is hydrogen-bonded is another factor. Thus, an alcohol molecule perturbed through the single hydrogen bond of type II by another alcohol molecule gives an O—H band at 2.76μ, and that perturbed through the single hydrogen bond of type I by another alcohol molecule (or ether molecule) gives an O—H band at about 2.86μ. While, an alcohol molecule perturbed through hydrogen bonds of both types (I and II) by other alcohol molecules gives an O—H band at 2.95μ. The carbonyl O in the peptide linkage is considered to be a stronger proton-acceptor than the ether or hydroxy O, because there is the electron migration from NH group towards the carbonyl group in the peptide linkage. It is expected, therefore, that the hydrogen bond O—H....O between the peptide C=O and the alcohol molecule, if it exists, should give O—H band at a longer wave-length than 2.86μ (Let its position be $2.86+\alpha\mu$).

Since the perturbation through the hydrogen bond of type II is weak as shown above, it is unlikely that the N—H....O bonding between the peptide N—H group and the bound-water molecule, which is one of the possible perturbing hydrogen bonds, is responsible by

(6) P. C. Cross, J. Burnham and P. A. Leighton, *J. Am. Chem. Soc.*, **59**, 1134 (1937).
(7) J. J. Fox and A. E. Martin, *Proc. Roy. Soc.(London)*, **A 174**, 234 (1940).
(8) J. J. Fox and A. E. Martin, *Trans. Faraday Soc.*, **36**, 897 (1940).
(9) F. A. Smith and E. C. Creitz, *J. Resear. Nat. Bur. Stand.*, **46**, 145 (1950).
(10) M. Tsuboi, This Bulletin **25**, 60 (1952).
(11) J. Errera and H. Sack, *Trans. Faraday Soc.*, **34**, 728 (1938).

itself for shifting the water band from 2.70μ (due to free H_2O) to 2.86μ. On the other hand, simultaneous perturbations of two types (I and II) as those in pure water may be ruled out for the bound-water molecule, because the O—H band under consideration is situated at a much shorter wave-length than that of pure water. The simple perturbation through hydrogen bonds of type I is the probable one for the present case. Calculations of the vibration frequencies of H_2O molecule[12] show that, if one of the two O—H's of a water molecule is perturbed through the hydrogen bond of type I by a peptide oxygen atom and the other O—H is left free, the molecule will give two O—H bands at about 2.7μ and at $2.86+\alpha\mu$, while, if both of its two O—H's are perturbed by peptide oxygen atoms, it will give two O—H bands, at a little longer wave-length than $2.86+\alpha\mu$ (corresponding to the symmetric stretching vibration) and at a little shorter wave-length than $2.86+\alpha\mu$ (corresponding to the antisymmetric stretching vibration). In the case now at issue no band attributable to the peptide-bound-water has been observed in the vicinity of 2.7μ,[13] showing that the bound-water molecule has no free O—H. Then, a view may be set forth here tentatively that the peptide-bound-water molecule has both of the two O—H's perturbed through O—H....O bondings by two peptide oxygen atoms (located near to each other),[14] and that the 2.86μ band corresponds to the antisymmetric vibration of that water molecule. The band due to the symmetric vibration, which, according to the above view, should appear at a little longer wave-length than $2.86+\alpha\mu$ has not been observed. This, however, may not necessarily be taken as vitiating the above view, for it is conceivable that this band is too weak to be observed, the dipole-moment-oscillation due to the symmetric vibration being smaller in amplitude than that due to the antisymmetric vibration.[15]

The bound-water band in the 2.90-3.03μ region observed on proteins may be attributed either to water molecules bound by much stronger proton-acceptor groups in the side chains such as ionized carbonyl groups, or to water molecules forming an aggregate around the polar groups just as those in liquid water.

A few words may be added here concerning the bound-water band at 2.86μ. In the writer's previous measurements of the 3μ region infrared absorption on egg albumin and horse serum albumin,[16] remarkable peaks at about 2.86μ were observed. This fact suggests that the water molecule bound to the carbonyl O in the backbone in the manner shown above are abundant in these proteins. On the other hand, the present writer's recent study on a film of poly-D,L-norleucine[17] (an isomer of amilan),

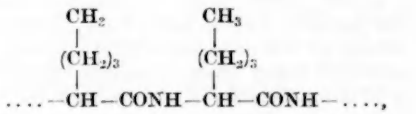

indicated that the film shows no absorption band at 2.86μ in the air of equal humidity as the air in which the measurement corresponding to the curve B for amilan (Fig. 2) was made. The crowded hydrophobic side chains ($-CH_2-CH_2-CH_2-CH_3$) seem to prevent the water molecule from reaching the backbone.

(12) In order to get knowledge about the coupling between the vibrations of two O-H's in a water molecule, the normal vibration frequencies of the water molecule were calculated, assuming the potential energy (V) of the molecule as,

$$V=\frac{1}{2}f_1(\Delta r_1)^2+\frac{1}{2}f_2(\Delta r_2)^2+\frac{1}{2}f_3(r_0\Delta\alpha)^2,$$

where r_1 and r_2 are the bond lengths of the two O-H's, r_0 the equilibrium O-H distance, α the angle HOH, and f_1 etc. the force constants. If we put $f_1=f_2=7.54655\times10^5$ dyne/cm, $f_3=0.70195\times10^5$ dyne/cm; we obtain three normal vibration frequencies: 3702, 3648, and 1600 cm^{-1}, which are close to the frequencies observed for water vapor (3750, 3650, and 1595 cm^{-1}). Fig. 3 and 4 show the two O-H stretching frequencies of H_2O molecule, as calculated by assuming that $f_1=f$(variable), $f_2=7.54655\times10^5$ dyne/cm., $f_3=0.70195\times10^5$ dyne/cm. (Fig. 3); and that $f_1-f_2=f$ (variable), $f_3=0.70195\times10^5$ dyne/cm. (Fig. 4). The dotted lines in the figures indicate the frequencies calculated for the case when the two O-H's vibrate independently of each other.

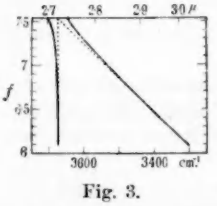

Fig. 3.

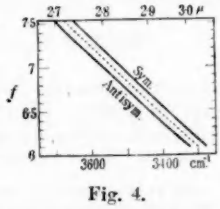

Fig. 4.

(13) Amilan shows a weak band at 2.7μ, but its intensity remains unchanged even when amilan is dried.

(14) The heat of adsorption of water into amilan from liquid water is, according to K. Hoshino and H. Yumoto (*J. Chem. Soc. Japan*, **70**, 104 (1949)), about -1 kcal/mol. From this the heat of adsorption from water vapor is calculated to be about -11 kcal/mol. This value is just as may be expected from the molecular state of the bound water here assumed.

(15) For instance, the symmetric O-H stretching vibration of H_2O gives much weaker infrared absorption band than the antisymmetric one in the CCl_4 solution (see reference (7)).

(16) M. Tsuboi, This Bulletin **22**, 255 (1949).

(17) This material was kindly placed by Dr. H. Tani (Osaka Univ.) at the writer's disposal.

In conclusion the writer wishes to express his sincere thanks to Professor San-ichiro Mizushima and Dr. Takehiko Shimanouchi for their kind guidance in this work, and to Mr. Hirosuke Yumoto for his valuable suggestions and for his placing the amilan film at the writer's disposal. The cost of this research has been partly defrayed from a Grant in Aid for Scientific Research from the Ministry of Education.

Department of Chemistry, Faculty of Science, Tokyo University, Tokyo

On the Electronic Structure of the Carbonyl and the Amide Groups

By Saburo NAGAKURA

(Received December 27, 1951)

Introduction

To the state of the molecule with the carbonyl or the amide group, the partially ionic structure, $\begin{matrix} R \\ R' \end{matrix}\!\!>\!C^+\!-\!O^-$ or $\begin{matrix} O^- \\ R \end{matrix}\!\!>\!C\!=\!N^+\!<\!\begin{matrix} R' \\ R'' \end{matrix}$ is expected to make large contributions.[1] By the use of these resonance structures, very satisfactory results have been obtained in the qualitative interpretation of many interesting physico-chemical properties of these groups, such as the large dipole moment[2] and the relatively low basicity of amide.[3]

In the present paper, the contributions of the partially ionic structures are theoretically treated by the molecular orbital method. The values of energy levels, resonance energies and π-electron densities are calculated for these two groups. Then these theoretical predictions are checked by the experimental values of resonance energies, dipole moments and near ultraviolet absorption spectra. Especially, as to absorption spectra, measurements were made in this laboratory with acetone, acetylchloride, acetic acid, ethyl acetate and N-methylacetamide. From these theoretical and experimental investigations, it is suggested that the weak near ultraviolet absorption spectrum characteristic of the unconjugated carbonyl group is due to the $n\rightarrow\pi^*$ transition, as was shown by Mulliken,[4] McMurry,[5] Baba[6] and Kasha.[7]

(1) L. Pauling, The Nature of the Chemical Bond, Cornell University Press 1940, p. 75, 133.
(2) W. D. Kumler and C. W. Porter, *J. Am. Chem. Soc.*, **56**, 2549 (1934).
(3) M. J. S. Dewar, The Electronic Theory of Organic Chemistry, Oxford University Press (1949), p. 94.
(4) R. S. Mulliken, *J. Chem. Phys.*, **3**, 564 (1935).
(5) H. L. McMurry, *J. Chem. Phys.*, **9**, 231 (1941).
(6) H. Baba, *J. Chem. Soc. Japan*, **72**, 214 (1951).

Theoretical

As is usual, only the π-electrons, of which there are two in the carbonyl group and four in the amide group, are considered. The molecular π-orbitals ψ_j $(j=1, 2, 3)$ in amide may be taken as linear combinations of the $2p$ atomic orbitals of oxygen, carbon and nitrogen atoms which are denoted by φ_O, φ_C and φ_N respectively. Using this approximation (LCAO), the following equation is obtained

$$\psi_j=a_{Oj}\varphi_O+a_{Cj}\varphi_C+a_{Nj}\varphi_N \qquad (1)$$

Neglecting the overlap integral S_{AB} between two atomic orbitals φ_A and φ_B, ies energthe E of these molecular orbitals are given approximately as the solutions of the following secular equation,

$$\begin{vmatrix} \alpha_O-E & \beta_{CO} & 0 \\ \beta_{CO} & \alpha_C-E & \beta_{CN} \\ 0 & \beta_{CN} & \alpha_N-E \end{vmatrix}=0 \qquad (2)$$

where α_A is the coulomb integral of A-atom and β_{AB} is the exchange integral between adjacent atomic orbitals φ_A and φ_B.

To evaluate the values of E, the following assumptions were made

$$\alpha_A=\chi_A\alpha/\chi_C,^{(8)}\ \beta_{AB}=S_{AB}\beta/S,^{(9)}\ \alpha=k\beta^{(8)}\ (3)$$

where χ_A represents the electronegativity of A-atom, S is the overlap integral between atomic orbitals belonging to adjacent carbon atoms

(7) M. Kasha, Discuss. Farad. Soc., Spectroscopy and Molecular Structure, 14. (1950).
(8) C. Sandorfy, *Bull. soc. chim. France*, (1949), 615.
(9) G. W. Wheland, *J. Am. Chem. Soc.*, **64**, 900 (1942).

Table 1

The Final Results of the Molecular Orbital Calculation with Amide

	I*	II*	III*	IV*	V*	VI*
α_C	4.297β	4.078β	4.378β	4.301β	4.085β	4.383β
α_O	5.355β	5.098β	5.546β	5.362β	5.106β	5.551β
α_N	5.109β	4.864β	5.331β	5.096β	4.849β	5.323β
β_{CO}	0.889β	0.891β	0.884β	0.919β	0.919β	0.919β
β_{CN}	0.822β	0.822β	0.818β	0.761β	0.761β	0.761β
E_1	6.081β	5.841β	6.240β	6.075β	5.833β	6.240β
E_2	5.213β	4.963β	5.422β	5.196β	4.945β	5.408β
E_3	3.466β	3.236β	3.593β	3.489β	3.262β	3.610β
Q_C	+0.360	+0.346	+0.404	+0.366	+0.356	+0.408
Q_O	−0.700	−0.680	−0.712	−0.700	−0.676	−0.702
Q_N	+0.338	+0.336	+0.308	+0.338	+0.324	+0.294

* Values of various parameters used in each calculation are as follows: $\chi_C=2.5$ in all calculations; $\chi_O=3.5$ and $\chi_N=3.0$ in I, II, IV and V; $\chi_O=3.6$ and $\chi_N=3.15$ in III and VI; $k=4.1$ in I, III, IV and VI; $k=3.9$ in II and V; $r_{CO}=1.23$ A. and $r_{CN}=1.32$ A. in I, II and III; $r_{CO}=1.21$ A. and $r_{CN}=1.37$ A. in IV, V and VI.

in benzene, α and β are the coulomb and the exchange integrals in the same molecule respectively, and k is the constant representing the ratio between α and β. Sandorfy has assigned 4.1 for the value of k. In the present calculation, two values of k, 4.1 and 3.9 were adopted. The latter value was determined as the ratio of the ionization potential of the carbon atom to the value of β estimated by Platt.[10] The overlap integrals necessary for the determination of the exchange integrals were obtained from the Table of Mulliken *et al.*[11] using the following two sets of bond distances:

C=O, 1.23 A., C−N, 1.32 A.;[12]

C=O, 1.21 A., C−N, 1.37 A..[13]

Under these conditions, three values of E can be evaluated in units of β. Then the values of a_{ai} in Eq. (1) can be calculated for each value of E. And it is possible to determine the π-electron density q_a of a-atom by the following equation,[14]

$$q_a=2\sum_i a^2_{ai} \qquad (4)$$

where the summation extends over the molecular orbitals which are occupied in the ground state.

From the value of q_a obtained by Eq. (4), the formal charge Q_a (in electron units) of a-atom can be known. Each atom having the positive or negative formal charge, correction terms for the electronegativity χ_a and the overlap integral S_{ab} should be considered. Corrections for these two quantities were made by the method of Pauling[15] and by the use of the table of Mulliken *et al.*[11] respectively. Thus it is possible to calculate new values of α_a and β_{ab} by Eq. (3). Using these new values, E, q_a and Q_a are calculated again by Eqs. (2) and (4). These procedures are repeated seven or eight times until the final results of these quantities are self-consistent.[16] They are given in Table 1, together with values of several parameters used in the last calculation.

Next, the similar calculation was made with

Table 2

The Final Results of the Molecular Orbital Calculation with the Carbonyl Group

	I′	II′	III′
χ_C	2.5	2.5	2.5
χ_O	3.5	3.5	3.6
k	4.1	3.9	4.1
α'_C	4.35β	4.16β	4.40β
α'_O	5.44β	5.20β	5.62β
β'_{CO}	0.838β	0.838β	0.838β
E'_1	5.895β	5.666β	6.045β
E'_2	3.895β	3.694β	3.975β
Q'_O	−0.544	−0.528	−0.590
Q'_C	+0.544	+0.528	+0.590

(10) The value of β estimated by Platt is −23,000cm.$^{-1}$ = −2.84 ev. J. R. Platt, *J. Chem. Phys.*, **18**, 1168 (1950).

(11) R. S. Mulliken, C. A. Rieke, D. Orloff and H. Orloff, *J. Chem. Phys.*, **17**, 1248 (1949).

(12) R. B. Corey and J. Donohue, *J. Am. Chem. Soc.*, **72**, 2899 (1950).

(13) The private communication from Mr. M. Kimura in Department of Chemistry, University of Nagoya.

(14) G. W. Wheland and L. Pauling, *J. Am. Chem. Soc.*, **57**, 2086 (1935).

(15) L. Pauling, The Nature of the Chemical Bond, Cornell University Press, 1940, p. 65.

(16) G. W. Wheland and D. E. Mann, *J. Chem. Phys.*, **17**, 264 (1949); Y. Kurita and M. Kubo, This Bulletin **24**, 13 (1951).

the carbonyl group because it was necessary for the evaluations of the resonance energy of the amide group and of the shift in the wave length due to the substitution of the methyl group of acetone by the amino group. In this case, the distance between carbon and oxygen atoms was set equal to 1.24 A.[17]

Experimental

N-methylacetamide is the same sample as used in the previous investigation.[16] Acetylchloride was prepared from glacial acetic acid and phosphorous trichloride. It was purified by the distillation in the atmosphere excluding moisture (b. p. 51.3°C.). Acetic acid, ethyl acetate and acetone were purified by the method of "Organic Solvent." Petroleum benzine used as the solvent was shaken with concentrated sulphuric acid for several days. Then it was treated with potassium permanganate and distilled after drying with sodium metal.

The absorption spectrum was measured with a Beckman spectrophotometer model DE. The results of the measurements are shown in Figs. 1 and 2. In these figures, molar extinction coefficients ε_M are plotted against wave lengths in mμ.

It was observed that the absorption intensities of ethyl acetate and acetylchloride decrease during the absorption measurements. This fact seems to mean that the decomposition of these molecules is induced by the near ultraviolet light. So the measured values of absorption intensities of these two molecules may not be said to be very accurate. But the wave length of the absorption maximum can be determined reliably as 220 mμ and 207 mμ for acetylchloride and ethyl acetate respectively in their solutions of petroleum benzine. The absorption maximum of acetic acid cannot be observed in this experiment, but it may be inferred from its absorption curve that its maximum probably appears near 200 mμ.[19] The absorption maximum of N-methylacetamide seems to appear in the side of shorter wave lengths rather than those of the above three substances as shown in Fig. 2.[20] This maximum cannot be measured with a Beckman spectrophotometer model DU.

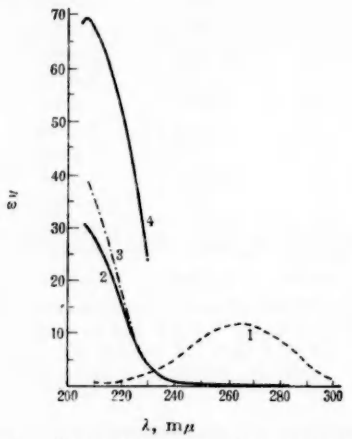

Fig. 1.—Absorption spectra of acetone, acetic acid and ethyl acetate: 1, acetone in water; 2, acetic acid in petroleum benzine; 3, ethyl acetate in water; 4, ethyl acetate in petroleum benzine.

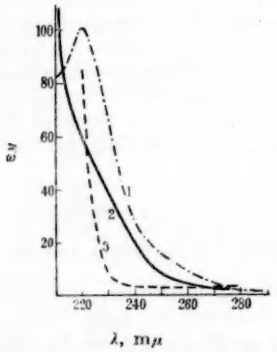

Fig. 2.—Absorption spectra of acetylchloride and N-methylacetamide: 1, acetylchloride in petroleum benzine; 2, N-methylacetamide in petroleum benzine; 3, N-methylacetamide in water.

At all events, it is evident from the above-mentioned experiments that the weak absorption band of acetone is intensified and shifted to the side of shorter wave lengths when one of the methyl groups is substituted by Cl atom, OR or NR_2 group.

Discussion

Calculated values of the resonance energies, π-electron distributions, and ground or exited energy levels of carbonyl and amide groups will be discussed comparing them with the observed or the estimated values of these quantities.

(17) M. Kimura and Y. Kurita, *J. Chem. Soc. Japan*, **72**, 396 (1951).

(18) S. Mizushima, T. Shimanouchi, S. Nagakura, K. Kuratani, M. Tsuboi, H. Baba and O. Fujioka, *J. Am. Chem. Soc.*, **72**, 3490 (1950).

(19) Ley and Arends observed the absorption maximum of acetylchloride, methyl acetate and acetic acid in pure liquids at 234.5 mμ, 208.5 mμ and 204 mμ respectively. The value of acetylchloride, which differs from that of the present experiment, seems to be incorrect because their measurements are not made in the wave lengths near the maximum. H. Ley and B. Arends, *Z. physik. Chem.*, (B) **17**, 177 (1932).

(20) Anslow pointed out with amide that very weak absorption maximum appeared about 280 mμ. In the present experiment, the similar phenomenon is observed in the concentrated aqueous solution of N-methylacetamide. Anslow regarded this absorption as due to associated amide molecules, but it seems more probable to consider that it is due to 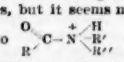 or some impurities.

G. A. Anslow, Discuss. Farad. Soc., Spectroscopy and Molecular Structure, 299 (1950).

Table 3

Calculated Values of ΔE_{res}, μ_π, and $\Delta\nu$ of Amide

	I	II	III	IV	V	VI
ΔE_{res}[a] (kcal./mole.)	19.2	18.3	18.0	18.2	17.3	17.5
μ_π (D)	5.54	5.38	5.42	5.51	5.32	5.32
$\Delta\nu$ (cm.$^{-1}$)[b]	7910	8200	7090	7550	7780	6810

a) The value of β is assigned -20 kcal./mole.
b) The value of β is assigned -23000 cm^{-1}.

(A) Resonance Energy of the Amide Group.—According to Pauling,[21] the resonance energy of amide is 21 kcal./mole. From the standpoint of the molecular orbital theory, this quantity can be represented approximately by the following equation, $\Delta E_{res}=2(E'_1+\alpha'_N)-2(E_1+E_2)$, where α'_N is the value of the coulomb integral for the neutral nitrogen atom. Calculated values of ΔE_{res} are given in Table 3. It is to be noticed that the values of ΔE_{res} evaluated by different methods I-VI may be regarded as almost the same,—that is to say, they are little affected by the values of various parameters used in each method. And it may be seen that the agreement between the calculated and the observed values are fairly good.

(B) π-Electron Densities and Dipole Moments of Carbonyl and Amide Groups.—The values of π-electron density, q_a calculated by the Eq. (4) indicate that in the carbonyl group about half of a π-electron moves from carbon to oxygen (see Table 2). This fact is in good accord with the conclusion derived by Pauling[1] from the study on the contribution of the polar resonance structure to the dipole moment of acetone or similar substances.

As to the amide group, it is shown that the non-bonding electrons in nitrogen partially migrate into the C=O bond. As the result of this electron migration, the nitrogen atom comes to have a partially positive charge. Thus it will be seen that the dipole moment of amide group becomes large, and the basic property of it decreases. From the values of Q_a, the dipole moment due to π-electron distributions, μ_π, can be calculated as shown in Table 3. The observed value of the dipole moment is 3.79D for dimethylacetamide in dioxan. So the calculated values are somewhat larger than the observed one.[22]

(C) Excited Electronic Levels and Near Ultraviolet Absorption Spectra of Carbonyl and Amide Groups.—Low intensity absorption band characteristic of unconjugated carbonyl bond appears at 279 mμ and 265 mμ in petroleum benzine and in water respectively. This absorption has been studied in detail by McMurry[5]; and from the theoretical investigation of the absorption intensity, it considered that this absorption might be due to the transition of non-bonding oxygen electron to the excited π-electron level of carbonyl group. This transition is shown schematically in Fig. 3. And it has been called the $n\rightarrow\pi^*$ or the $l\rightarrow\pi$ transition by Kasha[7] or Baba[6] respectively.

The results of our molecular orbital calculation on the electronic levels of carbonyl group are consistent with this view. The energy difference $\Delta E'$ between energy levels of the upper π-molecular orbital and of non-bonding oxygen electrons may be approximately represented by the following equation, $\Delta E'=E'_2-\alpha'_0$. The values of this quantity calculated by the methods I', II' and III' become -1.54, -1.51 and -1.64β respectively. The observed value can be determined as -1.56β, if the said absorption spectrum of acetone is due to the $n\rightarrow\pi^*$ transition. Therefore both values are in good agreement. But if it is assumed that this absorption band is due to the $\pi\rightarrow\pi^*$ transition, energy differences between upper and lower π-electron levels become -2.00, -1.97 and -2.07β. These values are larger than the observed value. Furthermore, the solvent effect of this absorption spectrum can be also explained from the same point of view. As shown in Table 4 the value of $\Delta E'$ calculated by the above equation becomes larger with the increase of $|\alpha'_0|$. This means that the above-mentioned absorption band shifts to the side of shorter wave lengths the contribution of the partially ionic resonance structure increases. The experimental result, namely that its wave length becomes smaller with he increment of the polarity of solvents,[23] conforms to the above theoretical expectation.

Table 4

The Relation between $\Delta E'$ and α'_0

α'_0	4.92β	5.41β	5.74β	6.07β	6.56β
Q'_0	-0.570	-0.640	-0.678	-0.710	-0.748
$\Delta E'$	-1.34β	-1.72β	-1.99β	-2.28β	-2.72β

Values of k, α'_c and β'_{co} used in these calculations are 4.1, 4.1β and 0.838β respectively.

Next the effect of substitution on the absorption spectrum of acetone will be discussed. When the methyl group of acetone is replaced by the group with non-bonding π-electrons such as amino or hydroxyl group, the absorption band shifts to the side of shorter wave lengths as shown in Figs. 1 and 2. On the other hand, in benzene the absorption spectrum due to the $A_{1g}\rightarrow B_{2u}$ transition shifts to the side of the longer wave lengths by

(21) L. Pauling, The Nature of the Chemical Bond, Cornell University Press (1940), p. 138.

(22) The dipole moment due to σ-electron distribution is expected to be very small for dimethylacetamide as well as C=O bond(1) So their dipole moments will be principally determined by π-electron distribution alone.

(23) According to Burawoy, this experimental result was regarded as one of the facts which could not be explained from the stand-point of $n\rightarrow\pi^*$ transition. But this difficulty for the $n\rightarrow\pi^*$ transition is surely removed by the present theoretical consideration. A. Burawoy, Discuss. Farad. Soc., Spectroscopy and Molecular Structure, 70 (1950).

the same substitutions.[24][25] It is interesting that the effect of the substitution on the absorption spectrum is quite different in acetone and benzene. This difference was discussed by Baba.[6] He applied the theory of the electron migration developed by Sklar[25] and Herzfeld[25] to explain qualitatively this fact. The same phenomenon can be treated by the LCAO molecular orbital method as follows. As shown in Fig. 3 and Tables 1 and 2, the calculated value of the empty π-electron level of amide group is higher than

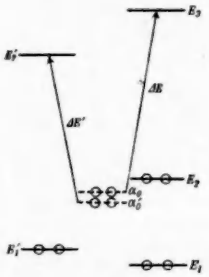

Fig. 3.—Energy levels of acetone and amide

that of acetone. So it may be regarded as reasonable that the absorption maximum of acetone appears in a longer wave length than that of amide. This fact can be readily understood by a glance at Fig. 3. And it is possible to calculate the wave number difference $\Delta\nu$ between these two absorption spectra by the equation, $\Delta\nu = (\Delta E - \Delta E')/ch = (E_2 - \alpha_0 - E'_2 + \alpha'_0)/ch$. The calculated values of $\Delta\nu$ are given in Table 3. The absorption maximum of N-methylacetamide appears probably below 205 mμ in petroleum benzine solution. So the observed value of $\Delta\nu$ may be estimated to be larger than 12900 cm.$^{-1}$ The calculated value for this quantity is smaller than the observed one. But it will be difficult to obtain more accurate values by the simple approximation of LCAO.

The shift of absorption spectra of acetylchloride, acetic acid and ethyl acetate can also be understood on the basis of the $n\rightarrow\pi^*$ transition. In these molecules as well as amide, the substituents have the non-bonding π-electrons which are able to migrate into carbonyl group, and the rate of electron migration probably increases in the order of Cl atom, OR and NR_2 groups as observed in the case of monosubstituted benzene.[25][27] It can be shown on the hand, that the value of E_2 becomes larger with the increment of the electron migration.[28] So it is expected from the standpoint of the $n\rightarrow\pi^*$ transition that these absorption spectra shift to the side of the shorter wave lengths in the order of acetylchloride, acetic acid or ethyl acetate, and N-metylacetamide. This expectation is qualitatively fulfilled by the present experiment.

Summary

1) Electronic structures of carbonyl and amide groups were investigated by the use of the molecular orbital method; calculated values of resonance energy and π-electron densities may be regarded as reasonable compared with these which were observed.

2) Near ultraviolet absorption spectra were measured with acetone, acetylchloride, acetic acid, ethyl acetate and N-methylacetamide. As the result of these measurements, it becomes evident that the low intensity absorption band of acetone shifts to the side of shorter wave lengths when the methyl group of acetone is replaced Cl atom or OR and NR_2 groups. These results can be explained by the present theoretical consideration if this absorption band is due to the $n\rightarrow\pi^*$ transition.

I wish to express cordial thanks to Prof. S. Mizushima and Prof. K. Higasi for stimulating and directing this research and to Mr. H. Baba for his helpful discussion. My thanks are also due to Mr. A. Kuboyama and Miss C. Tsurumi for their kind co-operation in performing this research. I am indebted to the budget of the Ministry of Education for this investigation.

Institute of Science and Technology, University of Tokyo, Tokyo

(24) S. Nagakura and H. Baba, *J. Chem. Soc. Japan*, **71**, 527 (1950).
(25) K. F. Herzfeld, *Chem. Rev.*, **41**, 233 (1947).
(26) A. L. Sklar, *J. Chem. Phys.*, **7**, 984 (1939).
(27) F. A. Matsen, *J. Am. Chem. Soc.*, **72**, 5243 (1950).
(28) This is apparent from the fact that $\partial E_2/\partial\alpha_N$ is positive.

Heats of Wetting of Polysaccharides. I. Heats of Wetting of Various Polysaccharides

By Toshio NAKAGAWA

(Received February 4, 1952)

Introduction

The interaction between polysaccharides and water has been investigated chiefly by graphing adsorption isotherms or X-ray patterns, and their heats of wetting have been relatively overlooked.

About fifty years ago, Rodewald and Kattein[1] measured heats of wetting of various starches, then in 1917 Katz[2] reported his data concerning adsorptions and heats of wetting of many substances including cellulose and inulin. More recently Schrenk *et al*[3]., Dumanskii and his collaborators[4], and Wahba[5] published their results in starch and cellulose.

The present writer also measured heats of wetting of various polysaccharides, such as potato starch, potato amylose, potato amylopectin, inulin, glycogen and konjac mannan, but found no regularity between heat of wetting and molecular constitution.

Apparatus and Procedure

The apparatus used resembles the one constructed by Harkins and his collaborator,[6] and is illustrated in Fig. 1a.

When the rod A is pushed down, the ampoule S breaks and the content is immersed into water, the temperature in D_1 rises owing to the heat of wetting of the sample and electrical potential difference appears at the ends of the thermocouple. This potential is measured with a potentiometer. Then a known amount of electric current is passed through H, the potential difference produced is measured again. We can estimate the heat of wetting by comparing these two potential differences.

The actual procedure of measurement is as follows. The apparatus is arranged as illustrated in Fig. 1a. When the thermal equilibrium is roughly attained, L is started. Potential difference at the ends of the thermocouple is recorded once every minute. The temperature in D_1 rises slowly because of the mechanical work of the stirrer (AB in Fig. 2). When the temperature-time curve results in a straight line, S is broken. The temperature is elevated rapidly owing to the heat of wetting (BC in Fig. 2), but in a short time returns again to a straight line (CD). When an amount of electric current is passed for a certain time through H, the temperature-time curve behaves as before (DEF).

Extrapolating these two straight lines (CD, EF), we can get temperature elevation S_1 by the heat of wetting and S_2 by the electrical work, and calculate the heat of wetting by comparing S_1 and S_2.

When the heat generation is relatively slow, necessary correction is given to S_1 and S_2. However in this experiment these corrections were usually small, and in most cases unnecessary.

If the value of an evacuated sample is to be obtained we put the sample in a thin walled ampoule S', evacuate under 1/1000 mm. Hg, and fuse off the neck, which remains an L-shaped

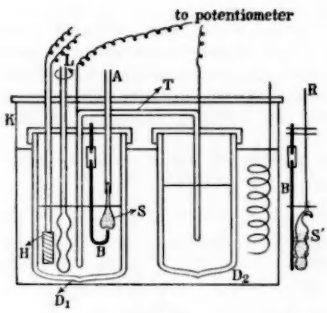

Fig. 1a. 1b.

K thermostat (constant within 1/100°C.)
D_1, D_2 Dewar's vessels
T Cu-constantan thermocouple with 36 pairs of junctions
S ampoule containing sample (usually about 0.8 g.)
A rod grasping ampoule
B brass rod with keen needle
H electric heater with resistance about 4.7 Ω
L glass stirrer
R string

(1) H. Rodewald and A. Kattein, *Z. phys. Chem.*, **33**, 579 (1900).
(2) J. R. Katz, *Kolloid. Beih.*, **9**, 1 (1917).
(3) W. G. Schrenk, A. C. Andrews and H. H. King, *Ind. Eng. Chem.*, **39**, 113, (1947).
(4) A. V. Dumanskii, Ya. F. Mezhennyi and E. F. Nekryach, *Kolloid. Zhur.*, **9**, 335 (1947); *Chem. Abst.*, **43**, 6042 (1949).
(5) M. Wahba, *J. Phys. Colloid. Chem.*, **52**, 1197 (1948).
(6) W. Harkins and Roy Dahlstrom, *Ind. Eng. Chem.*, **22**, 897 (1930).

hook. The rod A is removed and S' is fixed tightly to B, as shown in Fig. 1b. By pulling up the string R fastened to the hook, we can break the neck and bring out the sample into the water. In this case, heat development is somewhat slower, but the measurement can be performed without difficulty.

The accuracy of the apparatus was estimated in taking account of the sensibility of the potentiometer, and the exactness in determining electrical work. This is calculated to be about one per cent.

Furthermore, it is also deduced that the measured heat amount in the calorimeter has always uncertainty amounting to 0.05 cal., and this means, when we measure the heat smaller than 5 cal., the accuracy becomes less than one per cent.

The experimental values endorse the above presumption.

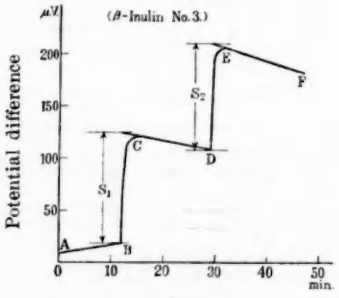

Fig. 2.

(1) Native potato starch: Native potato starch was dried in Abderhalden's desiccator under reduced pressure (2/100 mm. Hg.) so long as to reach constant weight.

(2) Potato starch in the form of paste: 6.5 g of native potato starch was mixed with 3 cc. of water, heated to 100°C. and dried at 100°C. Starch so treated was called by Katz "Verkleisterte" starch. It swelled to give paste when immersed into water.

(3) Retrograded potato starch: Potato starch paste was laid under saturated water vapor for a long time (from 22 to 162 days). Retrograded starch did not make paste.

(4) Potato amylose: Potato amylose was isolated by Schoch's method.(7) Potato starch was autoclaved with water for 3 hours at 110°C. To the 3 percent solution thus treated, excess amount of *n*-butanol was added and filtered. The filtrate which contained amylopectin, served as the source of the sample (6). Filtered precipitate was dissolved in hot water; then the solution was poured into a large amount of methanol, precipitating amylose. The resulting precipitate was filtered, washed with methanol and dried. This substance swelled well in cold water, dissolved partly in cold and perfectly in hot water, giving blue color with iodine.

(5) Retrograded amylose: The above-mentioned amylose was exposed to saturated water vapor for 25 days. The sample swelled in cold water but less than sample (4), and dissolved in hot water with difficulty.

(6) Potato amylopectin: The solution containing amylopectin (cf. sample (4)) was mixed with a large amount of methanol, the resulting precipitate was centrifuged, washed and dried. This sample swelled and partly dissolved in cold water. Iodine color was reddish violet.

(7) Retrograded amylopectin: Exposure of sample (6) to saturated water vapor for 29 days, gave retrograded amylopectin which swelled a little in cold water, but was entirely insoluble. This was confirmed by addition of iodine to the supernatant, which gave no color reaction.

(8) β-Inulin: "Takeda's" inulin was dissolved in hot water with active charcoal and filtered. The filtrate was cooled and frozen with freezing mixture; then melted. It remained a deposit. The precipitate was recrystallized three more times. β-Inulin is insoluble in cold water.

(9) α-Inulin: β-Inulin was dissolved in hot water, the solution was poured into a large amount of alcohol, the precipitate was centrifuged, washed and dried. α-Inulin dissolves in cold water.

(10) Retrograded inulin: α-Inulin was exposed to saturated water vapor for 10 days. This was insoluble in cold water.

(11) Konjac powder: Native konjac powder sold as "special grade", was dried under reduced pressure. This powder swells and dissolves in cold water. However, as the dissolution needed a very long time, it dissolved imperfectly in the course of the heat measurement.

(12) α-Konjac mannan: Native konjac powder was dissolved in cold water by shaking, and the solution filtered with cloth was mixed with alcohol. The resulting precipitate, after being washed and dried surves as the sample. α-Konjac mannan swelled and dissolved in cold water, but the perfect dissolution was not attained in the course of measurement because of slowness of the reaction.

(13) β-Konjac mannan: One per cent solution of α-konjac mannan was heated with $Ba(OH)_2$, and filtered. The deposit was treated with one per cent acetic acid solution for several days to remove Ba, then washed with water. The sample swelled a little in water, but did not dissolve even when boiled.

(14) Glycogen: "Takeda's" glycogen was dissolved in water, precipitated with alcohol, dissolved in water again, electrodialized, then precipitated with alcohol containing a trace of potassium acetate and washed thoroughly with alcohol. Glycogen dissolved well in cold water and gave a slightly turbid solution.

(7) T. J. Schoch, "Advances in Carbohydrate Chemistry." Vol. I. The fractionation of starch.

Results and Discussion

The results obtained are shown in Table 1. Each value is the mean of two or three experiments.

Table 1

		Heat of wetting cal./g. in the presence of air	Heat of wetting cal./g. evacuated
1	Native potato starch	28.2	27.2
2	Potato starch paste	24.6	
3	Retrograded potato starch	25.6 (22 days) 25.5 (162 days)	
4	Potato amylose	22.8	
5	Retrograded amylose	23.5	
6	Potato amylopectin	21.2	
7	Retrograded amylopectin	21.8	
8	β-Inulin	23.1	23.2
9	α-Inulin	17.9	
10	Retrograded inulin	21.2	
11	Konjac powder	21.3	
12	α-Konjac mannan	23.7	
13	β-Konjac mannan	16.2	16.7
14	Glycogen	23.5	

We see that the heats of wetting of polysaccharides lie in the range from 10 to 30 calories per gram of dried substance. The value of native potato starch (28.2 cal./g.) is in good accordance with that of Schrenk *et al*[3]. (29.1) and Dumanskii *et al*[4]. (28.06). The elevation of drying temperature from 34° to 64° or 100°C caused no decrease of weight and no change of heat-of-wetting exceeding experimental error (0.2 cal.). It is somewhat interesting that potato starch gives a higher value than either of its fractions (potato amylose, potato amylopectin.)

Inulin gives 23.1 cal./g. in agreement with Katz's[2] result. Heats of wetting of evacuated samples were also measured in three cases, namely potato starch, inulin and konjac mannan, but no or little effects were observed.

It seems to the present writer that there exists no correlation explicitly between the heat of wetting and the molecular constitution of polysaccharides.

Summary

Heats of wetting of various polysaccharides, such as potato starch, potato amylose, potato amylopectin, inulin, glycogen, and konjac mannan were measured, but no correlation between heat of wetting and molecular constitution was found.

The author wishes to express his hearty gratitude to Prof. Sameshima for his kind guidance and advice.

Department of Chemistry, Faculty of Science, Tokyo University, Tokyo

Heats of Wetting of Polysaccharides. II. A Rule Which Exists Between Adsorption Isotherms and Heats of Wetting of Polysaccharides

By Toshio NAKAGAWA

(Received February 4, 1952)

Net Heat of Adsorption

Net heat of adsorption defined by heat of adsorption minus heat of condensation, can be experimentally acquired by means of measuring heats of wetting of dried and partially saturated substance.

Denote the heat of wetting, obtained by throwing one gram of a dry substance into water, by H, and that obtained by a partially saturated substance, which consists of one gram of dry substance and m grams of water, by $H(m)$, then $H-H(m)$ gives the net heat of adsorption $N(m)$, generated when one gram of dry substance adsorbs m grams of water.[1]

$$N(m)=H-H(m) \qquad (1)$$

However, it should be remembered, that the processes are tacitly assumed to be reversible ones.

(1) A. B. Lamb and A. S. Coolidge, *J. Am. Chem. Soc.*, **42**, 1146 (1920).

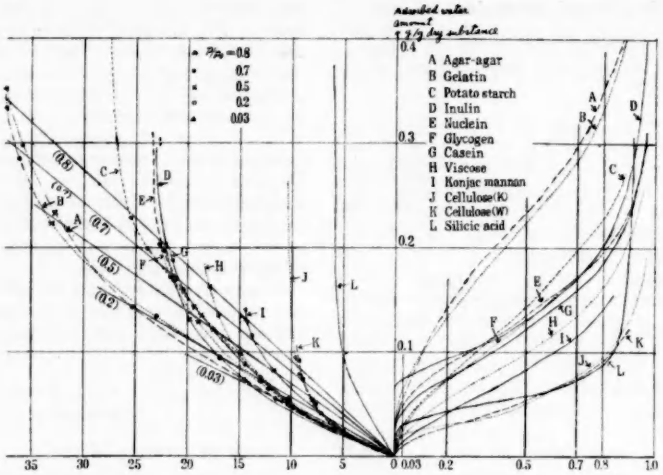

Fig. 1.

The Rule Found by the Author

The present writer arranged the data concerning heats of wetting, which were reported by J. R. Katz,[2] E. Rosenbohm,[3] A. V. Dumanskii *et al*,[4] and M. Wahba,[5][6] together with the author's own data, and plotted net heats of adsorption against water amounts adsorbed.

By comparing the curves thus obtained with the adsorption isotherms obtained by Katz,[2] H. Sato,[7] Wahba[6] and the author, it was found that there exists a simple rule, between the net heats of adsorption and water amounts adsorbed among the following substances: starch, inulin, cellulose, viscose, glycogen, konjac mannan, casein, nuclein, gelatin, and agar-agar.

The rule states: "When we bring one gram of each of the above-mentioned substances under the same relative humidity $x(p/p_0)$, generated net heats of adsorption $N(m)$ (heat of adsorption minus heat of condensation) are proportional to the amounts m of water adsorbed, independently of the varieties of substances, in the range of x smaller than 0.8".

The author wishes to expound the rule in further detail. In the right half of Fig. 1. are represented adsorption isotherms taking relative humidity x in abscissa and adsorbed quantity m (g. water/1 g. of dry substance) in coordinate.

The data were gathered from the works of the following investigators, Katz[2] (inulin, cellulose (K), casein, nuclein, gelatin, agar-agar at room temperature), H. Sato[7] (potato starch 20°C), Wahba[6] (cellulose (W), viscose 30°C), and the author (konjac mannan, glycogen 20°).

It should be mentioned here that in this paper Katz's values slightly differ from his original report. Katz obtained the relation between relative humidity and adsorbed water amount, by exposing the samples over sulfuric acid solution with various concentrations. To estimate the water vapor pressure over sulfuric acid solution, he used Regnault's[8] data, but it seems inadequate particularly at a concentration higher than 50 per cent. Relative humidities were therefore amended by Greenewalt's[9] report.

In the left half, net heats of adsorption $N(m)$, obtained using the method discussed above are plotted against adsorbed quantities m, taking the former in abscissa, and the latter in coordinate.

The data were collected from the experiments of the following investigators, Rosenbohm[3] (gelatine), Katz[2] (inulin, cellulose (K), casein, nuclein, agar-agar at room temperature), Dumanskii *et al*[4]. (potato starch, 30°C), Wahba[5][6] (cellulose (W), viscose 30°), and the author (konjac mannan, glycogen 30°C).

(2) J. R. Katz, *Kolloid Beih*, **9**, 1 (1917).
(3) E. Rosenbohm, *Kolloid Beih*, **6**, 177 (1914).
(4) A. V. Dumanskii, Ya. F. Mezhennyi and E. F. Nekryach, *Colloid Zhur.*, **9**, 355 (1917); *Chem. Abs.*, **43**, 6042 (1949).
(5) M. Wahba, *J. Phys. Colloid Chem.*, **52**, 1197 (1948).
(6) M. Wahba, *J. Phys. Colloid Chem.*, **54**, 1148 (1950).
(7) H. Sato, *J. Chem. Soc. Japan, Pure Chem. Sect.*, **72**, 790 (1951).
(8) Regnault, Landolt Tab. 3. Aufl. 166 (1905).
(9) G. H. Greenewalt, *Ind. Eng. Chem.*, **17**, 522 (1925).

The samples used in the two sets of experiments are the same excepting gelatin and starch. In the case of starch, it is ascertained by the author that Sato's sample has almost the same value of heat of wetting as the one used by Dumanskii (Sato's sample 28.2 cal./g., Dumanskii's 28.06 cal./g.).

When we draw a parpendicular line at a certain value of x in the right half of Fig. 1, its intersecting points with adsorption isotherms give the water amounts adsorbed by respective substances. Next we draw horizontal lines from these intersecting points toward the left half of Fig. 1. Intersecting points of these lines with net-heat-of-adsorption curves gives the values of net heats of adsorption, which will be developed when these substances are brought under the same relative humidity x. It will be recognized from Fig. 1. that these intersecting points lie on a straight line passing origin.

This rule holds well in the region from very small value of x (0.03) to relatively large value ($x=0.8$). This fact seems to the author too consistent to be considered as merely an accident. The rule cannot hold at any larger value of x, exceeding 0.8. The above-mentioned rule can be expressed mathematically as follows:

$$N(m)=a(x)m(x) \qquad (2)$$

where $N(m)$: a function of m, and depends also on the kind of substance.

$m(x)$: a function of x, and depends on the kind of substance.

$a(x)$: a function of x independently of the variety of substance.

Equation (2) indicates that net heat of adsorption is proportional to m at same x, independently of the variety of substance. Heat of adsorption $A(m)$ is also proportional to the adsorbed water amount m, because net heat of adsorption is defined by heat of adsorption minus heat of condensation.

$$\text{Thus} \qquad A(m)=N(m)+Lm=(a+L)m \qquad (3)$$

L: heat of condensation of 1 g. water.

From Fig. 1, values of $a(x)$ are obtained as follows relating to several values of x.

x	0.03	0.2	0.5	0.7	0.8
$a(x)$	205	178	145	123	109 cal./g. water

For the purpose of comparison, adsorption isotherm and net-heat-of-adsorption curve of silicic acid[2] are also represented in Fig. 1. Clearly it does not obey the rule.

It is difficult to explain why the rule holds in the above-mentioned substances, but it is also noticeable that these substances are polysaccharides, proteins, or their relatives.

The approximate value of net heat of adsorption can be obtained by drawing only one adsorption isotherm, in the case of the substance which obeys the rule, so it is interesting to explore what kinds of substances are governed by the rule.

The above-mentioned relation does not hold when x exceeds 0.8. Possibly this fact is due to the rapid increase of different kinds of adsorption in such a high humidity.

To the author, it seems an interesting fact that a regularity is found in the integral rather than in the differential heat of adsorption.

An example of polysaccharide which does not obey the rule, is reported. Namely, comparing the adsorption isotherm of "Künstliche Stärkekörper" obtained by Katz,[2] with the net heat of adsorption of the same substance reported by H. Rodewald and his collaborator,[10] we find the rule does not hold well. The net heat of adsorption expected from the adsorption isotherm using the above-mentioned rule, is lower than the experimental value.

But there is some reason to think the value given by Rodewald *et al.* is somewhat too high, possibly for the sake of lower experimenting temperature. For example, among the heats of wetting of potato starch reported by them and other more recent investigators, their value alone is somewhat higher than the others.

H. Rodewald *et al*[10]. (1900)	32.68 cal./gr. (at 0°C)	
A. V. Dumanskii *et al*[4]. (1947)	28.06	(20°)
W. G. Schrenk *et al*[11]. (1947)	29.2	(30°)
T. Nakagawa[12] (1949)	28.2	(30°)

Experiments

The samples of glycogen and konjac mannan, of which data are employed in the above discussion are the same ones as glycogen and β-konjac mannan in the preceding report of this series.[12]

A sample of each spread in a wide bottle, was put into a desiccator containing sulfuric acid solution with varying concentrations, and exposed for several months until constant weight was reached.

Adsorbed amount was measured as the increase of weight, relating to relative humidity.

Heats of wetting of partially saturated substances were measured using the same apparatus described in the preceding report. In this case, the sample enclosed in an ampoule, was put into the same desiccator that was mentioned above,

(10) H. Rodewald and A. Kattein, *Z. Phys. Chem.*, **33**, 579 (1900).

(11) W. G. Schrenk, A. C. Andrews and H. H. King, *Ind. Eng. Chem.*, **39**, 113 (1947).

(12) T. Nakagawa, Preceeding report in this journal.

and the ampoule was sealed off after the adsorption equilibrium had been roughly attained. Net heats of adsorption were then readily calculated.

In Fig. 1, curves thus obtained are represented with those derived from other investigators' data.

Summary

A simple rule which correlates adsorption isotherms and heats of wetting of polysaccharides was described.

The rule states: "When we bring one gram each of polysaccharides (and several other substances belonging to organic high polymer) under the same relative humidity, generated net heats of adsorption are proportional to the amounts of adsorbed water, independently of the varieties of substances."

The author wishes to express his sincere thanks to Prof. Sameshima for his kind guidance and encouragement.

Department of Chemistry, Faculty of Science, Tokyo University, Tokyo

Wettability of Solid Surface. V. The Effect of Metallic Cations on Wettability of Stearic Acid[1]

By Ayako INABA

(Received December 25, 1951)

Introduction

In one of the preceding reports,[2] it was pointed out that the wettability of stearic acid surface was increased by treating with aluminum or thorium salt solution, while it was not increased by treating with potassium or calcium salt solution. Langmuir also showed that the wettability of barium stearate built-up film was increased by treating with aluminum or thorium salt solution,[3][4] and further that some properties of stearic acid monolayer were changed by adsorption of these metallic ions.[5] However, the present author has found no explanation for the mechanism of wetting due to ions like aluminum and thorium. The present paper describes the effect of various metallic ions on the wettability of stearic acid as well as the explanation of its mechanism.

Experimental

Material.—Stearic acid of Kahlbaum was used after recrystallization from alcohol. Salts used were LiCl, NaCl, RbCl, $MgSO_4 \cdot 7H_2O$, $Ca(NO_3)_2 \cdot 4H_2O$, $Sr(NO_3)_2$, $BaCl_2 \cdot 2H_2O$, $Al_2(SO_4)_3 \cdot 18H_2O$, $CuSO_4 \cdot 5H_2O$, $AgNO_3$, $ZnSO_4 \cdot 7H_2O$, $3CdSO_4 \cdot 8H_2O$, $HgCl_2$, $Pb(NO_3)_2$, $Th(NO_3)_4$, $MnSO_4 \cdot 6H_2O$, $FeK(SO_4)_2 \cdot 12H_2O$, $Co(NO_3)_2$, and $NiSO_4 \cdot 7H_2O$. These salts were recrystallized from redistilled water before use. Special purification was made prior to the recrystallization if necessary. Water used for the wettability experiment was also redistilled using the apparatus of Vidrex glass of Kokura Glass Co. and was made free from carbon dioxide.

Measurement.—A clean glass rod of about 5 mm. diameter and 50 mm. length was dipped into molten stearic acid, withdrawn, and thus coated with a layer of stearic acid which was solidified in air. The surface of stearic acid thus obtained was treated with various salt solutions for about seventeen hours, after which the wettability of the surface was measured in relation to the same solution. The concentration of the solution used was kept to 10^{-4} mol unless mentioned otherwise. *p*H of the solution was controlled simply using hydrochloric acid or sodium hydroxide solution.

For wettability measurement, the sessile drop method was used. Namely, a drop of 0.5 mm. diameter was placed on the surface for measurement with the aid of a glass capillary having a paraffined tip. The image of the drop was magnified by a microscopic objective, projected on a screen, and sketched upon a piece of paper. A tangent was drawn for the silhouette thus obtained, and the contact angle θ was measured using a protracter. *p*H of the solution was determined by the color indicator method before and after each treatment of the surface. As the solution had no buffer action, the experiment was

(1) Reported before the annual meeting of the colloid chemistry held by the Chemical Society of Japan on Nov. 19th (1950).

(2) A. Inaba, This Bulletin, **23**, 146 (1950).

(3) I. Langmuir and V. J. Schaefer, *J. Am. Chem. Soc.*, **59**, 1405 (1937).

(4) I. Langmuir and V. J. Schaefer, *J. Am. Chem. Soc.*, **59**, 1762 (1937).

(5) I. Langmuir and V. J. Schaefer, *J. Am. Chem. Soc.*, **59**, 2400 (1937).

mainly conducted in the air free from carbon dioxide in the case of pH > 6. The use of a buffer solution was avoided owing to the probable effect of polyvalent anions and concentrated alkali ions which might obscure the effect of cation under investigation.

Results

The wettability of stearic acid surface treated by water, pH of which was controlled simply by hydrochloric acid or sodium hydroxide, is shown as a control curve in Fig. 1. In this case, wettability was constant in the range of pH < 8, being equal to that of untreated stearic acid towards distilled water ($\theta = 110°$), while the increase of wettability was remarkable at pH > 10, θ being reduced to almost 0°.

Addition of various metallic ions to the dipping solution affected the wettability of the stearic acid surface. These effects were divided into three types as follows:

(1) The Effect Produced by the Addition of Sodium, Potassium and Rubidium Salts.—The addition of these salts in concentration of 10^{-4} mol showed no effect on the wettability of stearic acid compared with the control as shown in Fig. 1. However, the increase of the concentration of the salts lowered pH at which wettability began to increase. For example, the addition of 0.05 mol Na_2HPO_4 or 0.2 mol KCl caused the wettability of stearic acid already at pH 7 (Fig. 1) to increase.

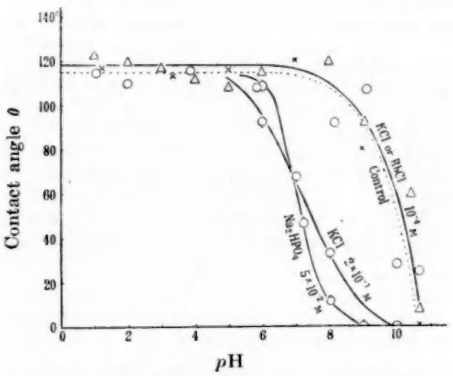

Fig. 1.—The effects of Na, K, and Rb ions (the 1st group) upon the wettability of stearic acid surface.

(2) The Effect Produced by the Addition of Thorium, Aluminum, Ferric, Chromic, Cobaltous and Cupric Salts.—These salts enhanced the wettability of the stearic acid surface in the pH region characteristic for each salt (Fig. 2a), although stearic acid showed only a small wettability in the absence of these salts (control curve). Cadmium, zinc, silver, and magnesium salts showed no effect at concentration of 10^{-4} mol but showed a perceptible wetting power at concentration of 10^{-3} mol (Fig. 2b). These salts may also be considered to belong to the preceding class, but for the reason mentioned later we should like to classify them as belonging to this class.

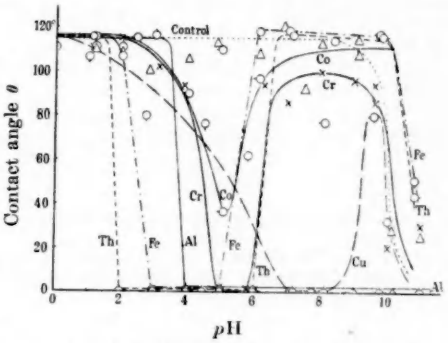

Fig. 2a.—The effects of Th, Fe, Al, Cr, Co, and Cu ions (the 2nd group) in concentration of 10^{-4} mol upon the wettability of stearic acid surface.

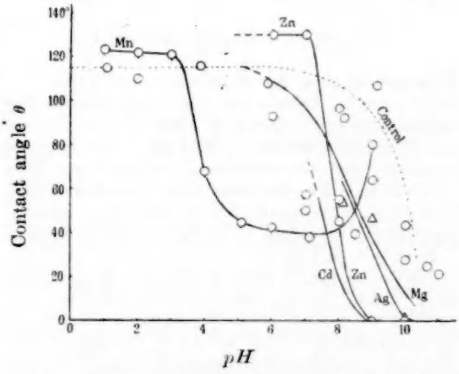

Fig. 2b.—The effects of Mn, Cd, Zn, Ag, and Mg ions (the 2nd group) in concentration of 10^{-3} mol upon the wettability of stearic acid surface.

(3) The Effect Produced by the Addition of Barium, Strontium, Calcium and Lithium Salts.—These salts reduced the wettability of stearic acid at pH > 10 (Fig. 3), in the region of which, however, stearic acid was wettable in the absence of these metallic ions except sodium ion which came from alkali for pH control. In this case increase in concentration of the ions of this group promoted the non-wetting properties of stearic acid as shown in Fig. 3. Mercuric, nickel, and lead salts showed apparently the similar effect (Fig. 4).

Discussion

Wettability of the stearic acid surface towards distilled water was small, the contact angle being

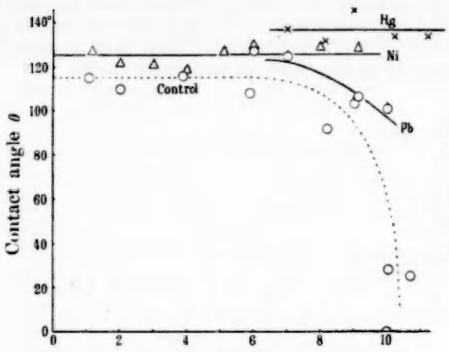

Fig. 3.—The effects of Ba, Sr, Ca, and Li ions (the 3rd group) upon the wettability of stearic acid surface.

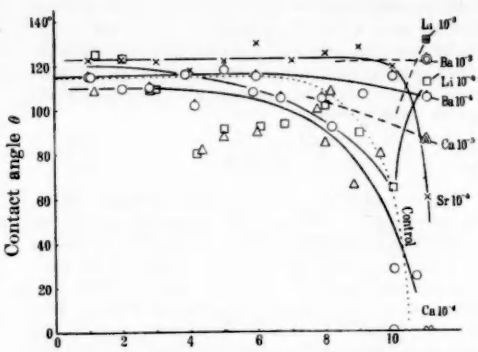

Fig. 4.—The effects of Hg, Ni, and Pb ions in concentration of 10^{-3} mol upon the wettability of stearic acid surface.

about 110°, and it did not change by being treated with hydrochloric acid. However, the surface showed increase in wettability towards sodium hydroxide solution. This increase can be explained by the polarity of the surface caused by the surface dissociation of stearic acid as follows:

$$StH + Na^+ + OH^- = St^-Na^+ + H_2O.$$

This will explain the control curve of Fig. 1. A more detailed calculation can even predict the wettability ~ pH curve similar to that found experimentally as shown in Fig. 1. It may be presumed that the addition of neutral salt like KCl or Na_2HPO_4 promotes the dissociation and that as a result wettability is increased. In fact, the wettability began to increase already at pH 7 as shown in Fig. 1.

Now we come to place where we can explain the effect of various metallic ions on the wettability of stearic acid. There have been some informations available for this purpose. For instance, we can cite Langmuir's study[5] on the stearic acid monolayer on the substrate containing metallic ions. There he confirmed the adsorption of metallic ions to the monolayer. Especially, in the case of barium salt, stearic acid monolayer was considered to be composed of neutral barium soap at pH 11,[6] and its built-up film was not wetted with water.[3] The author's experiment showed that the surface of stearic acid treated with 10^{-4} mol cupric salt solution at pH 6 ~ 8 was bright blue and the color was not removed after rinsing with water. From these and also other similar phenomena encountered we can safely conclude the adsorption or chemical reaction taking place between stearic acid and the metallic ions in solution, which profoundly affect the wetting condition of stearic acid surface. We can also confirm this point more precisely. Langmuir and others[5] introduced the following equation for this adsorption.

$$\log\{\tau_1/(1-\tau_1)\} = C_1 + m_1 \log[M_1^{Z+}] + Zm_1\,(p\mathrm{H})$$

Here τ_1 is the fraction of the number of surface cells occupied by the adsorbed substance, C_1 and m_1 are constants proper to M_1^{Z+} ion. According to this equation, it can be expected that apart from the characteristic properties of ions, higher valency ions can be adsorbed at still lower pH than that at which the lower valency ions are adsorbed. Langmuir's results showed that ferric ions were strongly adsorbed by stearic acid monolayer at pH 2, and aluminum ions at pH 3 to 5, barium at pH 6, and sodium at pH 8. On the other hand, in the author's experiment the various effects of the ions upon wettability appeared in the pH regions shown in Table 1, which were based upon the data of Figs. 2a, 2b, 3 and 4. It can be noted that these pH regions for various cations as a whole are in close relationship with those given for cations by Langmuir in the case of adsorption. The fact again confirms the above view, that the adsorption of ions is an important factor affecting the wettability of stearic acid. Disappearence of the remarkable wetting

Table 1

pH Regions at which Metallic Ions Affect the Wettability of Stearic Acid Surface.

Ion	pH	Ion	pH	Ion	pH	Ion	pH
Th^{++++}	2~6	Fe^{+++}	3~5	Co^{++}	5	Li^+	>10
		Al^{+++}	>4	Cu^{++}	7~8		
		Cr^{+++}	5~6	Mn^{++}	5~8 (10^{-3} mol)		
				Zn^{++}	>9 (10^{-3} mol)		
				Cd^{++}	>9 (10^{-3} mol)		
				Ba^{++}*	>10		

* Ba^{++} is considered to be partially adsorbed already at pH 6 or 7, but we cannot distinguish this surface from that of stearic acid at this pH, for both surfaces are non-dissociating and behave similarly at this pH.

(6) I. Langmuir and V. J. Schaefer, *J. Am. Chem. Soc.*, **58**, 284 (1936).

Table 2

Relation between Wetting Power and Co-ordination Tendency of Metallic Ions

Ion	Type of wetting	Degree of wetting*	Ionic potential	Ionization potential (1st), e. v.	Normal electrode potential, volt	Heat of hydration, kcal./mole	Free energy decrease of complex formation with stearate radical
Na^+	1st class	0	1.02	5.12	−2.71	114	—
K^+	〃	0	0.75	4.32	−2.92	94	—
Rb^+	〃	0	0.67	—	−2.92	—	—
Li^+	3rd class	−	1.28	5.37	−2.96	136	1.3
Ca^{++}	〃	−	1.89	6.09	−2.81	410	1.2
Sr^{++}	〃	−−	1.57	5.67	—	376	—
Ba^{++}	〃	−−	1.40	5.19	—	346	(1.1)
Ni^{++}	(3rd class)	−	2.56	7.61	−0.234	516	2.5
Hg^{++}	(〃)	−	1.79	10.38	+0.85	480	6.1
Pb^{++}	(〃)	−	1.52	7.38	−0.13	—	(3.4)
Mg^{++}	2nd class	+	2.56	7.61	−1.87	490	1.4
Cd^{++}	〃	+	1.94	8.96	−0.40	462	2.7
Zn^{++}	〃	+	2.41	9.36	−0.76	528	2.9
Mn^{++}	〃	+	2.20	7.41	−1.03	479	—
Ag^+	〃	+	0.88	7.54	+0.80	162	3.5
Co^{++}	〃	++	2.44	8.5	−0.26	504	2.2
Cu^{++}	〃	++	1.98	7.68	+0.35	536	3.4
Cr^{+++}	〃	++	4.69	6.74	−0.51	—	(4.3)
Fe^{+++}	〃	++	4.48	7.83	−0.04	185	(3.6)
Al^{+++}	〃	+++	5.26	5.96	−1.69	1149	(9.7)
Th^{++++}	〃	+++	3.64	—	—	—	—

* 0: Degree of wetting power exhibited under control condition.
−, −−: Relative degree of non-wetting power perceptible at 10^{-3} mol and 10^{-4} mol respectively.
+, ++: Relative degree of wetting power perceptible at 10^{-3} mol and 10^{-4} mol respectively.
+++: Remarkable wetting power exhibited at 10^{-4} mol.

power of ferric, thorium, chromic, cobaltous, and cupric, ions in high *p*H region can be attributed to the decrease of concentration of these ions in solution due to the precipitation as hydroxide.

Now, we feel much interest in the question, "What is the chief factor determining the wetting or non-wetting power of an ion?" To answer this question, we must know the nature of these adsorption products of metallic ions on stearic acid, which may presumably be attributed to the structural characteristics of the metallic ions themselves. In this connection, it is best to pay attention to the co-ordination tendency of the individual metallic ion concerned.

First of all, let us consider the aluminum ion which showed remarkable wetting power. It was known to have a marked co-ordination tendency and to form an aquo ion, $Al(H_2O)_6^{+++}$, in water, which was considered further to form so-called ol-compound and oxo-compound through hydrolysis and association of more than two aquo ions.[7] On the other hand, many fatty acid-aluminum compounds were considered by many investigators[8] to be hydrated macro-molecules. Sasaki and Matuura of our laboratory also confirmed the fact that stearic acid monolayer on the aqueous substrate containing aluminum ions showed a remarkable expansion and rigidity, while the monolayer on a substrate containing barium or calcium ions had no such properties.[9] Muramatsu and Sasaki observed that the thickness of the built-up film of stearic acid conditioned with aluminum salt solution, was remarkably increased compared with that without conditioning.[10] All these results lead us to the conclusion that the adsorption product or chemical compound between aluminum and stearic acid is composed of relatively large molecules of a complicated structure, which are also suitable for the explanation of the wetting power of aluminum ion. The complexity of the adsorption product may of course come from the marked co-ordination tendency exhibited by aluminum ion. From this point of view we may postulate further, that a marked co-ordination tendency of any metallic ion towards both water molecule and stearate

(7) N. Bjerrum, *Z. physik. Chem.*, **A 59**, 336, 581 (1907), **73**, 724 (1910), **110**, 656 (1924).

(8) V. R. Gray and A. E. Alexander, *J. Phys. & Colloid Chem.*, **53**, 26 (1949); E. Eigenberger and A. Eigenberger-Bittner, *Kolloid-Z.*, **91**, 287 (1940); Hi. Ikeda, K. Shiroyanagi and Ha. Ikeda, *Reports of The Scientific Research Institute*, **25**, 353 (1949); I. S. McRoberts and J. H. Schulman; *Proc. Roy. Soc.* (London), **A 200**, 136 (1950).

(9) T. Sasaki and R. Matuura, This Bulletin, **24**, 274 (1951). R. Matuura, This Bulletin **24**, 278 (1951)

(10) M. Muramatsu and T. Sasaki, This Bulletin, **25**, 21, 25 (1952).

radical favors the wettability of the treated surface. To ascertain this presumption, we examined the parallelism required to exist between the co-ordination tendency of metallic ion and wettability of stearic acid treated with the solution containing the same ions.

As the measure of co-ordination tendency or something closely related to this, the following factors are selected as shown in Table 2, namely free energy decrease of complex formation in aqueous solution, ionic potential,[11] ionization potential (1st ionization),[12] normal electrode potential,[13] and heat of hydration.[14] The value of free energy decrease of complex formation, $N/Z \cdot \log k + \log 55$ (Z, the co-ordination number of metallic ion, N, the number of ligands co-ordinated to central metallic ion,

$$\log k = \frac{1}{N} \log \frac{[MA_N]}{[M_{aq}]\,[A]^N},\ [MA_N], [M_{aq}] \text{ and } [A]$$

being the concentration of the complex, hydrated cation, and ligand respectively), which is proposed by Bjerrum,[15] is calculated for the case of stearate radical as ligand using the data for other ligand. As a whole, these five series are parallel to the series of the wetting power of metallic ions mentioned above (Table 2), though there are minor irregularities not completely explained yet. Among these the series of Bjerrum's free energy shows a good parallelism. In this case, it must be kept in mind that Bjerrum calculated the value for the complete exchange of aquo-molecule for other ligands, whereas in our case, we rather require the value for the exchange of the certain fraction of exchangeable aquo-molecule for stearate radical. The latter quantity may, however, be considered to be roughly parallel to the former.

Now, we should like to consider that cadmium, silver, and zinc ions belong to the second class because they have a rather large co-ordination tendency as can be expected from Table 2. The results of Muramatsu, Matuura and Sasaki[9][10] also confirm this view. It can be noted however that nickel, mercuric and lead ions, in spite of their marked co-ordination tendency for stearate and of rather large heat of hydration, not only showed no effect of promoting the wettability of stearic acid but also exhibited a further reduction, when compared with the case of untreated stearic acid. These facts together with those obtained by Sasaki and Matuura lead us to postulate that these three ions might form another group. The author will refer to this point in a paper which will follow. Apart from these exceptions, the effect of the second group ions is considered to come from the macro-molecular structure of their adsorption product formed on stearic acid surface as mentioned already.

Sonders and others[16] insisted that the polarizability of metallic ions played an important role in the wettability when they were adsorbed on the surface of glass or clay. But their idea does not explain the wetting phenomena observed in the author's experiment.

It is required further to explain the effect of reducing the wettability due to the third group ions such as barium or calcium. Here, contrary to the macro-molecular structure of aluminum soap, barium soap is known to be a simple compound composed of the linkage of principal valency only, similarly as in the case of stearic acid. Therefore, the surface of barium soap is probably non-wettable as in the case of stearic acid in the region of low pH. The non-wetting power of barium stearate at pH>10, being different from the wettable property of stearic acid, is explained by the consideration that barium-soap is more stable against surface dissociation than free stearic acid in alkaline region. The stability is probably caused by a stronger binding force of stearate radical to barium than to hydrogen.

Thus, the wetting or non-wetting effect of the ions towards the stearic acid surface is briefly explained by either macro or simple molecular structure of the adsorption product. For the support of this view, it is worth while to point out further the following facts. It is generally recognized that the wettability is profoundly affected by the orientation or overturning of the surface molecules.[3] According to this view, together with our opinion concerning wettability, it may be expected that aluminum salt treatment renders the surface layer of stearic acid more difficult to overturn than in the case of barium salt treatment. Certainly, an easiness of overturning contributes to some extent to the non-wetting properties of a surface treated by barium salt. Thus the overturn theory not only does not contradict the experimental results and the opinion mentioned above, but also supports the result of measurements on wettability of stearic acid built-up film, which was already reported briefly by Muramatsu and Sasaki,[10] and will be described by the present author in detail in a paper which will follow.

Summary

The effect of the solution of various metallic ions at varying pH upon the wettability of stearic acid surface has been studied. These ions are adsorbed by stearic acid surface in characteristic pH region and are classified into the following three groups, according to their effects on wettability.

(11) The values were calculated from those of ionic radii from W. L. Bragg, "Atomic Structure of Minerals", Cornel University Press, New York (1937).

(12) R. F. Bacher and S. Gaoudsmit, "Atomic Energy States" McGraw-Hill Book Co., Inc., New York and London (1932).

(13) M. de K. Thompson, "Theoretical and Applied Electrochemistry" The Macmillan Co., New York (1939).

(14) J. D. Bernal and R. H. Fowler, *J. Phys. Chem.*, **1**, 515 (1933).

(15) J. Bjerrum, *Chem. Rev.*, **46**, 381 (1950).

(16) L. R. Sonders, D. P. Enright and W. A. Weyl, *J. Applied Phys.*, **21**, 338 (1950).

(1) Wetting ions 1 (Formation of ionic adsoption compound (surface dissociation).) Na, K, and Rb.

(2) Wetting ions 2 (Formation of hydrated, macromolecular adsorption compound.) Al,Th,Fe, Cr,Co,Cu, Zn,Cd,Mn and Ag.

(3) Non-wetting ions (Formation of simple molecular non-dissociating compound of mere principal valency.) Ba, Sr, Ca, and Li.

The classification has been based upon the structural characteristics of the ions, especially the co-ordination tendency of the ions. The theory of overturning of molecules in surface layer is also one of the probable supports of these opinions.

The author wishes to express her gratitude to Prof. T. Sasaki for his kind advice and encouragement, and also to Miss. S. Miyazaki for her kind assistance throughout this study. The cost of this research has been defrayed by the Grant of the Ministry of Education given to Prof. Sasaki.

Department of Chemistry, Faculty of Science, Kyûshû University

Studies on the Conjugated Double Bond Systems. VIII. On the Electronic Structures of Furan, Pyrrole and Thiophen

By Saburo NAGAKURA and Toichiro HOSOYA

(Received January 21, 1952)

Introduction

Recently, remarkable advances have been made in the theoretical study on the electronic structures of unsaturated hydrocarbons containing conjugated double bonds. In particular, the electronic structures of benzene and other relatively simple molecules have been investigated in detail. Under these circumstances, therefore, the study on the electronic structure of hetero-cyclic compounds may be regarded not only as desirable from the stand-point of the theory of resonance, but also as necessary for the progress of the electronic theory of organic chemistry.

The first quantum mechanical treatment on hetero-cyclic compounds was made, probably, by Wheland and Pauling,[1] who used the molecular orbital method. It was, however, no more than merely making a guess at the π-electron distributions in the molecule which, apparently agreed with experimental facts on the condition that their assumed constant of electron affinity for the hetero-atom and of induced affinity for the adjacent atoms was suitable. Longuett-Higgins and Coulson[2] applied the same method to many hetero-cyclic compounds containing nitrogen, under some original assumptions about coulomb integrals. The method of Orgel *et al.*[3] which was applied to many hetero-cyclic molecules was essentially identical with that of Longuett-Higgins and Coulson. They calculated the values for dipole moment and compared them with the experimental results.

In the present paper, the molecular orbital method has been employed in the investigation of electronic structures of furan, pyrrole and thiophene under suitable assumptions about coulomb- and exchange-integrals. The results have been used for discussing resonance energies, dipole moments and near ultraviolet absorption spectra of these substances.

Outline of Method

In our treatment of furan, pyrrole and thiophene, we assume that they are all planar, and consider five $p\pi$ orbitals and six electrons, including an unshared pair on the hetero-atom. With the approximation of LCAO, the wave functions of molecular orbitals are as follows:

$$\Psi_j = C_{1j}\varphi_1 + C_{2j}\varphi_2 + C_{3j}\varphi_3 + C_{4j}\varphi_4 + C_{5j}\varphi_5 \quad (j=1,2,\ldots 5) \qquad (1)$$

(1) G. W. Wheland and L. Pauling, *J. Am. Chem. Soc.*, **57**, 2086 (1935).

(2) H. C. Longuett-Higgins and C. A. Coulson, *Trans. Faraday Soc.*, **43**, 87 (1947).

(3) L. E. Orgel, T. L. Cottrell, W. Dick and L. E. Sutton, *ibid.* **47**, 113 (1951).

where φ_1 is the $2p\pi$ or $3p\pi$ wave function of the hetero-atom, O, N or S, respectively, and $\varphi_2 \sim \varphi_5$ are the $2p\pi$ wave functions of the carbon atoms numbered as in Fig. 1. Assuming that φ_rs are all

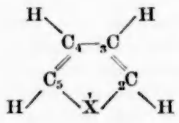

X=O, NH, S

Fig. 1.

normalized and mutually orthogonal, we reach to the following equation by the usual variation method:

$$\begin{vmatrix} H_{11}-E & H_{12} & H_{13} & H_{14} & H_{15} \\ H_{21} & H_{22}-E & H_{23} & H_{24} & H_{25} \\ H_{31} & H_{32} & H_{33}-E & H_{34} & H_{35} \\ H_{41} & H_{42} & H_{43} & H_{44}-E & H_{45} \\ H_{51} & H_{52} & H_{53} & H_{54} & H_{55}-E \end{vmatrix} = 0 \qquad (2)$$

where E is the energy of the molecular orbital Ψ_j, and $H_{rs}=\int \varphi_r H \varphi_s d\tau$.

Since these molecules belong to the symmetry group C_{2v}, the equation (2) is reduced to the following form

$$\begin{vmatrix} \alpha_1-E & \sqrt{2}\beta_1 & \sqrt{2}\beta_1' & 0 & 0 \\ \sqrt{2}\beta_1 & \alpha_2+\beta'_3-E & \beta_2+\beta_2' & 0 & 0 \\ \sqrt{2}\beta_1' & \beta_2+\beta_2' & \alpha_3+\beta'_3-E & 0 & 0 \\ 0 & 0 & 0 & \alpha_2-\beta_3'-E & \beta_2-\beta_2' \\ 0 & 0 & 0 & \beta_2-\beta_2' & \alpha_3-\beta_3-E \end{vmatrix} = 0 \qquad (3)$$

where following notations have been used, considering the symmetry of these molecules,

$$H_{11}=\alpha_1, \quad H_{22}=H_{55}=\alpha_2, \quad H_{33}=H_{44}=\alpha_3$$
$$H_{12}=H_{15}=\beta_1, \quad H_{23}=H_{45}=\beta_2, \quad H_{34}=\beta_3$$
$$H_{13}=H_{14}=\beta'_1, \quad H_{24}=H_{35}=\beta'_2, \quad H_{25}=\beta'_3.$$

That is, β_t $(t=1, 2, 3)$ is the exchange integral between adjacent atoms, and β_t' $(t=1, 2, 3)$ is the exchange integral between non-adjacent atoms. β_t' used to be neglected so far, but we will not neglect it, because in the penta-cyclic compounds, $|\beta_t'|$ is relatively large, owing to the smaller atomic distances compared with that of benzene. To make this point clear we have made calculations with and without neglecting β_t' in the case of furane and the results of two calculations have been compared with each other. (The method neglecting β_t' is named the first method, and the one including it, the second.)

These integrals are all represented with β[4], using the following approximations:

(a) the coulomb integral of the carbon atom in benzene is 4.1 β.[5]

(b) the coulomb integral of each atom is proportional to the electronegativity,[5] for which Pauling's values[6] have been adopted.

(c) the exchange integral is proportional to the overlap integral between two atoms.[7]

We have calculated the overlap integral with the aid of the table of Mulliken *et al.*[8] and the values of the atomic distances determined by Schomaker and Pauling.[9]

Under these assumptions, eigen values E_j $(j=1, 2, \ldots, 5$, numbered from the lowest level to the upper level) are evaluated and then C_{rj}s are determined for each value of E. With these values of C_{rj}s we can readily calculate the π-electron density q_r of r-atom by the following equation[10]

$$q_r = 2\sum_{j=1}^{3} C_{rj}^2$$

Now, it is possible to evaluate the formal charge of r-atom which is caused by π-electron migration from hetero- to carbon-atom. Owing to this formal charge, the correction term for the electronegativity and the overlap integral should be taken into consideration. We have obtained the correction for electronegativity according to Pauling,[10] and by the use of this corrected value the coulomb integral can be recalculated by the application of the above approximation (b). New values of overlap integrals are obtained from the tables of Mulliken *et al.*[8] and β_t's and β_t''s can be recalculated by the approximation (c). Using these values of the integrals, the equation (3) is resolved and q_rs are found.

These calculations are repeated several times until the final results are self-consistent.

Results and Discussion

In Table 1 are given our final values of energy integrals, energy levels and π-electron densities in the normal state.

Resonance Energy:—From the preceding results, we have calculated the resonance energy by the use of the following formula:

$$2(E_1+E_2+E_3)-2(\alpha_1+\alpha_2+\alpha_3+2\beta_2)$$

where α_1, α_2, α_3, and β_2 are the initial values of coulomb- and exchange integrals, *i. e.* the values

(4) β is the exchange integral between adjacent atoms of benzene.

(5) C. Sandorfy, *Bull. soc. chem. France*, (1949), 615.

(6) L. Pauling, "The Nature of the Chemical Bond," Cornell University Press, (1940) p. 64.

(7) G. W. Wheland, *J. Am. Chem. Soc.*, **64**, 900 (1942).

(8) R. S. Mulliken, C. A. Rieke, D. Orloff and H. Orloff, *J. Chem. Phys.*, **17**, 1248 (1949).

(9) V. Schomaker and L. Pauling, *J. Am. Chem. Soc.*, **61**, 1769 (1939).

(10) L. Pauling, "The Nature of the Chemical Bond" Cornell University Press, (1940) p. 65.

Table 1[a]

Values of Various Energy Integrals, Energy Levels and π-electron Densities.

	Furan (The First Method)	Furan (The Second Method)	Pyrrole (The Second Method)	Thiophene (The Second Method)
α_1	5.811	5.796	5.062	4.327
α_2	4.092	4.080	4.069	4.046
α_3	4.074	4.092	4.061	4.040
β_1	0.575	0.576	0.718	0.674
β_2	1.077	1.076	1.085	1.096
β_3	0.900	0.892	0.936	0.945
β_1'	—	0.086	0.116	0.147
β_2'	—	0.197	0.201	0.177
β_3'	—	0.193	0.204	0.130
E_1	6.304 (A_1)	6.515 (A_1)	6.429 (A_1)	6.221 (A_1)
E_2	5.383 (A_1)	5.364 (A_1)	4.876 (A_1)	4.512 (B_1)
E_3	4.804 (B_1)	4.488 (B_1)	4.453 (B_1)	4.360 (A_1)
E_4	3.190 (A_1)	3.174 (A_1)	3.026 (A_1)	2.908 (A_1)
E_5	2.462 (B_1)	2.599 (B_1)	2.536 (B_1)	2.499 (B_1)
q_1	1.869	1.896	1.745	1.578
q_2, q_5	1.011	1.036	1.060	1.100
q_3, q_4	1.055	1.016	1.068	1.111

a) In this Table, the energy values are represented in units of β.

obtained without the consideration of the resonance of π-electrons. The results are given in Table 2 together with the observed values[9] [11] which are obtained from the heat of combustion or hydrogenation. By a glance at the table, it is seen that the observed values themselves are different from each other. However, the following values may be regarded as the most probable: the resonance energy of thiophene, *i. e. ca.* 30 kcal./mol, and the difference between the resonance energy of furan and of pyrrole, *i. e. ca.* 8 kcal./mol, which was deduced by Schomaker andPauling[9] considering the resonance energies of many derivatives of furan and pyrrole. If these values are reliable, it is evident that the calculated values of these two quantities agree with the observed ones. In general, however, the calculated values are smaller than the observed, except in the case of the first method on furan. In addition, there is a serious difficulty in thiophene which requires a further discussion. It will be mentioned in the following section.

Dipole Moment:—The so called resonance moment which is caused by the migration of π-electron from the hetero-atom to the carbon atoms, *i. e.* μ_{mig}, can be calculated from the formal charges of the atoms and the atomic distances. The results are given in Table 3 together with the values which were determined by Schomaker and Pauling[9] using the observed values of dipole moments of these molecules and their tetrahydroderivatives. As for pyrrole, however, they stated that it seemed to be impossible to make a reliable estimate for resonance moments on account of uncertainty regarding the orientation of the N-H bond in pyrrole and pyrrolidine, and further that various methods of making the calculation gave values lying between 1.0 and 2.5 D, 1.5 D being the most probable value.

Table 2

Resonance Energy (kcal./mol)

		Furan	Pyrrole	Thiophene
Calculated Values[a]	1st Method	17.6	—	—
	2nd Method	11.6	20.0	26.2
Observed Values	Schomaker and Pauling[9]	23	31	(31)
	Wheland (from heat of combustion)[11]	24	24	29
	Wheland (from heat of hydrogenation)[11]	17.2	—	—

(*a*) It is assumed that β is equal to -20 kcal./mol

Table 3

μ_{mig} (D)

		Furan	Pyrrole	Thiophene
Calculated Values	1st Method	1.21	—	—
	2nd Method	0.62	1.33	2.50
Estimated Values by Schomaker and Pauling[9]		0.95	*ca.* 1.5	1.25

If, μ_{mig} of pyrrole is calculated by the rule of vector addition using the bond moments 1.3 and 0.4 D for N-H and N-C bond,[9] respectively and assuming that pyrrole is planar, it will be found that μ_{mig} is about 1.0 D. Anyhow, in the case of pyrrole, the calculated value may be considered to be reasonable. Though the calculated value for furan by the first method is larger and by the second is smaller than the value estimated by Schomaker and Pauling, the discrepancies are not serious. On the contrary, in the case of thiophene, the calculated value is very large compared with that estimated by them. This disagreement seems to be due to the fact that the non-bonding electrons of sulphur have been represented only by the $p\pi$ wave function in our calculation. Longuett-Higgins[12] treated this molecule theoretically using the hybridisation functions of $3p\pi$ and $3d$ wave functions as those of the non-bonding electrons of sulphur atom.

Bond Order:—The bond order between neighbouring atoms r and s is defined[13] as

$$p_{rs} = 2 \sum_j C_{rj} C_{sj}$$

(11) G. W. Wheland, "The Theory of Resonance" John Wiley and Sons, New York (1947), Chapter III.

(12) H. C. Longuett-Higgins and C. A. Coulson, *Trans. Farad. Soc.*, **43**, 83 (1947).

(13) C. A. Coulson, *Proc. Roy. Soc.* (London), **A 169**, 413 (1939).

where the summation is extended over all occupied molecular orbitals. Calculated bond orders of present molecules are given in Table 4.

Table 4

Calculated Values of Bond Orders

	Furan (The First Method)	Furan (The Second Method)	Pyrrole (The Second Method)	Thiophene (The Second Method)
p_{12}	0.30	0.26	0.41	0.50
p_{23}	0.87	0.91	0.85	0.79
p_{34}	0.45	0.38	0.45	0.52

The difference between p_{12}, p_{23} and p_4 in the same molecule tends to decrease in the order of furan, pyrrole and thiophene. The result seems to be in agreement with the order of aromaticity of these molecules.(14)

Transition Energy and Near Ultraviolet Absorption Spectrum:—When the transition energies are calculated assuming that the electronic transition from E_2 to E_3 corresponds to the absorption spectra of the longest wave length and $\beta=2.84$ e.V.,(15) it is found that they are 3.7, 4.0 and 4.1 e.V. in furan, pyrrole and thiophene, respectively. It is difficult to compare them with observed values, because we can not find reliable experimental data, but it seems that these values correspond to the absorption spectra,(16) 2650-2480 A. (4.6-4.9 e.V.), 2880-2540 A. (4.3-4.8 e.V.) and 2522-2246 A. (4.9-5.5 e.V.), respectively.

(14) The above mentioned view, however, is somewhat obscure owing to the following two reasons. Though it is reasonable to consider that p_{23} and p_{34} correspond to the strength of each bond, p_{12} does not do so, because as to the oxygen, nitrogen and sulphur atoms, which all have non-bonding electrons, the increase of the value of C means the decrease of bond formation character of these atoms. And as for thiophene, there is one more difficulty discussed in the preceding section.

Summary

Electronic structures of furan, pyrrole and thiophene were investigated by the use of the molecular orbital method. And values of energy levels, resonance energies, π-electron densities and bond orders were calculated. As the result of these calculations, it was found that non-bonding electrons of hetero-atoms migrate into carbon atoms and the degree of these electron migrations increases in the order of furan, pyrrole and thiophene.

The authors wish to express their sincere thanks to Prof. S. Mizushima and Prof. K. Higasi for their advice and encouragement throughout this research.

Institute of Science and Technology, and College of General Education, University of Tokyo, Meguro-ku Tokyo

(15) J. R. Platt, *J. Chem. Phys.*, **18**, 1168 (1950).
(16) H. Sponer and E. Teller, *Rev. Mod. Phys.*, **13**, 75 (1941).

Monolayers of Branched-Chain Fatty Acids I*

By Masami IZAWA

(Received February 18, 1952)

Branched-chain fatty acids have received much attention from biological points of view. Some of them are found in the normal cell of several kinds of bacteria, while some of them are strongly bactericidal. The bactericidal activity of a number of branched-chain fatty acids has been studied extensively by Adams and his coworkers,(1) and it has been stated that there is parallelism between the bactericidal activity and the surface activity of these acids. However, the exact mechanism of the bactericidal activity is still obscure.

A number of new branched-chain fatty acids have been synthesized at the Chemical Department, Institute for Infectious Diseases, Tokyo University, and their biological and chemical properties have been thoroughly investigated.(2)

* Part of this work was presented at the Meeting of the Chemical Society of Japan, held at Tokyo, Sept, 13 1947.

(1) W. M. Stanley and R. Adams, *J. Am. Chem. Soc.*, **54**, 1548 (1932).

(2) M. Asano, U. Kameta, T. Komai and I. Ishino, *Igakusoran (Japan)*, **1**, 41 (1945); M. Asano, U. Kameta and T. Wada, *J. Pharmaceut. Soc. Japan.*, **64**, 25 (1944); M. Asano and T. Yamakawa, *J. Pharmaceut. Soc. Japan*, **70**, 474 (1950); M. Asano, J. Ota and U. Ariyoshi, *Igakusoran (Japan)*, **1**, 42 (1945).

A detailed study of the monolayer behavior of these compounds may throw light on the mechanism of their action. In fact, it has been reported that there is a relation between the biological activity of alkyl substituted succinic acid half esters and the orientation of the molecules at air-water interface.[3] Unfortunately, at the present stage of our knowledge, it is not possible to correlate directly the surface properties of these acids with the biological activity. But, if we consider the surface behavior together with other properties of these acids, clearer understanding may be expected.

In this report, the measurements of force-area relations were made and the results were correlated with the structure and configuration of the molecules in the monolayer.

Techniques

The apparatus for measuring force-area curves was Langmuir-Adam type surface balance. It consisted of a nickel-plated brass trough and copper float with platinum ribbons. To avoid contamination, the whole surface of the trough, float system and glass barriers were heavily coated with solid paraffin in the usual manner, and they were rinsed with tap water about one hour before use.

The sample was dissolved with redistilled benzene and was spread on water by means of a micropipette. The volume of the micropipette was calibrated against the cross-sectional area of palmitic acid monolayer on distilled or acidic water substrates. The sensitivity of the torsion balance was 0.200 dyne per cm. per degree, and the surface pressure could be measured with the accuracy of ± 0.05 dyne/cm.

Since these compounds formed more stable films on acid substrates than on neutral or alkaline solutions, and since it was necessary to minimize the influence of heavy metal ions, experiments were made on 0.01 *N* hydrochloric acid solution.

Measurement was started at about one minute after spreading the material at zero pressure, and the time interval between adjacent points on the force-area curves was about thirty seconds. If the pressure changed rapidly with time owing to the hysteresis, it was read when no appreciable change was observed on the value within one minute. Generally, the coincidence between curves obtained by compression and expansion was relatively poor. Whether this is due to the instability of the monolayer or to the true hysteresis is uncertain. Each point on the curve was the mean of at least three independent measurements and was accurate within 3 per cent.

Materials

The branched-chain fatty acids used in this experiment were obtained from the Chemical Department, Institute for Infectious Diseases, Tokyo University, by courtesy of the late Prof. Asano. Palmitic acid was purchased from Dr. Theodor Schuchardt G. M. B. H. Chemische Fabrik, and was recrystallized from methanol. Its melting point was 62°C.

Results and Discussions

1. Trialkylacetic Acids.—Fig. 1 shows the force-area curves for two trialkylacetic acids with two long hydrocarbon chains at 20°C. These films are liquid-expanded, the limiting area of which is 75~80 A.^{2} per molecule, and are compressible to 60~65 A.^{2} The film of methylundecyldodecylacetic acid (I) collapses at about 7 dynes per cm., whereas monolayer of ethyldecyldodecylacetic acid (II) withstands higher pressures of 12~13 dynes. The reason for this difference may be due to the fact that while I is solid, II is liquid in

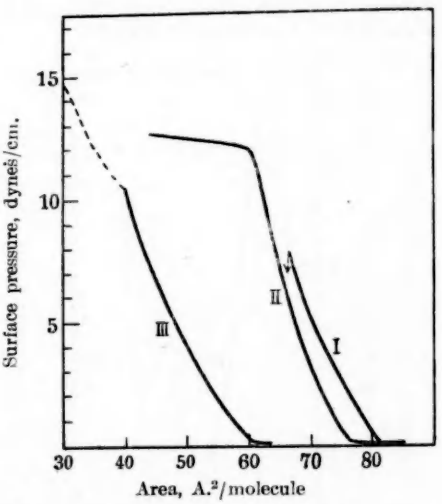

Fig. 1.—Force-area curves for methylundecyldodecylacetic acid (I) and ethyldecyldodecylacetic acid (II). Curve for phthioic acid (III) after Stenhagen is also shown in the figure. Substrate: 0.01 N HCl, 20°C.

(3) J. H. Schulman and W. McD. Armstrong, "Surface Chemistry", Interscience Publishers Inc., (1949), p. 263.

bulk state at room temperature. Below 60 A.^{2}, the curve of II shows a flat portion which indicates the existence of equilibrium between the monolayer and three-dimensional liquid drops on the substrate.

In Fig. 1, the curve for phthioic acid at 20°C (III), reported by Stenhagen,[4] is also shown. Phthioic acid is one of the normal constituents of tubercle bacillus with the formula $C_{26}H_{52}O_2$, isolated by Anderson,[5] and its molecular structure has been assumed to be a trialkylacetic acid, especially ethyldecyldodecylacetic acid (II), by Stenhagen[4] and Robinson.[6] Later, Polgar and Robinson[7] investigated the structure of the acid extensively and concluded that it was 3, 13, 19-trimethyltricosanoic acid. But the exact constitution still remains to be solved. It may be concluded at least from our results that phthioic acid is not identical with I or II.

2. β-Methylpalmitic Acid. — β-Methylpalmitic acid (IV) forms liquid-expanded film, whose limiting area is 63 A.^{2}, and compressible to about 30 A.^{2} as shown in Fig. 2.

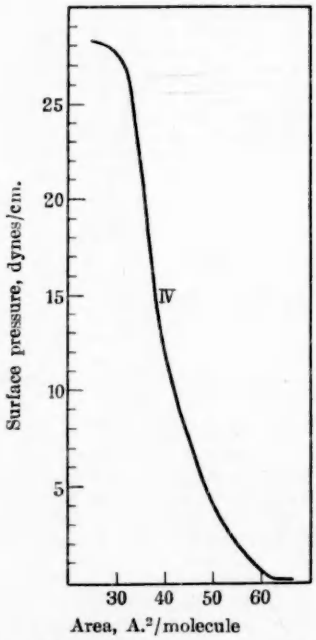

Fig. 2.—Force-area curve for β-methylpalmitic acid. Substrate: 0.01 N HCl, 25°C.

(4) E. Stenhagen and S. Ställberg, *J. Biol. Chem.*, **139**, 345 (1941).
(5) R. J. Anderson, *J. Biol. Chem.*, **97**, 639 (1932).
(6) R. Robinson, *J. Chem. Soc.* (*London*), 505 (1940).
(7) N. Polgar and R. Robinson, *J. Chem. Soc.*, (*London*), 389 (1945).

3. β, β', β'' - Trialkylpropionic Acids Having Only One Long Chain.—Fig. 3 shows the curves for β-methyl-β'-ethyltridecanoic acid (V) and β-methyl-β'-ethylpentadecanoic acid (VI). Both films are liquid-expanded and compressible to about 35 A.^{2}

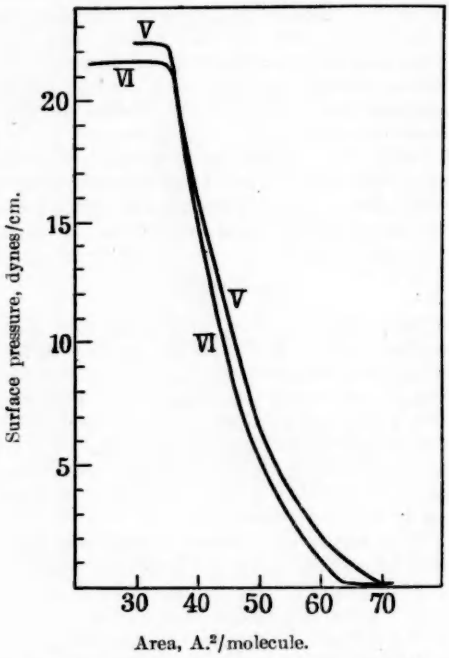

Fig. 3.—Force-area curves for β-methyl-β'-ethyltridecanoic acid (V) and β-methyl-β'-ethylpentadecanoic acid (VI). Substrate: 0.01 N HCl, 20°C.

4. Diheptylacetic Acid, β, β'-Diheptylpropionic Acid and γ, γ'-Diheptylbutyric Acid.—The effect of the position of diheptylmethyl group [$(C_7H_{15})_2$—CH—] with respect to the carboxyl group of the acids was examined (VII, VIII and IX). As shown in Fig. 4, the limiting areas become smaller and the force-area curves steeper as the position of the substitution is separated from the carboxyl group. These monolayers collapse at about 50 A.^{2}

5. α-Ethyl Fatty Acids.—α-Ethylnonylic, α-ethylpalmitic (X), α-ethylstearic (XI) and α-ethylarachidic acids(XII) were examined (Fig. 5). α-Ethylnonylic acid does not form a stable monolayer, probably because of the high solubility of the compound. The monolayer of X is liquid-expanded, whereas monolayers of

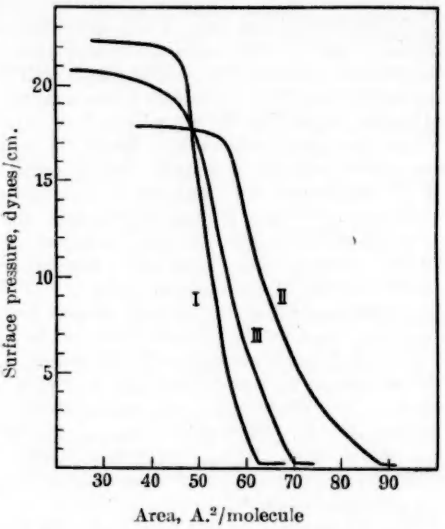

Fig. 4.—Force-area curves for diheptylacetic acid (VII), β,β'-diheptylpropionic acid (VIII) and γ,γ'-diheptylbutyric acid (IX). Substrate: 0.01 N HCl, 12°C.

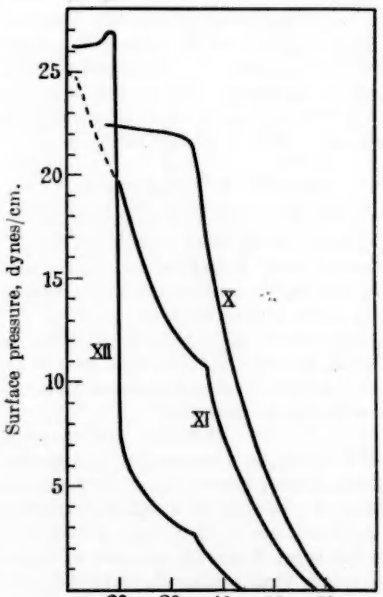

Fig. 5.—Force-area curves for α-ethylpalmitic acid (X), α-ethylstearic acid (XI) and α-ethylarachidic acid (XII). Substrate: 0.01 N HCl. 20°C.

XI and XII show a transition from liquid-expanded to condensed states. The latter two substances show a marked temperature effect as shown in Fig. 6.

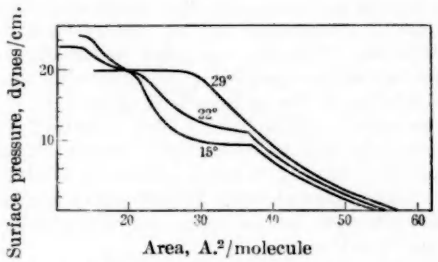

Fig. 6.—Temperature effect on the force-area curve for α-ethylstearic acid. Substrate: 0.01 N HCl.

6. α-Methyl-and α-Propylmyristic Acids.—The effect of α-substituted groups of myristic acid on the force-area curve is shown in Fig. 7 (XIII and XV). As the side chain becomes longer, the limiting area is larger and the equilibrium pressure is lower. The curve for

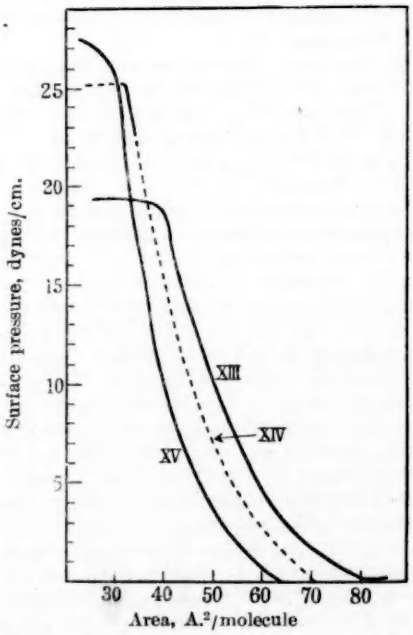

Fig. 7.—Force-area curves for α-propyl- (XIII) and α-methyl- (XV) myristic acids. XIV indicates the curve for α-methylpentadecylic acid after Stenhagen. Substrate: 0.01 N HCl, 20°C (XIV and XV) and 18°C (XIV).

α-ethylpalmitic acid (XIV) reported by Stenhagen[8] falls between these curves as indicated by a dotted line in the figure.

The monolayers reported above are all of liquid-expanded type. In 1933, Langmuir proposed a theory for the liquid-expanded state.[9] According to his theory, liquid-expanded films are composed essentially of two layers, the upper being an insoluble oil layer consisting of the hydrocarbon portion of the molecules, and the lower a layer of hydrophilic groups of the molecules which exists at the interface of oil and water phases and which acts as a gaseous film. The force-area relation for this state can be represented by the following equation:

$$(F-F_0)(a-a_0)=kT,$$

where F: surface pressure,
a: area per molecule,
k: Boltzmann constant,
T: absolute temperature,
F_0: a constant relating to the spreading coefficient of an assumed oil layer consisting of the hydrocarbon portion of the molecules in the film.
a_0: a constant relating to the actual cross-sectional area of one molecule on the surface.

The force-area relations for the branched-chain fatty acids examined fit this equation well. This theory has been opposed by several authors,[10] but essentially it will be right, as was pointed out by Adam,[11] irrespective of minute difficulties.

Since two constants, F_0 and a_0, in the equation may be considered as relating to the structure of molecules in the monolayer, it may be reasonable for these constants as well as the limiting area or the area at collapse to be characteristic to the molecular structure. The values of F_0 and a_0 calculated from the experimental curves are listed in Table 1. From the table, it can be seen clearly that there are close relations between the structure of the molecules and the values of F_0 and a_0. These relations are summarized as follows:

i) When two long hydrocarbon chains exist in the molecule, constant a_0 becomes about 40 A.^{2} This is shown in series 1 (except phthioic acid) and 4. Especially in series 4, the a_0 value of the three acids is determined by the diheptylmethyl radical $[(C_7H_{15})_2-CH-]$ and is about 40 A.^{2}, which is twice the value of the cross-sectional area of one hydrocarbon chain, in spite of the quite different shapes of the force-area curves. Shereshefsky and Wall[12] reported that dilauryl maleate forms a liquid-expanded film, the a_0 of which is 39.0 A.^{2} Hence, two long hydrocarbon chains of these compounds consist of a hydrophobic portion of the molecules, and stand side by side in the monolayer. It may be mentioned here that a_0 is practically equal to the "area at collapse", because the force-area curves are nearly vertical at the collapse point.

ii) The a_0 of the films which possess only one long chain in the molecule is about 20 A.^{2} Series 2, 3, 5 and 6 correspond to this structure. But as shown in series 6, the longer the side chain is, the larger is a_0, and, presumably, the smaller is $-F_0$. The value of the a_0 of tuberculostearic acid $[C_8H_{17}-CH(CH_3)-(CH_2)_8-COOH]$ is also about 20 A.^{2} if calculated from the published data.[4]

iii) An increase in the length of the long chain results in the increase in $-F_0$ value, but a_0 seems to be independent of it. Calculations were made on two other acids of similar structure (α-ethyltridecanoic and α-ethylpentadecanoic acids) based on the curves reported by Stenhagen,[4] and they are included in Table 1. From these figures, the influence of the chain length on the F_0 value will be evident. It has been reported by Langmuir[9] that, in normal chain fatty acids, there is a linear relation between the number of carbon atoms of the acids and F_0 as follows:

$$F_0=4.8-1.3n,$$

where n is the number of carbon atoms of the alkyl portion of the acid ($C_nH_{(2n+1)}COOH$). It can be concluded that there is a similar relation in the branched-chain fatty acids examined here at least qualitatively.

iv) As the branching shifts from the position of α, through β, to γ, with respect to the carboxyl group, $-F_0$ increases in this order. This is shown in series 4.

v) As the side chain in the α position becomes longer, a_0 increases and, apparently, $-F_0$ diminishes. Series 6 shows this regularity.

These relations are of a qualitative nature, and hold as long as films are of the liquid-expanded type. Using these relations, it should be expected that branched-chain fatty acids or other compounds newly synthesized or extracted from natural products can be identified, and in favorable cases, information about the

(8) E. Stenhagen, *Trans. Faraday Soc.*, **36**, 597 (1940).
(9) I. Langmuir, *J. Chem. Phys.*, **1**, 755 (1933).
(10) For example, W. D. Harkins and E. Boyd, *J. Phys. Chem.*, **45**, 20 (1941).
(11) N. f. Adam, "The Physics and Chemistry of Surfaces", Oxford University Press, (1938), p. 67.
(12) J. L. Shereshefsky and A. A. Wall, *J. Am. Chem. Soc.*, **66**, 1072 (1944)

Table 1

The Values of F_0 and a_0 in the Langmuir Equation for Liquid-Expanded Films of Branched-Chain Fatty Acids

Series No.	Sample No.	Formula	Temperature	a_0	$-F_0$
1	I	$\begin{matrix}CH_3\\C_{11}H_{23}\\C_{12}H_{25}\end{matrix}\!\!>\!CHCOOH$	20°	45.0	11.8
	II	$\begin{matrix}C_2H_5\\C_{10}H_{21}\\C_{12}H_{25}\end{matrix}\!\!>\!CHCOOH$	20°	45.5	12.9
	III†	Phthioic acid	20°	20.	9.8
2	IV	$\begin{matrix}CH_3\\C_{13}H_{27}\end{matrix}\!\!>\!CHCH_2COOH$	25°	22.0	10.4
3	V	$\begin{matrix}CH_3\\C_7H_5\\C_{10}H_{21}\end{matrix}\!\!>\!C\ CH_2\ COOH$	20°	24.9	9.1
	VI	$\begin{matrix}CH_3\\C_2H_5\\C_{12}H_{25}\end{matrix}\!\!>\!C\ CH_2\ COOH$	20°	24.3	10.4
4	VII	$\begin{matrix}C_7H_{15}\\C_7H_{15}\end{matrix}\!\!>\!CHCOOH$	12°	42.0	8.6
	VIII	$\begin{matrix}C_7H_{15}\\C_7H_{15}\end{matrix}\!\!>\!CH\ CH_2\ COOH$	12°	38.5	12.5
	IX	$\begin{matrix}C_7H_{15}\\C_7H_{15}\end{matrix}\!\!>\!CH\ CH_2CH_2COOH$	12°	37.2	15.8
5	†	$\begin{matrix}C_2H_5\\C_{11}H_{23}\end{matrix}\!\!>\!CHCOOH$	18°	22	6.9
	X	$\begin{matrix}C_2H_5\\C_{14}H_{29}\end{matrix}\!\!>\!CHCOOH$	20°	22.2	9.9
	XI	$\begin{matrix}C_2H_5\\C_{16}H_{33}\end{matrix}\!\!>\!CHCOOH$	20°	20.2	10.1
	XII††	$\begin{matrix}C_2H_5\\C_{15}H_{37}\end{matrix}\!\!>\!CHCOOH$	20°	(13)	(11.9)
6	XIII	$\begin{matrix}C_7H_7\\C_{12}H_{25}\end{matrix}\!\!>\!CHCOOH$	20°	26.3	7.5
	XIV†	$\begin{matrix}C_2H_5\\C_{13}H_{27}\end{matrix}\!\!>\!CHCOOH$	18°	22	7.6
	XV	$\begin{matrix}CH_3\\C_{12}H_{25}\end{matrix}\!\!>\!CH\ COOH$	20°	19.1	9.8

† F_0 and a_0 were calculated from the $F-a$ curves reported by Stenhagen *et al.*[4]

†† The values of F_0 and a_0 are uncertain because the film shows a transition from liquid-expanded to condensed states.

structure of them may be obtained.

Summary

(1) Force-area relations for the monolayers of a number of branched-chain fatty acids have been investigated.

(2) These monolayers are of the liquid-expanded type, on acidic substrates, and force-area curves fit the Langmuir equation well.

(3) Constants F_0 and a_0 in the Langmuir equation have been calculated from the curves. It has been shown that there is a definite regularity between these constants and the structure of the molecules in the films.

(4) It was revealed that the structure of phthioic acid is not of the trialkylacetic acid type as postulated by Stenhagen and Robinson.

This work was started at the Department of Chemistry, Faculty of Science, Tokyo University under the direction of Prof. Sameshima. The author wishes to express his sincere appreciation to Prof. Sameshima for his kind direction, and also to Dr. Akamatsu and Dr. Tachibana of Tokyo University, and Dr. Umezawa of the National Institute of Health for their advice in the present study. He is also greatly indebted to the late Prof. Asano for a number of samples of branched-chain fatty acids.

National Institute of Health, Tokyo

The Crystal Structure of Trinitrotriammine-cobalt (III), $[Co(NH_3)_3(NO_2)_3]$

By Yoshimichi TANITO, Yoshihiko SAITO and Hisao KUROYA

(Received December 19, 1951)

Introduction

According to Y. Shibata and R. Tsuchida,[1] the third absorption bands of co-ordinated compounds in aqueous solutions may be attributable to a pair or pairs of negative radicals co-ordinated in *trans*-positions and, from this point of view and because of the existence of the third absorption band at 120.4×10^{13} sec^{-1} ($\lambda=2492$ A.) with $\log\varepsilon=3.81$, it has been postulated that, to the trinitrotriammine-cobalt (III), $[Co(NH_3)_3(NO_2)_3]$, a *cis-trans*-configuration, instead of a *cis-cis* form, should be assigned (Fig. 1).

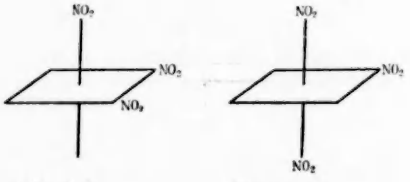

Cis-cis form *Cis-trans* form

Fig. 1.—Two possible forms of trinitrotriammine-cobalt (III).

In order to verify the above-mentioned conclusion by determining directly the configuration of the complex molecule, we have attempted to investigate the crystal structure of this compound.

Material

Trinitrotriammine-cobalt (III) was prepared by the method of Jörgensen.[2] Recrystallization from water containing a small amount of acetic acid yielded thin tabular crystals. The crystals belonging to the orthorhombic bisphenoidal class, are usually platy in habit with (010) extended.

According to Jaeger[3] the axial ratios are:

$$a:b:c=0.8682:1:0.6020\ ;$$

and the density is 1.992 g./cc. at 25°C.

Experimental

The X-ray work was carried out with Fe K_α radiation ($\lambda=1.937$ A.)

The crystals selected for the present study were $1\times1\times0.1$ mm. in effective dimensions. Only very thin platy crystals were available. Oscillation photographs about [100] and [001] gave the dimensions:

$$a=10.20\text{ A.},\ b=11.77\text{ A. and }c=6.99\text{ A.},$$

with the axial ratios

$$a:b:c=0.867:1:0.594$$

in agreement with the values obtained morphologically.

The space group is $D_2^4-P2_12_12_1$. There are four molecules in the unit cell, the calculated density being 1.972 g./cc. All the atoms are in the general positions: xyz; $1/2+x, 1/2-y, -z$; $1/2-x, 1/2+y, 1/2-z$; $-x, -y, 1/2+z$.

The reflections were estimated visually by comparison with a time calibrated scale of exposures, and they were converted into structure amplitudes by applying the appropriate correction factors, as shown in Fig. 2.

Analysis

At the outset of the analysis the following characteristics of intensity distribution were found:

(hkl); $h+l=2n$: strong
$(hk0)$; $h=2n$: strong
$(0kl)$; $k=2n$, $l=2n$: strong
and $(h0l)$; $h+l=2n$: strong.

This may indicate that the cobalt atoms are at $(x, 1/4, 1/4)$ etc., the arrangement of cobalt atoms alone thus having the symmetry D_{2h}^7-Bbmm. This was confirmed by synthesizing Patterson projections $P(xy)$ and $P(yz)$. These lead us to fix the positions of the cobalt atoms at 0.0686, 0.2500, 0.2500, etc.

Preliminary Fourier projections of electron density upon (001) and (100) were synthesized using $F(hk0)$'s with h even and $F(0kl)$'s with k, l

(1) Y. Shibata, *J. Chem. Soc. Japan*, **36**, 1243 (1915); R. Tsuchida, *J. Chem. Soc. Japan*, **59**, 586 (1938).
(2) S. M. Jörgensen, *Z. anorg. Ch.*, **17**, 463 (1898).
(3) F. M. Jaeger, *Z. Krist.*, **39**, 568 (1904).

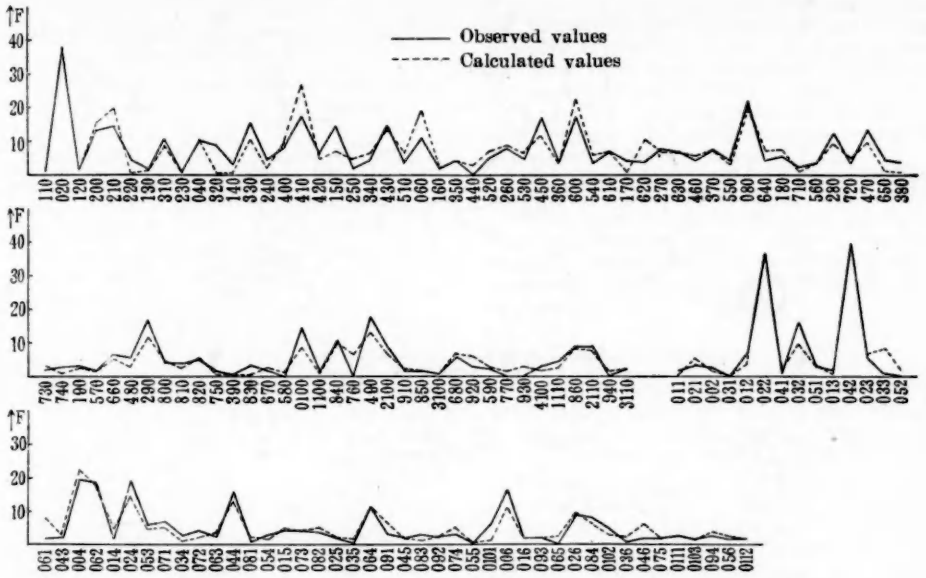

Fig. 2.—Observed and calculated F-values for trinitrotriammine-cobalt (III).

all even respectively, the signs of which were calculated from the parameter values of cobalt. From these projections we could assign approximate parameters for nitrogen atoms which form a distorted octahedron around each cobalt atom. These were in good accord with the conclusion drawn from Patterson projections $P(xy)$ and $P(yz)$. However, from the Fourier maps so obtained we could not locate the oxygen atoms unequivocally and we tried to determine the positions of these by trial and error. Bond angles and distances usual in nitro-compounds were used to locate oxygen atoms. Since the structure amplitudes $F(hk0)$ and $(F(0kl)$ could be accounted for only by one of the models having the *cis-trans* configuration, we regarded it as an approximate structure of trinitrotriammine cobalt (III) and started to determine the atomic parameters by successive approximations. The final parameters are listed in Table 1.

Table 1

Parameters of atoms in trinitrotriammine-cobalt (III)

	x/a	y/b	z/c
Co	0.0686	0.2500	0.2500
N(1)	−0.116	0.210	0.227
N(2)	0.020	0.360	0.450
N(3)	0.118	0.140	0.050
$NH_3(1)$	0.255	0.288	0.273
$NH_3(2)$	0.049	0.366	0.046
$NH_3(3)$	0.088	0.134	0.455
O(1)	−0.139	0.119	0.143
O(2)	−0.199	0.275	0.300
O(3)	0.135	0.393	0.472
O(4)	−0.068	0.401	0.558
O(5)	0.240	0.153	0.072
O(6)	0.076	0.054	−0.036

The values of $F(hk0)$ and $F(0kl)$ calculated from the parameter values in Table 1 are generally in good agreement with the observed values as shown in Fig. 2. In the calculation of the structure factors the atomic scattering curves in Internationale Tabellen (1935) were employed and corrected for temperature according to the Debye-Waller formula, the constant B being given the value 2.50×10^{-16} cm^2. For nitrogen belonging to the NH_3 group an appropriate correction,[4] due to the embedded hydrogen atoms, was made. A correction[5] for the anomalous dispersion for the Co atom ($\Delta f=2.2$) was also taken into account.

Description of the structure

The structure projected on the plane (001) is shown in Fig. 3 and the Fourier diagram in Fig. 4.

The cobalt atom occupies a general position. The arrangement of the cobalt atoms themselves has the symmetry D_{2h}^{7}—*Bbmm*. The proper symmetry of a cobalt atom is C_1—1 and this is surrounded by three nitrogen atoms of nitro-groups and three ammonia molecules, which form

(4) T. Watanabé, M. Atoji and C. Okazaki, *Acta Cryst.*, **3**, 405 (1950).

(5) H. Hönl, *Ann. Phys. Lpz.*, **18**, 625 (1935); R. W. James, "The Optical Principles of the Diffraction of X-rays" p. 609, G. Bell and Son, London, (1950).

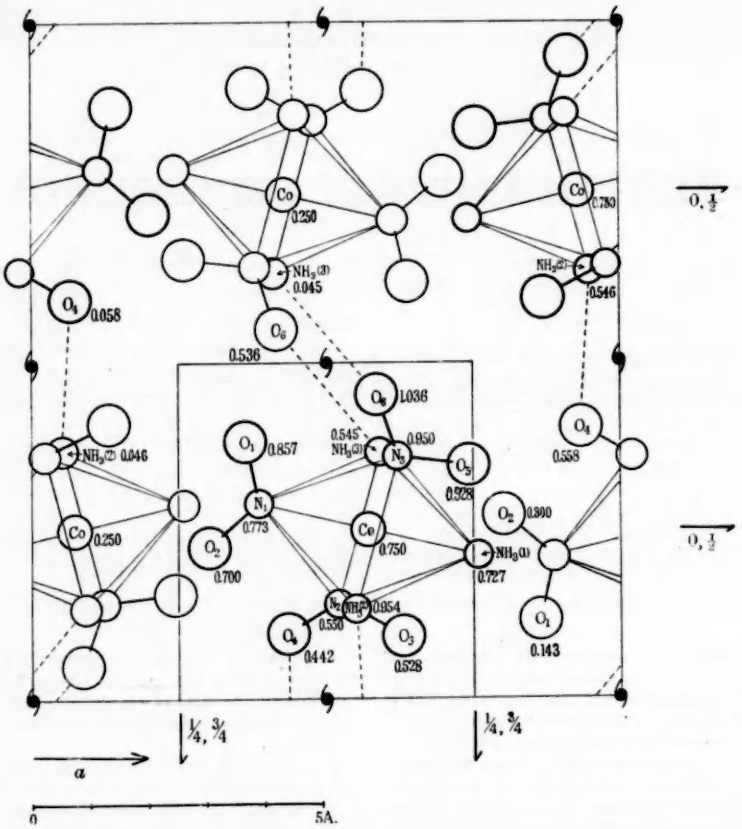

Fig. 3.—Projection of the structure upon (001) for trinitrotriammine-cobalt (III). Numbers give the height of atoms from (001) as fractions of the translation. N—H...O bonds are shown by dotted lines. The part of the cell corresponding to Fig. 4 is indicated.

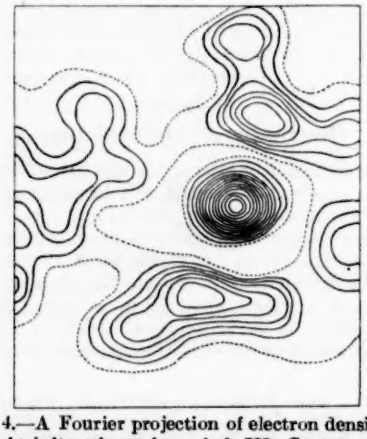

Fig. 4.—A Fourier projection of electron density of trinitrotriammine-cobalt(III). Contours at intervals of 2 e. A^{-2}., the first being broken.

a slightly distorted octahedron around the cobalt atom. Two of the nitro-groups are co-ordinated to a cobalt atom in *trans*-positions with respect to each other.

The interatomic distances as well as interbond angles are listed in Table 2.

Owing to the complexity of this crystal structure, involving the determination of 39 parameters and the overlapping of atomic peaks in both of the Fourier projections of electron density $\rho(xy)$ and $\rho(yz)$ it was not possible to determine the interatomic distances and interbond angles very accurately. The shape and size of the nitro-groups (N-O=1.25 A., $\angle$ONO=120°) may be compared with the values (N-O=1.25 A.. $\angle$ONO=112°) for the Erdmann's salt,(6) or with the values recently obtained for aromatic nitro-compounds.(7)

(6) A. F. Wells, *Z. Krist.*, **94**, 74 (1935).
(7) For example, F. J. Llewellyn, *J. Chem. Soc.*, **1947**, 884.

Table 2

Interatomic distances and angles in trinitrotriammine-cobalt (III).

Within a complex radical			Between neighboring molecules		
		A.			A.
Co	N(1)	1.96	$NH_3(2)$	O(4)	2.74
	N(2)	1.97	$NH_3(3)$	O(6)	2.78
	N(3)	1.97	$NH_3(1)$	O(1)	3.29
Co	$NH_3(1)$	1.97	$NH_3(1)$	O(2)	3.10
	$NH_3(2)$	1.98	O(1)	O(6)	3.10
	$NH_3(3)$	1.99	O(2)	O(5)	2.76
N(1)	O(1)	1.24			
	O(2)	1.25			
	∠ONO	127°			
N(2)	O(3)	1.25			
	O(4)	1.27			
	∠ONO	119°			
N(3)	O(5)	1.27			
	O(6)	1.25			
	∠ONO	121°			
O(1)	O(6)	2.65			
O(2)	O(4)	2.69			
$NH_3(1)$	O(3)	2.23			
	O(5)	2.13			

The closest approach of the molecules is between O atom of NO_2 group of one molecule and NH_3 of another. It seems likely that the binding forces between the molecules are mainly due to the N-H...O bonds between ammonia and nitro-groups. This N-H...O bonds are evidenced by characteristic short NH_3-O distances (2.75 A., 2.80 A.). They are shown in Fig. 3 by dotted lines. Somewhat analogous hydrogen bridges have been recently reported in the case of ammonium tetrametaphosphate.[8] Such bridges of length 2.8 A. have also been reported in several other cases.

By these NH...O bonds the complex molecules form a spacial network parallel to the plane (010). The NH_3...O distances between the molecules in the adjacent (010) layers (3.10 A., 3.29 A.) are longer by far than those between the molecules in the (010) layers. This fact may suggest that the interactions which are responsible for uniting molecules in the (010) planes would be greater than those which exert between the molecules of adjacent (010) layers. It is to be noted here that the shorter N-H...O bonds are formed between the nitro-groups in *trans*-positions and the ammonia groups also in *trans*-coordination.

Unlike other complex salts consisting of neutral molecules, trinitrotriammine-cobalt (III) is fairly soluble in water (0.177 g. in 100 parts of water at 16.5°C.[9]) This fact may be related to the presence of hydrogen bonds between molecules in crystals and also between these molecules and water in solution.

Summary

The crystal structure of trinitrotriammine-cobalt (III) prepared accoding to the method of Jörgensen has been studied by X-rays, using rotation methods (Fe K_α, λ=1.937 A.). This structure belongs to the orthorhombic system and the dimensions of the unit cell which contains four molecules of $[Co(NH_3)_3(NO_2)_3]$ are a=10.20 A., b=11.77 A., and c=6.99 A. The space group is $D_2^4-P2_12_12_1$. The cobalt atom is surrounded by six nitrogen atoms approximately in octahedral coordination. The shape and size of the nitro-groups are like those in $Ag[Co(NH_3)_2(NO_2)_4]$. Two of the nitro-groups are found to be (coordinated to) the cobalt atom in the *trans*-positions with respect to each other in conformity with the conclusion drawn from spectroscopic investigations.

The authors express their hearty thanks to Profs. I. Nitta and R. Tsuchida of the Osaka University for their kind advice and encouragement in the course of this study. Part of the cost of this study has been defrayed by a Grant of the Ministry of Education, to which the authors' thanks are due.

Institute of Polytechnics, Osaka City University, Osaka

(8) C. Romers, J. A. A. Ketelaar and C. H. MacGillavry, *Acta Cryst.*, **4**, 114 (1951).

(9) A. Werner, P. Larish and F. Ephraim., *Ber.*, **56**, 1532, (1923).

The Crystal Structure of Alpha-amino Isobutyric Acid*

By Sakutaro HIROKAWA, Shunsuke KURIBAYASHI and Isamu NITTA

(Received January 9, 1952)

Introduction

Since the war, crystal structures of some amino acids have been determined by several authors[1),(2),(3),(4)] using the three-dimensional Fourier method. These works have revised several points of older knowledge; for example, the value of C—N distance has now turned out to be nearly equal to the sum of covalent radii of carbon and nitrogen atoms. Still it is desirable to collect more X-ray data extended to other amino acids in order to study the nature of chemical bonds as well as protein structure. Thus the present authors have carried out the investigation on the crystal structure of α-amino isobutyric acid, of which an account will be given below.

Crystallographic and Other Data

Alpha-amino isobutyric acid $(CH_3)_2C(NH_2)COOH$ was for the first time found by T. Yabuta[5] in 1938 in the decomposition products of a protein. The melting point of this new substance is 319~320°C. and it sublimes already fairly below the melting point like many other amino acids. The reaction of this substance with thymol-hypobromite is shown to be positive.

Single crystals used in this investigation were prepared from aqueous solution by slow evaporation. These show monoclinic symmetry, and cleavage parallel to (110) is very perfect and that cleavage parallel to (001) is fairly perfect. Specimens were cut into cylindrical shape being not more than 0.05 mm. in diameter. From the oscillation photographs of a-, b- and c-axes respectively, the unit cell of this crystal was determined to be of the following dimensions; $a=10.59\pm0.04$ kx, $b=8.97\pm0.01$ kx, $c=11.34\pm0.03$ kx and $\beta=94\pm0.5°$, the number of molecules in this unit being calculated to be eight from the density $\rho=1.27_5$ measured by the flotation method. The determined space group is $C^6_{2h}-C2/c$.

Determination of the Structure

The eight molecules in the unit cell should be arranged so that every set of eight atoms all occupy the eight-fold general positions of $C2/c$. The Patterson and Harker series were synthesized along a-, b- and c-axes, of which $P(x, y)$, $P(y, z)$ and $H(x, 1/2, z)$ were especially useful to find the atomic parameters. These are shown in Figs. 1, 2 and 3.

Using the results of the trial and error

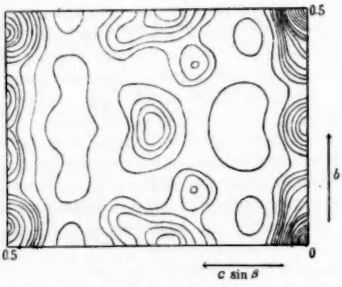

Fig. 1.—$P(y, z)$. The contour lines are drawn at equal intervals of an arbitrary scale.

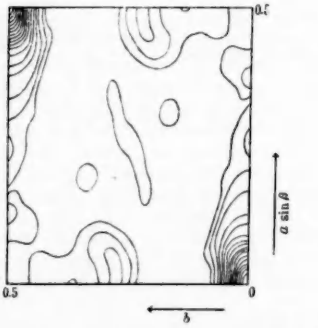

Fig. 2.—$P(x, y)$. The contour lines are drawn at equal intervals of an arbitrary scale.

* A preliminary study of this problem was reported at the anual Meeting of the Chemical Society of Japan in April, 1950.

(1) E. W. Hughes and W. T. Moor, *J. Am. Chem. Soc.*, **71**, 2618 (1949).

(2) J. Donohue, *J. Am. Chem. Soc.*, **72** 949 (1950)

(3) G. B. Carpenter and J. Donohue, *J. Am. Chem. Soc.*, **72**, 2315 (1950).

(4) D. Shoemaker, J. Donohue, V. Schomaker and R. B. Corey, *J. Am. Chem. Soc.*, **72**, 2328 (1950).

(5) T. Yabuta, *Gakujyutsu Kyokai (Japanese Scientific Association) Ho*, **13**, 80 (1938).

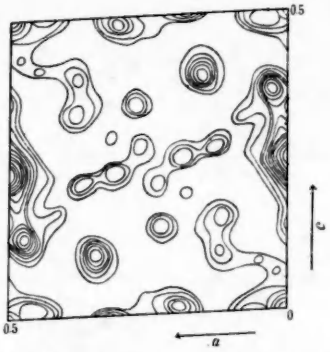

Fig. 3.—H $(x, 1/2, z)$. The contour lines are drawn at equal intervals of an arbitrary scale.

method, the two-dimensional Fourier series were synthesized along the three principal axes. As the resolution of the obtained projections for the whole unit cell was rather poor, the part-cell projections were prepared. However, in these projections the atoms were not yet sufficiently resolved. Thus we proceeded to the three-dimensional Fourier analysis, which was done by the method of the Beevers-Lipson strips. The result is shown in Fig. 4.

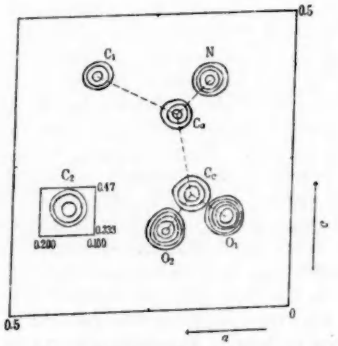

Fig. 4.—Composite drawing of electron density which were made from a section of $\rho(x, y, z)$ at several values of y. The contour lines are drawn at equal intervals of an arbitrary scale.

The refined locations of peaks were calculated by the method proposed by G. B. Carpenter and J. Donohue[3] in the paper on *N*-acetylglycine. Final parameter values obtained are listed in Table 1. Another table of comparison between observed and calculated *F*-values is omitted because of scarcity of space. Copies of this table will be available if required. In calculting structure factors a temperature factor with B=2.25 A.^{2} was used. For the accuracy of determination expressed in the usual way as

$$\Sigma(|F_{obs.}| - |F_{calc.}|)/\Sigma|F_{obs.}|$$

a figure of 0.199 was obtained for 1110 (hkl) reflections. It is to be added that this determination neglects the contributions of the hydrogen atoms.

Table 1

Parameter Values of Atoms

	N	C_c	C_α	C_1	C_2	O_1	O_2
x	0.154	0.178	0.212	0.355	0.148	0.112	0.224
y	0.100	−0.025	−0.031	−0.027	−0.167	0.083	−0.121
z	0.388	0.199	0.331	0.365	0.382	0.159	0.138

Discussion of the Structure

The determined atomic configuration and dimensions of the α-amino isobutyric acid molecule in the crystal are shown in Fig. 5. as well as in Table 2.

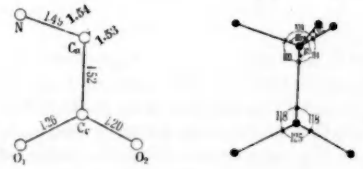

Fig. 5.—The molecule of the α-amino isobutyric acid, showing interatomic distances and bond angles. The hydrogen atoms are not drawn.

Table 2

Interatomic Distances and Bond Angles

Distances kx	Angles
$O_1-C_c=1.26$	$O_1-C_c-O_2=125.3°$
$O_2-C_c=1.20$	$O_1-C_c-C_\alpha=117.9°$
$C_c-C_\alpha=1.52$	$O_2-C_c-C_\alpha=117.7°$
$C_\alpha-N=1.49$	$C_c-C_\alpha-N=108.8°$
$C_\alpha-C_1=1.53$	$C_c-C_\alpha-C_1=114.0°$
$C_\alpha-C_2=1.54$	$C_c-C_\alpha-C_2=108.7°$
	$N-C_\alpha-C_1=107.5°$
	$N-C_\alpha-C_2=104.9°$
	$C_1-C_\alpha-C_2=112.2°$

The two C_α—C (methyl) distances and the C_α—N distance were found to be 1.53, 1.54 and 1.49 kx, respectively, in agreement with the sum of the covalent radii of Pauling. Among the bond angles of carbon atoms which are mostly nearly equal to the standard tetrahedral angle, there are observed some appreciable

deviations, for example, $C_c-C_\alpha-C_1=114.0°$ and $N-C_\alpha-C_2=104.9°$. As for the structure of the carboxylic group it was found that the bond distances $C-O_1$ and $C-O_2$ are somewhat

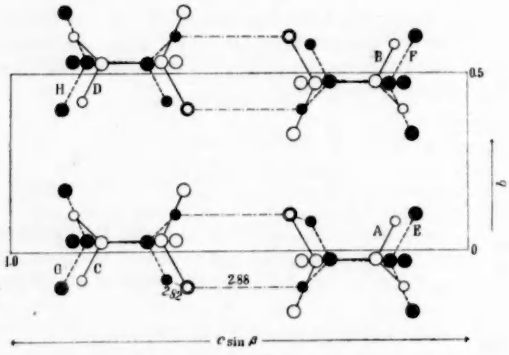

Fig. 6a.—Projection of molecules upon the (100) plane of the crystal, showing some significant interatomic distances. To distinguish molecules which superpose one another, atoms of one kind are drawn in white circles and those of the other kind are drawn in black circles.

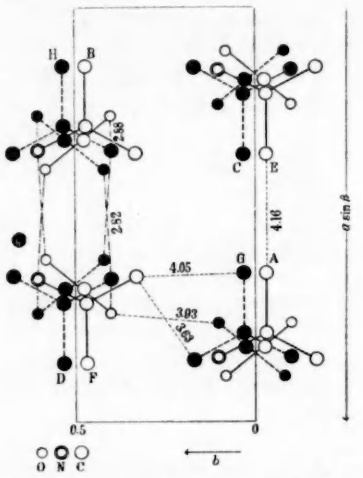

Fig. 6b.—Projection of molecules upon the (001) plane of the crystal, showing some significant interatomic distances. To distinguish molecules which superpose one another, atoms of one kind are drawn in white circles and those of the other kind are drawn in black circles.

different, 1.26 and 1.20 kx. respectively. It is to be noted that in the case of DL-alanine $C-O_1=1.21$ Å. is shorter than $C-O_2=1.27$ Å. Like all the amino acids hitherto analysed, the *N* atom lies approximately in the same plane as the carboxylic group. The value of the interatomic distance between N and O_1 in the molecule was calculated to be 2.61 kx.

The projections of the molecules along *a* and *b* axes respectively are given in Figs. 6a and 6b. The principal intermolecular interatomic distances between molecules are listed in Table 3. In these, the letters A to H refer to equivalent points in the space group as follows:

A: x, y, z; B: $1/2+x, 1/2+y, z$; C: $-x, -y, -z$; D: $1/2-x, 1/2-y, -z$; E: $-x, y, 1/2-z$; F: $1/2-x, 1/2+y, 1/2-z$; G: $x, -y, 1/2+z$; H: $1/2+x, 1/2-y, 1/2+z$.

It is seen that there are two types of hydrogen bonds in intermolecular contacts, one of which is formed between N and O_1, *e. g.* N in (B) and O_1 in (F) and its dimension is 2.82kx, and the other is between N and O_2, *e. g.* N in (B) and O_2 in (H) and its dimension 2.88 kx. It can be said that the molecules are tied to one another with hydrogen bonds in two dimensions between amino groups and carboxylic groups. There is seen considerably short intermolecular contact with respect to methyl groups, *e. g.* C_2 in (F) and C_2 in (G). The dimension of this contact is 3.63 kx. still shorter than that 3.79 A. in L-threonine crystal.

Considering the intermolecular contacts observed, the cleavages parallel to (110) and to (001) are interpreted quite naturally. For reference molecular dimensions found in some crystals of amino acids are listed in Table 4, where those of α-amino isobutyric acid are given in the last column.

Table 3

Principal Intermolecular Atomic Distances (kx)

N (B) – O (F) = 2.82	N (A) – O (B) = 5.56
N (B) – O (H) = 2.88	N (A) – O (G) = 4.20
O (A) – O (B) = 3.20	C (F) – C (G) = 3.63
N (A) – N (C) = 4.61	C (F) – C (G) = 4.05
N (A) – N (D) = 4.14	C (A) – C (E) = 4.16
N (A) – N (E) = 4.23	O (F) – O (G) = 3.93
N (A) – O (E) = 4.50	C (F) – O (G) = 5.86
N (A) – O (F) = 4.75	

Summary

X-ray examination of crystals of α-amino isobutyric acid shows them to be built upon a composite monoclinic unit having $a=10.59$ kx, $b=8.97$ kx, $c=11.34$ kx, and $\beta=94°$, containing eight molecules. The space group is $C2/c$ with all atoms being in the general positions with the following parameters which were determined by the three-dimensional

Table 4

A Comparison of Dimensions found in Some Crystals of Amino Acid.

	N-acetyl-glycine.	*β*-glycyl-glycine.	DL-alanine.	L-threonine.	*α*-amino isobutyric acid.
C_c-O	1.19	1.21	1.21	1.24	1.26
	1.31	1.27	1.27	1.25	1.20
C_c-C_α	1.51	1.53	1.54	1.52	1.52
$C_\alpha-N$	1.45	1.48	1.50	1.49	1.49
$C_\alpha-C$	—	—	1.51	1.54	1.53
	—	—	—	—	1.54
$C_\beta-C$	—	—	—	1.50	—
$O_1...N$	—	—	2.69	2.67	2.61
Hydrogen Bond;					
O...N	3.03	2.80	2.88	2.90	2.88
	—	2.81	2.84	2.80	2.82
Bond Angles;					
$O-C_c-O$	124	125	125	127	125
$O-C_c-C_\alpha$	124	123	121	117	118
	112	112	113	116	118
$C_c-C_\alpha-N$	110	111	108	110	109
$C_c-C_\alpha-C$	—	—	111	113	114
	—	—	—	—	109
$N-C_\alpha-C$	—	—	110	108	108
	—	—	—	—	105
$C-C_\alpha-C$	—	—	—	—	112
$C_\alpha-C_\beta-O_H$	—	—	—	104	—
$O-C_\beta-O_H$	—	—	—	111	—

Fourier analysis; nitrogen: $x=0.154$, $y=0.100$, $z=0.388$; carboxylic carbon: $x=0.178$, $y=-0.025$, $z=0.199$; α-carbon: $x=0.212$, $y=-0.031$, $z=0.331$; methyl carbon 1: $x=0.355$, $=-0.027$, $z=0.365$; methyl carbon 2: $x=0.148$, $y=-0.167$, $z=0.382$; oxygen 1: $x=0.112$, $y=0.083$, $z=0.159$; oxygen 2: $x=0.224$, $y=-0.121$, $z=0.138$. Bond distances are 1.26 and 1.20 kx. for carbon-oxygen, 1.52, 1.53 and 1.54 kx. for carbon-carbon and 1.49 kx. for carbon-nitrogen. There are observed a considerably close intramolecular approach between nitrogen and oxygen atoms and also close contact between two methyl groups.

The authors are indebted to Dr. J. Noguchi who kindly supplied the material for the present experiment. The cost of this investigation was partly defrayed by a grantfic of the Ministry of Education, to which the authors wish to express their thanks.

Faculty of Science, Osaka University, Osaka

X-Ray Study of Carbon Brushes

By Tokiti NODA and Shinya SATO

(Received February 7, 1952)

Carbon brushes for electrical machines must have specific qualities requisite for their uses. There are quite a good many kinds of carbon brushes on the market made from various kinds of raw materials by different procedures, details of which, however, are generally kept secret. The properties of carbon brushes depend on their structures, such as the mode of aggregation and distribution of carbon particles, and the form, size and degree of distortion or

Table 1

Unit Cell Dimensions of Graphite Crystal

Name of brush	c Dimension from (004) A.	(006) A.	a Dimension from (110) A.	(112) A.	mean A.	$C=c/a$ from (004)	(006)
HM-5	6.66_0	6.702	2.446	2.447	2.447	2.72_7	2.739
HM-6	6.71_2	6.708	2.461	2.462	2.462	2.72_6	2.725
PD-2	6.69_0	6.690	2.455	2.457	2.456	2.72_4	2.724
GE-D	6.72_4	6.699	2.460	2.461	2.460	2.73_3	2.723
8601-N	6.76_4	6.738	2.454	2.457	2.455	2.75_5	2.745
NCC-258	6.74_6	—	2.457	—	2.457	2.74_5	—
NCC-259	6.76_5	—	2.453	—	2.453	2.75_9	—
NCC-255	6.79_9	—	2.458	—	2.458	2.76_6	—
SA-45	6.79_6	—	2.455	—	2.455	2.76_6	—
E	6.71_2	6.720	2.458	—	2.458	2.73_3	2.736
Graphite							
Bacon[2]	6.708±0.001		2.4614			2.725_3	
Hofmann[3]	6.69 ±0.01		2.455 ±0.002			2.725	

imperfection of graphite crystallites in carbon particles. The structure may be divided into macroscopic, microscopic and submicroscopic ones. Although there are many studies concerning the macroscopic and microscopic structures, the apparent and true densities, the porosity, and other physical properties, no one has yet succeeded in making clear the relationship between the dynamic characteristics and the structure of brushes by having recourse to the macroscopic and microscopic observations alone. The authors now intend to make clear the submicroscopic structure of carbon brushes by X-ray and electronmicroscopic methods.

K. Hayashi and Y. Uto[1] measured the unit cell dimensions of graphite crystallites of several carbon brushes and divided them into three groups, *i. e.* (a) the natural graphite type, (b) the 2600 type or the pitch coke type, and (c) the SA-type or the soot type. The a dimension of graphite crystallite was constant for all kinds of brushes, but the c dimension was not uniform, being 6.72 A. for the natural graphite type, 6.78 A. for the 2600 type, and 6.85 A. for the SA-type. In the present paper, the results of the measurements of the unit cell dimensions and crystal sizes of graphite crystallites of several natural graphite and electrographite type of carbon brushes are reported.

Experimental

Specimens of carbon brush powder pulverized to pass 300 mesh per inch sieve and packed in a cellophane tube of about 0.3 mm inner diameter were employed, using FeK radiation in a 6.1 cm. camera. The diameter of the camera was calibrated by NaCl reflexions. Samples investigated were,

HM-5 (Morganite), natural graphite type,
HM-6 (Morganite), natural graphite type,
PD-2 (Hitachi), electrographitized pitch coke type (electrode for a vaccum tube),
GE-D (General Electric), electrographitized pitch coke type,
8601-N (Ringsdorff), electrographitized pitch coke type,
NCC-258 (National Carbon), electrographitized pitch coke type,
NCC-259 (National Carbon), electrographitized soot type,
NCC-255 (National Carbon), electrographitized soot type,
SA-45 (National Carbon), electrographitized soot type,
E (Nippon Carbon), electrographitized pitch coke type (Laboratory product).

Unit Cell Dimensions and Calculate Density.—The results of the meaurements of unit cell dimensions are shown in Table 1. The spacing values of HM-6, GE-D, 8601-N, NCC-255, and SA-45 were taken as the mean of those found from two films, but the others from one film.

The c dimensions were calculated from the (004) and (006) reflexions. For the a dimensions, the measurements were of the (110) and (112) reflexions. The c dimension from the (006) reflexion was used to calculate the a dimension from the (112) reflexion. The coincidence of the a dimensions from the (110) and (112) reflexions on the same film is satisfactory. The (006) and (112) reflexions could not be detected on films of some of the specimens, especially those of the soot type brushes. On the films of the soot type brushes, the (100) and (101) reflexions could not be resolved.

(1) K. Hayashi and Y. Uto, *Journ. Inst. Elec. Engrs., Japan*, **63**, 452, 592 (1943).
(2) G. E Bacon, *Acta Cryst.*, **3**, 137 (1950).
(3) U. Hofmann und D. Wilm, *Z. Elektrochem.*, **42**, 504 (1936).

The accurate measurement of the graphite unit cell dimensions of Bacon[3] (1950) showed that the value of the c dimension increased inversely proportionally with the thickness of graphite crystal, and that the value of the a dimension showed no change for graphite samples investigated, whose thicknesses of graphite crystals were larger than *ca.* 100 A. According to Taylor's paper[4] (1942), there was no genuine change of the a dimension for carbon layers having widths greater than a few tens of Ångstron unit. As shown later, graphite crystallites of our samples have width larger than 100 A. and overall height H larger than a few tens of Ångstron unit, it may reasonably be assumed that the a dimension of all the samples has the same value as that of the natural graphite. As all the spacings of HM-5 have smaller values than the other samples, there must be a systematic error due to the film treatment. Mean value of the a dimension of the eight samples except HM-5 is 2.457± 0.001 A. This value is almost equal to Hofmann's value 2.455 A., but smaller than the more accurate value of Bacon by 0.004 A. The main source of the error came from the camera diameter determination, as the camera diameter was calculated from NaCl reflexions on a separate film. We can eliminate the film error and compare the degree of graphitization of each sample by taking the axial ratio $C=c/a$. The (004) and (006) reflexions occur at 35° and 60° respectively. As the mean error of the a dimensions calculated from the (110) ($\theta=52°$) and (112) reflexions ($\theta=57°$) is ±0.0001 A., the mean error of the c dimension from the (006) reflexions may be the same as or less than that of the a dimensions. Therefore the mean error of the C (006), the axial ratio calculated from the (006) reflexions and the a dimension, was assumed to be ±0.001. The accuracy of the C (004) may be less than the C (006). From the standard deviation of the C (004) to the C (006) and the mean error of the C (006), the mean error of the C (004) was calculated to be ±0.008.

Among five specimens of which the values of C were obtained from the (006) reflexions, the values of C (006) of HM-6, PD-2, and GE-D should be looked upon as equal to the value of the natural graphite of Hofmann and Bacon. These brushes could be regarded as being composed of well crystallized graphite crystallites. The C (006) value of HM-5 is greater than the above three values, but smaller than that of 8601-N. The C (006) value of E is smaller than that of 8601-N, but larger than that of GE-D. The larger value of C indicates the smallness of graphite crystallite. From the C (004) values, it is difficult to tell the difference between HM-6, PD-2, GE-D, E and HM-5. The C (004) value of NCC-258 can be distinguished from that of PD-2, but not from that of GE-D. The C (004) value of 8601-N can be distinguished from that of GE-D, but not from that of NCC-258. The value of NCC-259 can barely be distinguished from that of NCC-258, but it cannot be distinguished at all from that of 8601-N. The value of NCC-255 is equal to those of SA-45 and NCC-259, but can clearly be distinguished from that of NCC-258. Summarizing the above observation, the order of the value of C of the brushes can be shown by the following inequality.

$$\text{HM-6}=\text{PD-2}=\text{GE-D}<\text{E}\leq\text{HM-5}<\text{8601-N},$$
$$\text{GE-D}\leq\text{NCC-258}\leq\text{8601-N}\leq\text{NCC-259}\leq$$
$$\text{NCC-255}=\text{SA-45}.$$

Densities d (X) of the graphite crystallites were calculated from the C (004) or C (006) values taking the a dimension as 2.461_4 A. from Bacon's paper. This value is also very near to the value 2.461_2 A., previously obtained by Nelson and Riley[5]. Both values are shown in Table 2 with densities d(p) measured by the picnometer method. Calculated *Kryptoporen*[6] are also shown in the table.

Table 2

Density and *Kryptoporen* of Carbon Brushes

Name of brush	d (X) from (006)	d (X) from (004)	d (P)	*Kryptoporen* from (006)	*Kryptoporen* from (004)
HM-5	2.240	2.24_9	2.101	6.20	6.6
HM-6	2.251	2.25_6	2.229	0.98	0.9
PD-2	2.252	2.25_2	2.254	0.00	0.0
GE-D	2.253	2.24_4	2.210	5.90	5.5
8601-N	2.235	2.22_6	1.999	10.5	$10._6$
NCC-258	—	2.23_5	2.120	—	5.1
NCC-259	—	2.22_1	2.068	—	7.0
NCC-255	—	2.21_8	2.000	—	9.8
SA-45	—	2.21_8	1.990	—	$10._3$
Graphite					
Bacon	2.250_8				
Hofmann	2.251				

Crystallite Size and Intensity Ratio of Reflexions.—Relative intensities of the (100), (101), (110) and (112) reflexions and widths at half intensity of the (004), (110) and (112) reflexions were measured from the microphotometric curves of the X-ray photographs. Sizes of graphite crystallites were calculated from the widths at half intensity by Laue's equation. Sizes of crystallites larger than 200 A. could not be determined and it was possible to compare sizes smaller than 100 A. The true thickness of the graphite crystal t ($=m_2c$) was calculated from the (112) reflexion, the width of the crystal w ($=m_1a$) from the (110) reflexion, and the overall height of the crystal H from the (004) reflexion. The results are shown in Table 3 with the values of $I(101)/I(100)$ and $I(112)/I(110)$. The t value and the intensity ratio of reflexions of the soot type brushes could not be obtained, as their (112) reflexions were not observed, and their (100) and

(4) A. Taylor, *Nature*, **152**, 462 (1942).

(5) J. B. Nelson and D. P. Riley, *Proc. Phys. Soc., London*, **57**, 477 (1945).

(6) $Kryptoporen=[d(\text{X})-d(\text{p})]\times 100/d(\text{X})$.

Table 3

Crystal Size and Intensity Ratio

Name of brush	Crystal Size×10 A. H	t $(=m_3c)$	w $(=m_1a)$	Intensity Ratio I (101)/I(100	I (112)/I(110)
HM-5	>20	15	>20	1.8	0.9
HM-6	>20	12	>20	4.3	1.8
PD-2	>20	10	>20	3.2	1.6
GE-D	>20	7	>20	2.5	1.2
8601-N	7	2	15	1.6	0.6
NCC-258	10	7	>20	1.6	0.9
NCC-259	10	—	15~20	—	—
NCC-255	10	—	15~20	—	—
SA-45	10	—	10	—	—
Natural graphite (Hofmann)				4.9	1.6

(101) reflexions could not be resolved.

Discussion

HM-6 and HN-5 are the natural graphite-carbon type brushes. From the C value or the calculated density and the value of the *Kryptoporen* of HM-5, it was shown that HM-5 must contain α considerable amount fo amorphous (or ungraphitized) carbon. By the influence of the presence of amorphous carbon, calculated thicknesses of crystallites of HM-5 and HM-6 appeared to be too small. Intensity ratios of the reflexions of HM-6 are approximately the same as those of the natural graphite, but those of HM-5 are far smaller. The content of amorphous carbon of HM-5 must be large enough to influence the intensities of reflexions. The fact that the C value or the calculated density of PD-2 is equal to the values of the natural graphite and that the value of *Kryptoporen* is zero shows the completeness of the graphitization of PD-2, the electrographitized pitch coke. The C value of GE-D is equal to that of the natural graphite, but the value of *Kryptoporen*, 6 %, shows that the degree of graphitization is not yet sufficient. But among the electrographitized pitch coke type brushes, GE-D is the most highly graphitized one. Judging from the C values, the crystallite sizes, and the intensity ratios of the reflexions, NCC-258 is next to GE-D in the graphitization. 8601-N is the least graphitized one among these three piteh coke type brushes. Among the electrographitized soot type brushes, the degree of graphitization of NCC-259 is larger than the degrees of NCC-255 and SA-45. The thickness of crystallites of the soot type brushes must be very small, though the (hkl) reflexions of these brushes could not be observed on the films. SA-45 appeared to be composed of graphite crystallites of the smallest size among the above three soot type brushes.

The X-ray study of carbon brushes may be said to be useful, and a finer conclusion may be obtained by improving the experimental method.

This research was supported by the Grant in Aid for Developmental Scientific Research of the ministry of Education and was made as a part of the work of the committee No. 117 (Carbon Materials for Electrical Machines) of the Japan Society for the Promotion of Scientific Research.

Department of Applied Chemistry, Faculty of Engineering, Nagoya University, Nagoya.

On the Acidity of Boric Acid. I. Neutral-Salt Effect Observed by Alkali-titration

by Shunsuke SHISHIDO

(Received January 21, 1952)

Introduction

It is a well known fact that the solution of boric acid is too weak to be determined by alkali-titration. But the solution is so strongly acidified by the addition of polyalcohol, glycerine, mannit, etc., that it can be titrated by adopting phenolphthalein as indicator. This is one of the methods of quantitative analysis of boric acid.(1) A. Deutsch and S. Osoling(2) studied the complex formation between boric acid and mannit by the conductometric and potentiometric methods and concluded that the equilibrium is as follows:

$$H_3BO_3 = H^+ + H_2BO_3^-$$
$$H_2BO_3^- + \text{Mannit} = [H_2BO_3\ \text{Mannit}]^-$$
$$H_2BO_3^- + 2\ \text{Mannit} = [H_2BO_3\ 2\ \text{Mannit}]^-.$$

Recently, D. Setten(3) has shown that the boric acid solution becomes more acidic than expected from the law of mass action in the case of concentrated solution (above 0.1 M), and that the polymerization of H_3BO_3 molecule occurs.

It is clear that the increase of acidity could be caused by the stabilization of the dissociated ion $H_2BO_3^-$ or H^+ owing to the complex formation or polymerization, but the reason why the stabilization and the ionization could be correlated directly with each other has not been explained sufficiently.

The new fact of neutral-salts effect has been discovered in this laboratory, which gives the hint for the explanation of this phenomena as shown in the following section.

Experimental Procedure and Result

(A) Titration by the addition of mannit, glycerine, ethylene glycol and methyl alcohol.—20 cc. of the solution of boric acid (0.1 M/1) added with 10 cc. of distilled water the mixture is titrated with 0.2 N. sodium hydroxide solution in the presence of phenolphthalein. The alkali solution is added until the colour of the solution turns to light pink (pH-8.5) and the added volume of alkali solution is read. This is the initial titration volume (itv). Then, the moderate volume of alcohol (volume added) is added. When the solution discolours, it is again titrated with the alkali solution in order to read the second titration volume. The titration is repeated and the titration curves can be obtained. When the quantity of alcohol is enough, the colouring points (each end point) become clearer, because the dissociation constant is increased. Some results are shown in Fig. 1. We can easily understand from these

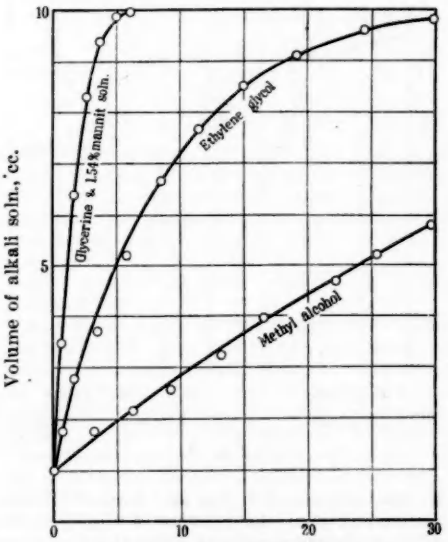

Fig 1.

curves that the strength of acidifying effect is demonstrated by the initial inclination of the titration curve. These values are listed in Table 1. Similar effects are observed in the system of two components of CH_3OH–$C_2H_4(OH)_2$ and CH_3OH–$C_3H_5(OH)_3$, and the results are shown in Table 2 and Fig. 2.

Supplementally, the effect of aceton and dioxan has been investigated without virtue, and the results are rather negative.

(B) Titration by the addition of neutral-salts.—20 cc. of the solution of boric acid (0.1 M) is added

(1) F. P. Treadwell, "Analytische Chemie".
(2) A. Deutsch and S. Osoling, *J. Am. Chem. Soc.*, **71**, 1637 (1949).
(3) D. Setten, *Anal. Chem.*, **23**, 1777 (1951).

Table 1

Subst.	Initial inclination cc./cc.	cc./mol	Relative value
Methyl alcohol	1/6	6.7	1
Ethylene glycol	4/6	36	5.4
Glycerin	4/1	280	42
1.54% Mannit Soln.	4/1	4000	100

Table 2

Methyl alcohol~Ethylene glycol Mol ratio (M:E)	Init. incli., cc./cc.	Methyl alcohol~Glycerin Mol ratio (M:G)	Init. incli., cc./cc.
4 : 0	0.17	4 : 0	0.17
3 : 1	0.35	3 : 1	2.2
2 : 2	0.60	2 : 2	3.2
1 : 3	0.65	1 : 3	4.0
0 : 4	0.67	0 : 4	4.0

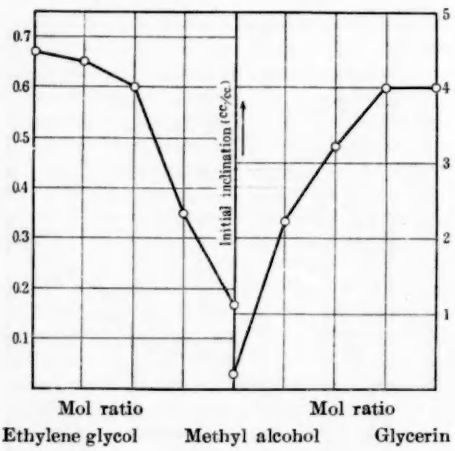

Fig. 2.

by the neutral-salt at first and 10 cc. of distilled water, and then the mixture is titrated by the similar way described in (A). The titration curves are obtained mainly with ethylene glycol. The results in the presence of NaI and K_2SO_4 are shown in Fig. 3. The curves are displaced from the original (ethylene glycol only) mainly in the next two points:

(1) initial titration volume (itv).

(2) sufficient quantity of ethylene glycol which needs to reach the final end point decreases when the initial titration volume increases as compared with the case of ethylene glycol only.

From these observations, the effects examined are divided into three classes, which are,

(a) strongly effecting salts: LiCl, $CaCl_2$, $BaCl_2$, NaBr, NaI, $Ca(NO_3)_2$, $Ba(NO_3)_2$,

(b) moderately effecting salts: NaCl, $NaNO_3$, KBr, KI,

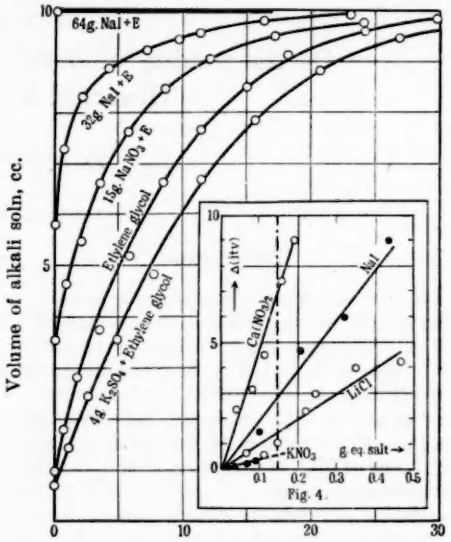

Fig. 3.

(c) little or negatively effecting salts: KNO_3, Na_2SO_4, K_2SO_4.

In order to discuss the effect quantitatively, the author examined the relation between initial titration volume and salt concentration. Generally, the change of initial titration volume $\triangle$(itv) is linear with the salt concentration. Some results are shown in Fig. 4. From this linearity, we can determine the strength of acidifying effect as the change of initial titration volume $\triangle$(itv)* at the salt concentration of one gram equivalent to the solution of 20 cc. of 0.1 M boric acid and 10 cc. of distilled water. These values are listed in the last column in Table 3.

Result and Discussion

The effects of polyalcohols and their mixtures, as well as acetone and dioxan, showed the results expected from the previous works. But the neutral-salt effect was remarkable. Therefore, it is important to discover the correlation between the acidifying effect and the other properties of salts.

After various speculation, the author has concluded that there is a distinct relation between the strength of the acidifying effect ($\triangle$(itv)*) and the energy of hydration of ions. When we compare the $\triangle$(itv)* with the difference of the hydration energy between positive and negative ions ($\triangle U$(Cal./g. eq. ion) $= U_+ - U_-$) in Table 3,[4] we can easily perceive the simple relation as

(4) J. D. Bernal and R. H. Fowlers, *J. Chem. Phys.*, **1**, 538 (1933). The values for NO_3^- and 1/2 SO_4^{--} are assigned as 58 kcal./g.eq. ion and 85 kcal. respectively from the expectation that the effect of KNO_3 and Li_2SO_4 lies on the curve on Fig. 5.

Table 3

Salts	Hydration energy, kcal./g. eq. ion				△(itv)*, cc.
	U_+	U_-	ΣU	$\triangle U$	
LiCl	136	65	200	75	+1.7
$LiNO_3$	136	(56)	(192)	(80)	+1.8
NaCl	114	65	179	49	+1.6
NaI	114	47	161	67	+3.0
$NaNO_3$	114	(56)	(170)	(58)	+1.2
$\frac{1}{2}Na_2SO_4$	114	(85)	(199)	(29)	±0
KCl	94	65	159	29	±0
KBr	94	57	151	37	+0.5
KI	94	47	141	47	+1.4
KNO_3	94	(56)	(150)	(38)	+0.6
$\frac{1}{2}K_2SO_4$	94	(85)	(179)	(9)	−1.0
$\frac{1}{2}CaCl_2$	207	65	272	142	+4.5
$\frac{1}{2}Ca(NO_3)_2$	207	(56)	263	(151)	+6.7
$\frac{1}{2}BaCl_2$	174	65	239	109	+4.7
$\frac{1}{2}Ba(NO_3)_2$	174	(56)	230	(118)	+3.0

shown in Fig. 5, that is, △(itv)* is larger as $\triangle U$ increases.

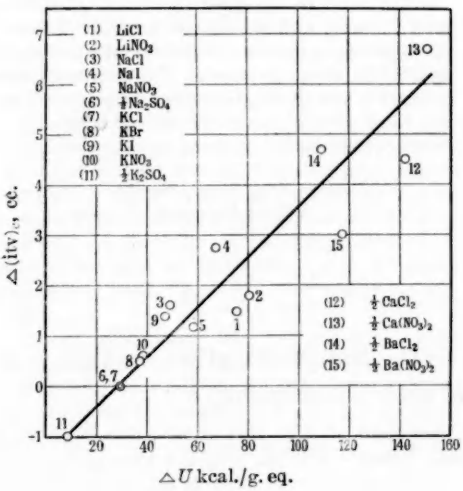

Fig. 5.

Concerning the acidity of boric acid solution, the following three principal features have been discovered;

(1) complex formation with polyalcohol[1][2]

(2) polymerization of itself in concentrated solution[3]

(3) present neutral-salt effect.

In virtue of the effort to obtain the consistent explanation of these three features, the author has reached the following conclusion:

(A) Since the electron configuration in boron atom is $(1s)^2(2s)^2(2p)^1$, it could be bound in either of two ways; that is, tricovalent bond as trimethyl boron B $(CH_3)_3$ molecule (pyramidal) or of tetracovalent bond as fluoroboronate ion $(BF_4)^-$ (tetrahedral). Actually, the various structures, which are derived from the above principal bond, are reasonating.[5]

(B) The structure of crystalline boric acid is considered, from the various facts,[5] to be a resonance form mainly among the tetravalent plane structures (Fig. 6) accompanied with the separation of formal charge, rather than tricovalent.

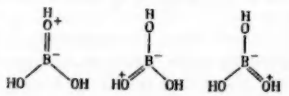

Fig. 6.

Therefore, when there are favourable circumstances for the separation of the formal charge of bond as in H_3BO_3 and $(BF_4)^-$, boron prefers to be bound in tetracovalent. In the case of aqueous solution of boric acid, the separation of charge becomes more easy in the process of electrolytic dissociation (complete separation of charge):

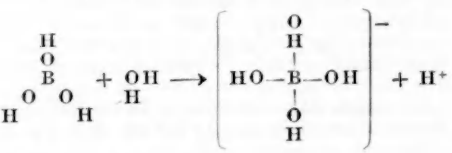

This is the mechanism of electrolytic dissociation of H_3BO_3, although it is very weak. The unstabilization accompanied slightly with the complete separation of charge can be cancelled by the increase of bond energy of regular tetrahedral bond which may be larger than that of the deformed tetravalent plane structure of H_3BO_3 molecule.

(C) When methyl alcohol coexists in an aqueous solution of boric acid the combination can form the methyl ester of boric acid more or less by the dehydrating action owing to the strong affinity of methyl alcohol to water. The separation of formal charge in the molecule of this ester becomes more difficult. Consequently, the bond nature should be inclined to tricovalent and becomes more unstable (for an example $B{\cdot}(OCH_3)_3$ molecule). But, if the ionization of methyl ester is easy, it can be stabilized by the possibility of complete separation of charge (*i.e.*, ionization) and of formation of regular tetracovalent bond.

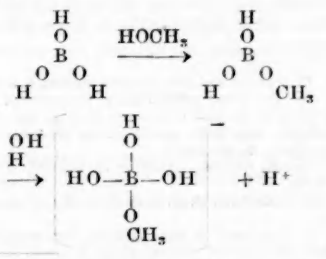

(5) L. Pauling, "The Nature of the Chemical Bond".

The ester formation and the ionization are parallel in this example, because any system should be existing in the most stable state. This is the acidifying mechanism of these compounds and their mixtures, and it depends mainly on the possibility of ester formation. Aceton and dioxan may have the sufficient affinity of water, but not the possibility of ester formation, therefore, they can not show the acidifying effect, but are rather negative.

(D) The fact that the acidity of the more concentrated aqueous solution of boric acid is larger than the value predicted from the law of mass action in the dilute solution is considered to be caused from polymerization.[3] According to the author's theory, this is the expectable result of the cooperative separation of charge to form a regular tetracovalent bond, for an example:

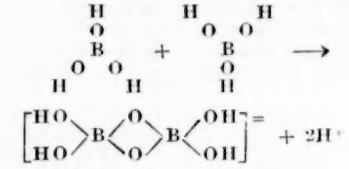

(E) Since the water molecule in the salt solution is hydrated strongly by the ion as in Fig. 7,

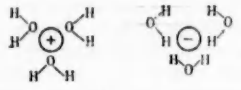

Fig. 7.

the water molecule behaves like the OH radical in polyalcohol or the O atom in the aceton and dioxan molecule in the neighborhood of the cation or anion, respectively. In a more concentrated neutral-salt solution, these two tendencies are counter-balancing, according, to the relative strength of hydration of cation and anion.

When the hydration of cation is greater than that of anion, the water molecule of the solution may behave like polyalcohol, and for the above reasons (A, B, C and D) the acidity of boric acid is increased. On the contrary, when the anion hydrates the water molecule more strongly than cation, the water molecule behaves like aceton or dioxan and rather decreases the acidity of boric acid solution.

This is the mechanism of the acidifying effect of neutral-salt solution. The author will give the quantitative explanation in detail later on.

Summary

The acidifying effect of various solutions (CH_3OH, $C_2H_4(OH)_2$, $C_3H_5(OH)_3$, $C_6H_8(OH)_6$, their mixture, CH_3COCH_3, $O(CH_2CH_2)_2O$, and neutral-salts) is measured by the alkali-titration method, and the simple relation between the hydration energy of neutral-salts and their acidifying effect is found. The consistent explanation for these phenomena is proposed on the view of the nature of the tricovalent and tetracovalent bond of boron atom.

Chemical Department, Faculty of Science, Niigata University, Niigata

Studies on Nitrate Reductase. VII. Reinvestigation on the Identity of the Enzyme with Cytochrome *b*[1]

By Ryo SATO[2] and Makoto NIWA

(Received November 22, 1951)

Previous studies in this laboratory,[3~6] together with informations from other laboratories,[7~10] have clarified that nitrate reductase is the enzyme functioning as the terminal component of the catalytic system, by which hydrogen atoms (or electrons) are transported from metabolites such as succinate, formate and alanine to the final acceptor

(1) The results and discussions described in this paper were, for the most part, already presented at the 3rd Symposium on Enzyme Chemistry, October 1950, TOKYO. Its abstract has been published in Japanese (*Symp. Enzyme Chem.*, **6**, 40 (1951))

(2) Present address: Faculty of Science, Kanazawa University.

(3) F. Egami and R. Sato, *J. Chem. Soc. Japan*, **68**, 39 (1947).

(4) F. Egami and R. Sato, *J. Chem. Soc. Japan*, **69**, 160 (1948).

(5) R. Sato and F. Egami, This Bulletin, **22**, 137 (1949).

(6) R. Sato, *Science Reports*, **2**, 122 (1950).

(7) S. Yamagata, *Acta Phytochimica*, **10**, 283 (1938).

(8) S. Yamagata, *Acta Phytochimica*, **11**, 145 (1939).

(9) E. Aubel and F. Egami, *Compt. rend. acad. sci.*, **202**, 675 (1936).

(10) E. Aubel and F. Egami, *Bull. soc. chim. biol.*, **18**, 301 (1936).

nitrate. The role of this enzyme in nitrate reduction is therefore quite analogous to that of the terminal heme enzyme in respiratory mechanisms. Corresponding to this functional similarity, one of the present authors (Sato) and Egami[5] suggested in an earlier report of this series that nitrate reductase of *Escherichia coli* may be an iron enzyme and is probably identical with cytochrome *b* of *E. coli* type.[11] This view appeared to be able to account for almost all the results obtained up to that time. As to this identity, however, some doubts were presented even at that time, since there was no evidence to indicate that the cytochrome in question does combine with cyanide, a well known inhibitor of nitrate reductase. On the contrary, Pappenheimer and Hendee[12] have reported that cytochrome *b* of *Corynebacterium diphtheriae*, apparently identical with that of *E. coli*, is insensitive to cyanide in its aerobic function. Sato (one of the present authors) and Egami[5] themselves also failed to observe any change in the absorption bands of the cytochrome *b* contained in a cell-free preparation of nitrate reductase from *E. coli* when cyanide was added to this preparation. In order to correlate this observation with the above view, they had to assume a rather incredible fact: cyanide does combine with the cytochrome *b* and so inhibit the activity of nitrate reductase, but this combination causes no alteration of the absorption spectra of the cytochrome (at least α- and β-bands of the reduced cytochrome). It has been since considered desirable to study the problem more extensively and to settle the contradictory points.

In our attempts to solve the problem, it was discovered that thiourea inhibits nitrate reductase considerably. This reagent differed from the other known inhibitors of nitrate reductase such as cyanide, azide and carbon monoxide in exerting only a slight inhibition upon the oxygen uptake by *E. coli*. The fact that such an inhibitor as thiourea does exist seemed to provide another support for the invalidity of the suggested identity, because it was clear that the very cytochrome *b* is required in this thiourea-insensitive respiration.

Further investigations were then carried out using thiourea as a tool in order to obtain more advanced informations on the nature of nitrate reductase. The results of these investigations as well as consideration of the other data have shown that the previously proposed hypothesis is incorrect. Instead, it has been now clarified that cytochrome *b* of *E. coli* type is not identical with nitrate reductase itself, though it is closely related to the nitrate-reducing activity of this organism. The "nitrate reductase" which we previously so called is in fact a complex system consisting of the cytochrome *b* and a cyanide- and thiourea-sensitive factor, nitrate reductase itself.

Despite the revision of the view, it seems still tenable that nitrate reductase is an iron enzyme, because the carbon monoxide inhibited-activity of the enzyme can be restored by light.

Experimental

Materials and Methods

The resting cell suspension of *E. coli* grown on a nitrate-containing peptone-bouillon-agar medium was prepared as described in the preceeding paper.[13] The cell-free preparation of nitrate reductase employed in this investigation was obtained from *E. coli* by ultrasonic destruction of the cells and ammonium sulfate precipitation as previously described.[5] In the present study, however, the preparation was brought to dryness by lyophilization after 10 hours dialysis against a stream of water and stored at 0° in a vacuum desiccator. The presence of cytochrome *b* of *E. coil* type in this preparation was readily demonstrable by a hand spectroscope. It also contained a powerful activity of formic dehydrogenase as measured by the methylene blue technique.

Nitrate reduction was carried out anaerobically using Thunberg tubes. The rate of the reduction was measured by determining the amount of nitrite formed in the reaction mixtures by a colorimetric method as used in the previous studies.[13] The activity of dehydrogenases was followed by the ordinary Thunberg method. Manometric experiments were conducted with the use of a Warburg manometer. Spectroscopic observations with the resting suspension were made as follows. A Thunberg tube containing the samples was illuminated by a projector from a distance of about 5 cm. and the spectrum was observed by a hand spectroscope. A Beckman spectrophotometer was employed in spectroscopic investigations with the cell-free preparation.

Further details of the experimental conditions and methods are given in the tables and figures.

Results

Effect of Thiourea on Nitrate Reductase, Dehydrogenase and Oxygen Uptake of E. coli.— Fig. 1 shows the effect of thiourea on nitrate reduction by the cell-free preparation of nitrate

(11) This type of cytochrom *b* is also called cytochrome b_1, according to D. Keilin and C. H. Harpley (*Biochem. J.*, **35**, 688 (1941)).

(12) A. M. Pappenheimer Jr. and E. D. Hendee, *J. Biol. Chem.*, **177**, 701 (1947).

(13) R. Sato, M. Ebata and F. Egami, *This Bulletin*, **25**, 56 (1952).

reductase using sodium formate and methylene blue as hydrogen donator and intermediary carrier respectively.[3] It can be seen that the reduction was completely inhibited by about 0.1 M. of thiourea; half maximum inhibition was attained by $10^{-2.9}$ M. of the inhibitor. Under these conditions, however, the reduction occurs by a co-operative action of formic dehydrogenase and nitrate reductase; the former reducing methylene blue and the latter transfering electrons from the reduced dye to nitrate.[3,7] It was therefore necessary to decide which of the two enzymes concerned was actually inhibited by thiourea. This problem was pursued by studying the effect of the inhibitor on formic dehydrogenase using Thunberg technique. The results of these experiments, together with those on succinic dehydrogenase, are recorded in Table 1. As is shown in the table, the activity of formic dehydrogenase as well as that of the succinic enzyme was not inhibited by thiourea even at a concentration of 0.2 M. It is accordingly evident that nitrate reductase was the actual site of the thiourea inhibition.

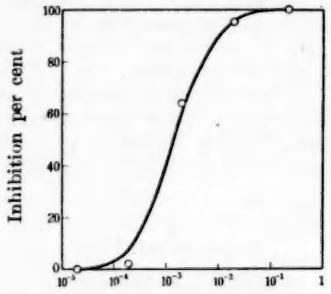

Fig. 1.—Inhibition of nitrate reduction by varying concentrations of thiourea. Each Thunberg tube contained 1 mg. of the cell-free enzyme preparation, 0.004 M. KNO_3, 0.02 M. sodium formate, 10^{-5} M. methylene blue, 0.1 M. phosphate buffer (*p*H 7.4), and varying concentrations of thiourea in a final volume of 5 ml. Temperature: 35°. Reaction time: 50 minutes. Control experiment without thiourea produced 165 μ M./l. nitrite under these conditions.

Table 1

Effect of Thiourea on Formic and Succinic Dehydrogenases of *E. coli*.

Each Thunberg tube contained 12 mg. of the resting cells, 0.1 M. phosphate buffer (*p*H 7.6), 0.002 M. substrate, and 1 : 25000 methylene blue in a final volume of 5 ml. Temperature: 36°. Figures indicate the decolorization time of the dye (in minutes).

Substrate	Without thiourea	With thiourea		
		0.2 M	0.1 M	0.01 M
Formate	15	—	16	16
"	14	10	—	—
Succinate	8	—	—	5
"	5	9	5	—

The effect of thiourea on the oxygen uptake by *E. coli* using formate (Fig. 2) and succinate (Fig. 3) as substrate was then studied. As shown in

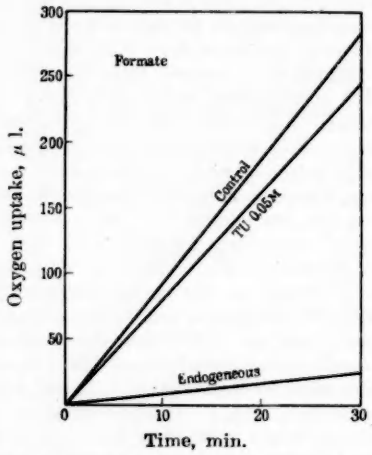

Fig. 2.—Effect of thiourea on respiration of *E. coli* (formate as substrate). Each vessel contained 2.5 mg. of the resting cells, 0.017 M phosphate buffer (*p*H 7.4), 0.017 M. sodium formate with or without thiourea (0.05 M.) in a final volume of 3 ml. Endogeneous respiration was measured without the addition of formate. Temperature: 36°. TU = thiourea.

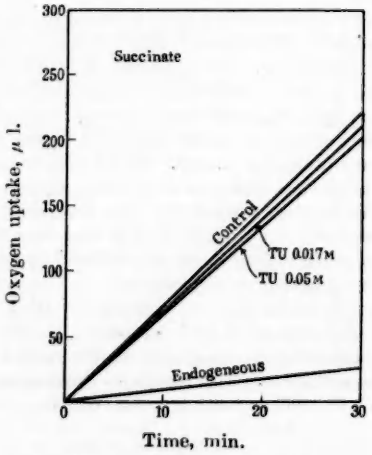

Fig. 3.—Effect of thiourea on respiration of *E. coli* (succinate as substrate). The same conditions as Fig. 2 except sodium succinate was used as substrate instead of formate.

Table 2

Qualitative Spectroscopic Observations using Resting Cell Suspension of *E. coli*

In the main compartment of a Thunberg tube the reactants in Column A were placed, and in the hollowed stopper those in Column D. After evacuation, the tube was incubated at 37° for about 20 minutes. The absorption bands of the ferrocytochrome *b* (at 560 mμ and 530 mμ) and the color of methylene blue (Mb) were observed and recorded in Column B. Then air was introduced into the mixture by removing the stopper and shaking vigorously. Changes observed after this procedure were recorded in Column C. The stopper was again plugged and the tube was incubated as before. Then the contents of the two parts of the tube were mixed and changes which occurrod as a result of this mixing were observed and recorded in Column E. All observations were conducted at room temperature. The *E. coli* suspension contained 7.5 mg. of the cells per ml. (in 0.2 M phosphate buffer of *p*H 7.6). ⧺, +, and ± indicate the intensity of the bands or the color. − shows the absence of the bands or the color.

	A Main compartment						B		C		D Hollowed stopper		E	
	E. coli suspension	Na succinate (0.1 M.)	Na formate (0.1 M)	KCN (0.1M)	Thiourea (1 M.)	Mb (0.02 %)	Bands of cytochrome	Color of Mb	Bands of cytochrome	Color of Mb	KNO_3 (0.5M)	Mb (0.02 %)	Bands of cytochrome	Color of Mb
1	2.0ml	0.5					⧺		−		0.5		±	
2	2.0		0.5				⧺		−		0.5		±	
3	2.0	0.5		0.5			⧺		⧺		0.5		⧺	
4	2.0		0.5	0.5			⧺		⧺		0.5		⧺	
5	2.0	0.5			0.5		⧺		−		0.5		+	
6	2.0		0.5		0.5		⧺		−		0.5		+	
7	2.0	0.5				0.5	⧺	−	−	⧺	0.5		±	⧺
8	2.0	0.5		0.5		0.5	⧺	−	⧺	+	0.5		⧺	−
9	2.0	0.5			0.5	0.5	⧺	−	−	⧺	0.5		⧺	±
10	2.0	0.5					⧺		−			0.5	−	⧺
11	2.0	0.5		0.5			⧺		⧺			0.5	−	⧺
12	2.0	0.5			0.5		⧺		−			0.5	−	⧺

Fig. 2 and Fig. 3, thiourea caused only a slight inhibition on the respiration of formate and that of succinate; only 12 per cent inhibition was seen in the respiration of formate by 0.05 M. of thiorea, a concentration sufficient to inhibit nitrate reductase almost completely. De Ritis and Scalfi[14] have also reported that thiourea does not appreciably influence the respiration of bacteria.

Spectroscopic Observations using Resting Suspension of E. coli.—One of the facts on which Sato and Egami[5] depended in suggesting the identity of nitrate reductase with cytochrome *b* of *E. coli* type was their spectroscopic observation that the reduced cytochrome *b* was rapidly oxidzed by the addition of nitrate. It seemed, therefore, of interest to use thiourea as an inhibitor in such spectroscopic experiments. Thus, we set ourself first to a qualitative investigation with the use of the resting cell suspension of *E. coli*. A hand spectroscope was employed for this purpose.

The results of this investigation are summarized in Table 2. On anaerobic incubation of the suspension with formate or succinate, the cytochrome *b* was converted to the reduced (or ferro-) form as indicated by the appearance of the absorption bands of the ferrocytochrome *b* (α-band at 560 mμ and β-band at 530 mμ). Thiourea and cyanide did not prevent this reduction. When air was introduced into the mixture, the bands disappeared at a rapid rate and the spectrum became that of the oxidized (or ferri-) cytochrome *b*. This aerobic oxidation of the ferrocytochrome *b* was completely inhibited by cyanide, but thiourea failed to inhibit it. In confirmation of the previous data,[5] the bands of the reduced cytochrome also greatly decreased their intensity by the addition of potassium nitrate. This oxidation by nitrate was also found to be sensitive to cyanide just like the aerobic process. A remarkable difference was, however, recognized between the two oxidation processes; in the former case, nitrate as oxidant, the disappearance of the reduced cytochrome bands was greatly inhibited by the presence of thiourea, in contrast to what was seen in the aerobic oxidation.

Incubation of the suspension with succinate or formate in the presence of methylene blue under anaerobic conditions resulted in, as is well known, the decolorization of the dye; the addition of nitrate into the decolorized mixture caused the immediate recolorization of the leuco methylene blue as previously reported.[3,7] This oxidation of the leuco dye by means of nitrate was found to be also inhibited by thiourea as well as by cyanide. Spectroscopically, it was confirmed that this recolorization of methylene blue was always accompanied by the disappearance of the bands of the reduced cytochrome *b*.

(14) F. De Ritis and L. Scalfi, *Boll. soc. ital biol sper.*, **22**, 703 (1946); *Chem. Abst.*, **41**, 3167 (1947).

Moreover it was found that the reduced cytochrome bands also disappeared when methylene blue was added to the mixture. But this disappearance was not inhibited by either cyanide or thiourea.

Finally, the effect of thiourea on the absorption spectra of the cytochrome *b* was examined. No change, however, could be detected in the spectra of either the oxidized or the reduced cytochrome even when 0.2 M. of thiourea was added.

Spectroscopic Experiments using the Cell-free Preparation.—A quantitative investigation by the use of a Beckman spectrophotometer was then undertaken with the object of ascertaining the findings of the above qualitative observations using a hand spectroscope. The cell-free preparation of nitrate reductase was adopted for this purpose.

Due to the turbidity and the relatively minute concentration of the cytochrome *b* contained in the preparation, the spectra obtained were rather indistinct. Nevertheless, it was not so difficult to identify the absorption maxima due to the reduced cytochrome *b*. Fig. 4 illustrates the spectra of the preparation at both the oxidized and reduced states measured at the wave length region ranging from 525 mμ to 575 mμ. The reduced state was realized by two methods; by the addition of sodium hydrosulfite and by incubation of the preparation with formate under an anaerobic condition (using liquid paraffin as a seal). In the latter procedure the incubation was carried out without any added intermediary hydrogen carrier such as methylene blue, but the cytochrome *b* was reduced to about 80 per cent of completion after 30 minutes (the reduction by hydrosulfite being assumed complete). This enzymatic method was used in the later experiments in preference to the hydrosulfite method; the reason of which was described in the previous paper.[5] It is clearly shown in Fig. 4 that the reduced spectra have two peaks at 560 mμ and 530 mμ corresponding to the α- and β-bands of the ferrocytochrome *b* respectively. On the other hand, no absoption maxima could be detected in the oxidized spectrum at least in this wave length region. The increasing optical density toward the shorter wave length region is not largely due to true absorption; the most part of this apparent absorption is a mere result of the scattering of light caused by the turbidity. (It is known that light scattering intensifies itself as the wave length becomes shorter). Net absorption at 560 mμ caused by the ferrocytochrome *b*, therefore, may

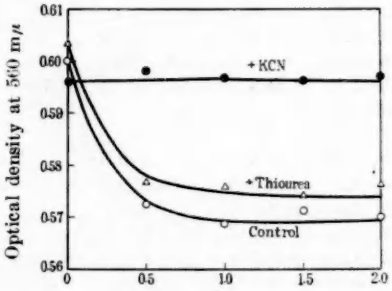

Fig. 5. Effect of KCN and thiourea on aerobic oxidation of ferrocytochrome *b*. The cell-free preparation of nitrate reductase was dissolved in 0.05 M. (*p*H 7.4) phosphate buffer containing 0.05 M. sodium formate (200 mg. of the preparation per 3 ml.). 3 ml. of this solution was pippetted into a cuvette of the Beckman spectrophotometer and liquid paraffin (1.5 cm. thick) was placed on it. The cuvette was then incubated for 30 minutes at 37°. Then each 1 ml. of either distilled water (control), or 0.04 M. KCN (+KCN), or 0.2 M. thiourea (+Thiourea) was added and the optical density at 560 mμ was measured. Then the liquid paraffin was removed by pipetting out as quickly as possible and air was bubbled into the mixture by a small syringe. The changes of the optical density was followed at each 30 seconds interval. Measurements were conducted at room temperature.

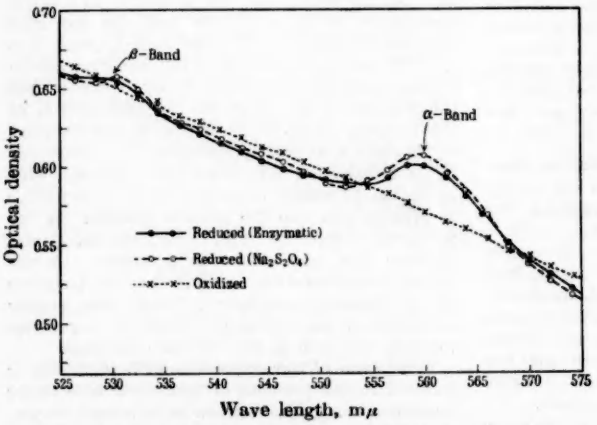

Fig. 4.—Absorption spectra of cell-free preparation of nitrate reductase. Each cuvette of the Beckman spectrophotometer (light path 1 cm.) contained 200 mg. of the cell-free preparation in a final volume of 4 ml. (phosphate buffer, 0.05 M, *p*H 7.4). Enzymatic reduction was carried out by incubating with 0.05 M sodium formate for 30 minutes at 37°. Liquid paraffin (1.5 cm. thick) was placed on the mixture to keep the anaerobic condition. Nonenzymatic reduction was carried out by adding a small amount of solid $Na_2S_2O_4$ and then placing liquid paraffin.

be estimated as about 0.03—0.04 in optical density unit.

By following the decrease of optical density at 560 mμ, the oxidation of the ferrocytochrome *b* by atmospheric oxygen (Fig. 5) and by potassium nitrate (Fig. 6) together with the effect of cyanide and thiourea on these processes were then studied. As shown in Fig. 5 and Fig. 6, it was confirmed that the reduced cytochrome *b* undergoes rapid oxidation by either introduction of air or by addition of nitrate. In both the cases the oxidation proceeded to completion within 30 seconds. In confirmation of the qualitative observations, it was further found that cyanide prevented both

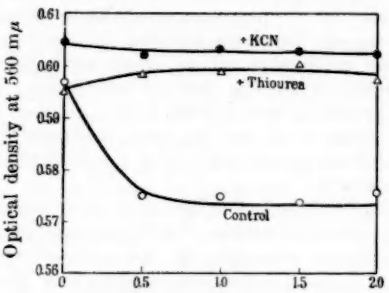

Fig. 6.—Effect of KCN and thiourea on oxidation of ferrocytochrome *b* by nitrate. Conditions and methods were the same as Fig. 5, except the following. Instead of removing the liquid paraffin and bubbling air, small amounts of solid potassium nitrate was added at zero time.

of the processes completely, but thiourea was inhibitory only for the oxidation by nitrate. No appreciable retardation of the aerobic oxidation was observed by the presence of thiourea (0.05 M.).

Attempts were also made to test the possibility that methylene blue may oxidize the ferrocytochrome suggested by the qualitative observation. But high concentration of methylene blue (0.001 per cent) used in these experiments made it impossible to conduct desirable measurements due to the intense general absorption of the dye. Even at lower concentrations of the dye no definite results were obtained.

Discussion

Nitrate reductase can be defined as the terminal enzyme of hydrogen (or electron) transporting pathways from suitable hydrogen (or electron) donators to nitrate; *viz.*, it is the enzyme which reacts directly with nitrate. If this enzyme is actually identical with cytochrome *b* of *E. coli* type as previously suggested,[5] the only possible scheme accounting for both the nitrate reduction and the aerobic respiration by *E. coli* should be as follows:

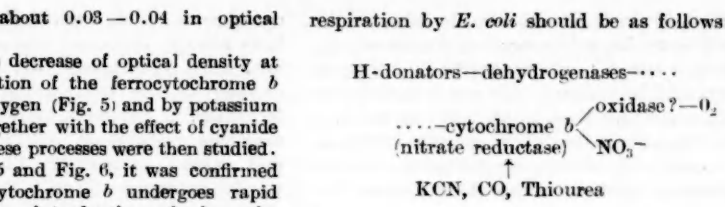

Here, the arrow indicates the site of action of the inhibitors. The intermediary components between dehydrogenases and the cytochrome *b* are not shown in this scheme for several reasons; (1) no definite information is as yet available, (2) this part of the scheme may be different according to the hydrogen donators, and (3) they are not important for the later discussions. The oxidase inserted between the cytochrome *b* and molecular oxygen will be discussed later.

The results reported in the present study, however, suggest that the above scheme as such is unlikely. First of all, this scheme can not provide any satisfactory explanations for the finding that thiourea does not appreciably influence the aerobic respiration of *E. coli*, in contrast to its fairly marked inhibitory action upon the nitrate reduction. Spectroscopic evidence also indicates that thiourea is not capable of preventing the oxidation of the ferrocytochrome *b* by atmospheric oxygen, while the disappearance of the reduced cytochrome bands by nitrate is completely inhibited by the same reagent. Furthermore, as already mentioned the above scheme is not consistent with the observations that no changes occur in the cytochrome bands by the addition of cyanide. The view claimed by Pappenheimer and Hendee[12] that diphtherial cytochrome *b* is not inhibited by cyanide further makes a protest against the scheme.

A satisfactory settlement of the matter, however, suggests itself on the basis of the very results obtained in the present study. The marked inhibition exerted by thiourea upon the nitrate reduction and the failure of the same reagent to inhibit the respiration necessarily lead to the assumption that a certain thiourea-sensitive factor may be involved in the nitrate-reducing mechanism, whereas no such factor may be required in the respiratory system. The role of this factor is suggested by the spectroscopic results to consist in the catalysis of the oxidation of the ferrocytochrome *b* by nitrate (but not by molecular oxygen). We should therefore regard this factor, according to the definition, as nothing but nitrate reductase itself. The contradiction concerning the cyanide inhibition of the nitrate reduction

mentioned above would also be able to be settled by taking this factor into consideration, because it seems more reasonable to attribute the cyanide inhibition to this new factor (nitrate reductase) rather than to the cytochrome *b*.

On the basis of the above considerations, a more acceptable scheme can be drawn for the processes in question instead of the former one.

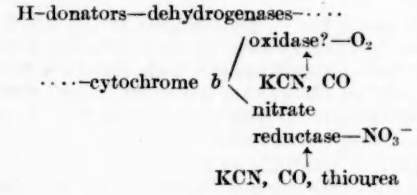

This revised scheme is in agreement with all the results reported in this paper as well as with those in the foregoing studies. The reason why thiourea exerts marked inhibition upon the nitrate reduction without seriously affecting the aerobic respiration will be readily explained by this scheme. (The slight inhibition of the respiration by thiourea may be due to an entirely different mechanism from that for the nitrate reduction.) This scheme can also interpret the spectroscopic findings with ease. Furthermore, the cytochrome *b* is shown in this scheme not to be inhibited by either cyanide or carbon monoxide in accordance with the generally held concept that the cytochrome does not combine with these reagents. Thiourea should also be regarded as being inert to the cytochrome because of the inability of this substance to inhibit the respiration which requires the cytochrome as an essential catalyst.

A brief account of the aerobic pathway presented in the scheme seems desirable. Although there remains little doubt about the participation of the cytochrome *b* in the respiration of *E. coli*, further details of the process are as yet obscure. Pappenheimer and Hendee[12] have obtained evidence indicating that diphtherial cytochrome *b* is autoxidizable and the greater part of the oxygen uptake by a cell-free diphtherial extract can be accounted for in terms of this autoxidation. It is not clear, however, whether the same respiratory mechanism is functioning also in *E. coli*. From our spectroscopic observations it appears preferable to consider that the autoxidation of the cytochrome, if any, does not greatly contribute to the respiration of *E. coli*, because the aerbic oxidation of the reduced cytochrome *b* was strongly inhibited by cyanide. This fact in turn suggests that a cyanide-sensitive oxidase is necessary as a link between the cytochrome and oxygen. Keilin and Harpley[11] have already suggested that an iron enzyme, designated cytochrome a_2, functions as an oxidase of the cytochrome *b* in *E. coli*. Moreover, it has been found spectroscopically that this cytochrome combines with cyanide and carbon monoxide. The presence of a similar oxidase in Type I Pneumococcus and some other bacteria which lack cytochrome *c* and cytochrome oxidase has been reported by Sevag and Shelburne,[15] who found that the respiration of these bacteria is sensitive to both cyanide and carbon monoxide and attributed the inhibitions to this oxidase. It seems therefore by no means unreasonable to assume such an oxidase as the terminal enzyme in the aerobic mechanism of a group of bacteria characterized by the lack of cytochrome *c*-cytochrome oxidase system. The absence of this system in *E. coli* has been confirmed by the negative indophenol oxidase reaction of the organism.[16]

The role of methylene blue as an intermediary hydrogen carrier between dehydrogenase systems and nitrate reductase in the reconstructed system[3] may require an explanation. Previously, assuming the identity of the cytochrome *b* with nitrate reductase, the dye was simply considered as an artificial link between dehydrogenase systems and the cytochrome. Our spectroscopic observations, however, have provided indications, though qualitative and inconclusive, that the dye can serve also as an oxidant of the ferrocytochrome *b*. In addition, it has been confirmed that the reoxidation of the leuco dye by nitrate is sensitive to both cyanide and thiourea. These facts lead to the view that methylene blue might mediate between the cytochrome and nitrate reductase in this simple reconstructed system.

Throughout the above arguments the selective inhibition by thiourea on the nitrate reduction has been taken as the most conclusive evidence in favour of the nonidentity of nitrate reductase with the cytochrome *b*. A selective toxicity[17] of this compound on nitrate metabolism has been also reported by Fleury,[18] who found that thiourea exerts a strong fungistatic action on *Aspergillus niger* in media with nitrate as the sole source of nitrogen, while the toxicity is much less (or absent) when ammonium salts or organic nitrogen

(15) M. G. Sevag and M. Shelburne, *J. Gen. Physiol.*, **26**, 1 (1942).

(16) R. Sato, Unpublished data.

(17) W. W. Wainio *et al.* have reported (*J. Biol. Chem.*, **192**, 349 (1951)) that thiourea, even at a concentration of 10^{-2} M., does not exert any inhibition on cytochrome oxidase activity of a heart muscle preparation.

(18) C. Fleury, *Bull. soc. suisse botan.*, **58**, 462 (1948); *Chem. Abst.*, **43**, 3880 (1949).

sources are available. From these findings Fleury has concluded that thiourea inhibits the nitrate-reducing enzyme system of the mold. The precise mechanisms involved in these specific inhibitions, however, are left to be clarified. Presumably, the capacity of thiourea to form complexes with various metal ions might play a part in these phenomena in some manners. At any rate, further research about this point appears to be of promise for the elucidation of the nature of nitrate reductase.

As a result of the denial of the identity previously suggested between nitrate reductase and cytochrome *b* of *E. coli* type, the necessity has come to the fore again to consider the chemical nature of this enzyme. Neverthless, it seems still valid that the activity of nitrate reductase of *E. coli* is inseparably associated with the presence of iron in the molecule. The most clear-cut support for this view comes from the results of the previous study[5] showing the carbon monoxide inhibition of this enzyme and its reversal by light. Recently it has been further confirmed in this laboratory[19] that a small but definite inhibition by carbon monoxide is also seen in the nitrate reduction by *Bacillus subtilis* and *Acetobacter xylinum*; light reversed the inhibition also in these cases, This suggests that a similar iron enzyme may be responsible for the reduction also in these organisms. Its detailed features, however, are not yet clear.

The iron-protein nature of nitrate reductase receives further indirect support from an investigation dealing with the effect of iron-deficiency on the nitrate-reducing activity of *E. coli*.[20] It has been shown that the organism grown on iron-deficient media has a considerably low activity of nitrate reductase as compared to the cells supplied with a sufficient amount of iron. The activity of succinic dehydrogenase was not influenced by the iron content of the media. Similar results has also been obtained with *C. diphtheriae*.[21] In this connection, observations by Granick and Gilder[22] are worthy of special attention. Studying the growth-promoting activity of various porphyrin derivatives on strains of *Hemophilus influenzae*, they found that several iron porphyrin compounds such as iron meso- and iron hematoporphyrin can substitute iron protoporphyrin as an essential growth factor for this organism. But the organism grown on these unnatural growth factors was found to be completely devoid of the nitrate-reducing activity. On the basis of these observations they have concluded that iron protoporphyrin is required either for the formation of the function of the nitrate-reducing mechanism, the vinyl side chains of protoporphyrin being assumed to be essential.

There are, however, no definite indications in support of the possibility that nitrate reductase is actually a heme protein enzyme, and the clarification of the chemical nature of this enzyme is largely left for the future.

Summary

1. It has been found that thiourea has a marked inhibitory effect on the nitrate reduction by *E. coli*, but dehydrogenase activity and the aerobic respiration of the same organism are not considerably influenced by this compound.

2. Spectroscopically it has been further clarified that thiourea completely prevents the anaerobic oxidation of the ferrocytochrome *b* by means of nitrate, whereas the same reagent can not inhibit the aerobic oxidation of the cytochrome. Cyanide prevents both of the oxidation processes.

3. On the basis of these findings the previously suggested identity of nitrate reductase with cytochrome *b* of *E. coli* type has been criticized and it has been concluded that the cytochrome *b* is not identical with nitrate reductase itself, though it is closely associated with the nitrate-reducing mechanism of *E. coli*.

4. A scheme has been proposed which can account for both the nitrate-reducing and the respiratory mechanisms of *E. coli*.

5. The chemical nature of nitrate reductase has been discussed and the iron-protein nature of this enzyme has been again emphasized.

Addendum I: In a review quoting a previous paper[5] of this series, Wurmser[23] wrote that in the nitrate reduction nitrogen replaces oxygen for the Slater's respiratory scheme. In spite of the validity of this statement, it should be considered that nitrate, but not nitrogen, replaces it.

Addendum II: After this paper had been submitted to the editors, we were informed of the criticism by G. N. Cohen[24] against our earlier hypothesis on the identity of nitrate reductase with the cytochrome *b*. The nitrate-reducing mechanism of strict anaerobes and its differences from that of *E. coli* have been

(19) I. Yamashina, Unpublished data.
(20) M. Niwa, Unpublished data.
(21) R. Sato and M. Yoneda, Unpublished data.
(22) S. Granick and H. Gilder, *J. Gen. Physiol.*, **30**, 1 (1946).
(23) R. Wurmser, *Ann. Rev. Biochem.*, **20**, 8 (1951).
(24) G. N. Cohen, *Ann. Rev. Microbiol.*, **5**, (1951).

investigated by Mr. Tadao Katsura at the Institute of Infectious Diseases of Tokyo University in connection with us. This material will be published shortly.

The present authors are deeply indebted to Prof. F. Egami for his continuous encouragement and valuable advice for this study. The spectroscopic experiments by the use of a Beckman spectrophotometer were carried out at the National Institute of Health (Japan). The kindness of Dr. H. Fukumi and Mr. H. Uchida who permitted us to use the instrument is gratefully acknowledged. Thanks are also due to Prof. S. Hosoya of the Institute for Infectious Diseases for his kindness in giving us many conveniences in preparing the cell-free enzyme preparation. A part of the cost of this investigation was defrayed from the Scientific Research Encouragement Grant from the Ministry of Education.

Chemical Institute, Faculty of Science,
Nagoya University

Études sur les Lactones dérivés des Acides Chrysanthémiques

par Masanao MATSUI, Takashi OHNO, Seiichi KITAMURA et Misao TOYAO

(Reçu Octobre 1, 1951)

Si l'on chauffe l'acide chrysanthémique jusqu'à 400° dans un tube à vide, la majeure partie des substances se transforme en lactones. Ainsi, on obtient le pyrocin qui fond à 83.5-84.5° de l'acide chrysanthémique naturel[1][2] et de la même façon on obtient le (±)-pyrocin qui fond à 61-62° des acides chrysanthémiques synthétiques.[2] Mais, la majeure partie des lactones reste à l'état d'huile. Si l'ouverture de l'anneau se produisait à quelques degrés par le chauffage, des lactones se produiraient comme exprimé par les formules suivantes.

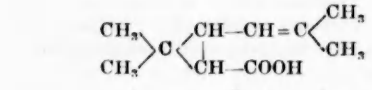

I.

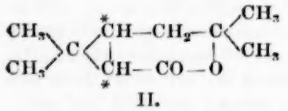

II.

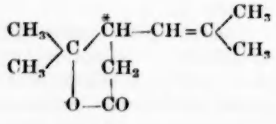

III.

* carbone asymétrique.

L'un de nous a suggéré que la formule constitutionelle du pyrocin pourrait être II d'après les produits d'oxydation et les réactions par son radical alcoolique du pyrocin.[2]

Il y a huit ans, le Dr. Makoto Nagase et l'un de nous[1] ont oxydé le pyrocin avec le permanganate de potassium et nous avons obtenu l'acétone et un corps qui fut considéré comme de l'acide *trans*-caronique par son point de fusion (212.5°) et par le résultat de la microanalyse.

Après cela, la constitution du pyrocin fut discutée sur la base de cette expérience. Cette même année, pourtant, nous avons su que le Dr. S. H. Harper[3][4] avait obtenu avec de l'acide (±)-*cis*-chrysanthémique en le traitant par l'acide sulfurique dilué un lactone qui fond à 52° et il proposait que ce corps est le lactone de l'acide 2-(2-hydroxyisobutyl)-3,3-diméthylcyclopropane - 1 - carboxylique (II). Pourtant, l'un de nous a aussi obtenu des acides (±)-*cis*-*trans*-chrysanthémiques synthétiques en chauffant dans un tube à vide, un lactone qui fond à 62° et il a conclu aussi à la même constitution que le Dr. Harper. L'abaissement du point de fusion du mélange de ces deux corps indique qu'ils sont des corps tout à fait différents.

Nous avons, alors, réexaminé des réactions

(1) Makoto Nagase et Masanao Matsui, *J. Agr. Chem. Soc. Japan*, **20**, 250 (1944).

(2) Masanao Matsui, *Botyu-Kagaku* (Japan) **15**, 1(1950).

(3) S. H. Harper, Pyrethrum Post, Janvier et Avril (1949), **1**, No. 3, 9-15, No. 5, 10-16.

(4) Nous tenons à remercier ici Monsieur le Docteur S. H. Harper des précieux specimens qu'il nous a prodigués.

de pyrocins et essayé, de nouveau, l'oxydation du pyrocin et du (±)-pyrocin purifiés avec soin. Les deux corps décolorisèrent la solution alcoolique ou acétonique de permanganate de potassium. Alors, nous avons ozonisé les deux lactones et nous avons obtenu de l'ozonide du pyrocin l'acide (+)-térébinique qui fond à 200° et qui fond à 202° mélangé avec l'acide (+)-térébinique fondant à 201-204° [207.5-210.5° (corrigé)] qui est obtenu par nous de l'acide (±)-térébinique par son sel de cinchonine. Mme. Arne Fredga[5] a obtenu de l'acide térébinique actif qui fond à 201-205°, $[\alpha]_D^{25°}$, ±13.2° par oxydation de l'acide isopropylsuccinique. Or le corps fondant à 212.5° (corrigé) qui est obtenu par le Dr. Nagase et l'un de nous par l'oxydation du pyrocin avec le permanganate de potassium et regardé comme de l'acide *trans*-caronique[1] était réellement l'acide (+)-térébinique.

Nous avons obtenu aussi de l'ozonide du (±)-pyrocin l'acide (±)-térébinique qui fond à 173 et à 174°, étant mélangé avec l'acide (±)-térébinique fondant à 175°.

Alors la formule consitutionelle du pyrocin doit être le lactone lévogyre de l'acide 3-isocrotyl-4-méthyl-4-hydroxyvalerianique.

Le (±)-pyrocin se transforme en un corps $C_{10}H_{18}O_3$ qui fond à 159° ajoutant une molécule d'eau par le traitement de l'acide sulfurique dilué. Il donne l'éther-sel de *p*-bromophénacyl. Pourtant, à cause du point de fusion bas on ne peut pas le purifier suffisamment. Ce corps probablement est VI, parce que γ-lactone ne donne pas ordinairement l'ether-sel de *p*-bromophénacyl; On ne peut pas obtenir l'éther-sel de *p*-bromophénacyl du pyrocin.

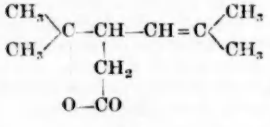

III.

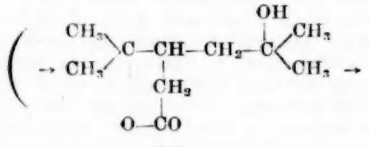

IV.

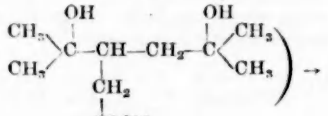

V.

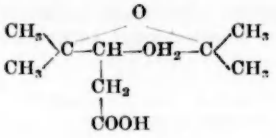

VI.

En outre, nous avons ozonisé aussi les liqueurs-mères du (±)-pyrocin. Pourtant nous n'avons pas obtenu des ozonides des corps cristallins sauf une petite quantité d'acide (±)-térébinique qui fond à 174°.

Alors, nous avons essayé de synthétiser du pyrocin et du (±)-pyrocin d'après la formule constitutionelle présomptive, en partant de l'acide (+)-térébinique et de l'acide (±)-térébinique respectivement, suivant les schèmes ci-dessous.

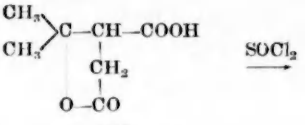

VII.

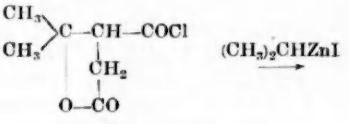

VIII.

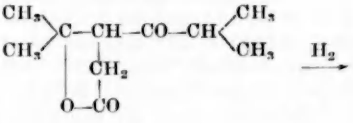

IX.

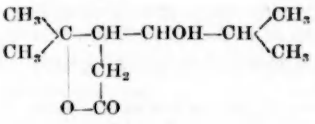

X.

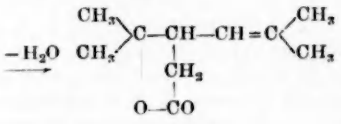

III.

La réaction de VIII à IX n'a pas été normale. Nous avons obtenu directement III par la réaction entre le chlorure de l'acide térébinique et l'iodure de zinc-isopropyl. Il

(5) Arne Fredga, Svensk Papperdtidn, **50**, No. 11, B 91-3 (1947), (*Chem. Abs.*, **42**, 123 (1948).

s'est manifesté par l'action réductrice de l'iodure de zinc-isopropyl suivi par la déhydration.

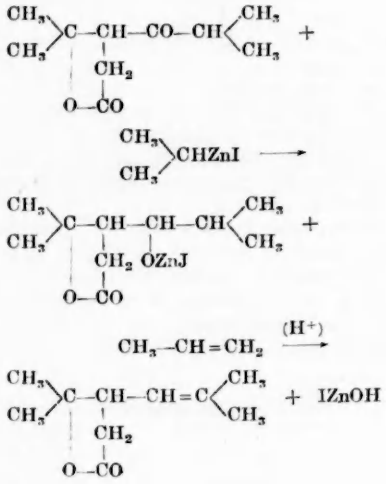

Les points de fusion des corps synthétiques sont 83-84° et 61-62° en partant de l'acide (+)-térébinique et l'acide (±)-térébinique respectivement et le point de fusion mélangé de ce corps-là avec le pyrocin fondant à 83.5-84.5° a été 83-84° et celui de ce corps-ci avec le (±)-pyrocin fondant à 61-62° a été 61-62°.

Le (±)-pyrocin totalement synthétique via l'acide (±)-térébinique aussi se transforme en corps qui fond à 159° ajoutant une molécule d'eau en chauffant dans l'acide sulfurique à 5% que le corps transformé de l'acide (±)-*cis-trans*-chrysanthémique par le chauffage.

Or, nous avons confirmé enfin que le pyrocin et le (±)-pyrocin sont respectivement la forme lévogyre et la forme racémique du lactone de l'acide 3-isocrotyl-4-méthyl-4-hydroxyvalérianique.

Pourtant par les études ci-dessus il est mis en évidence comme par miracle que le point de fusion de l'acide térébinique actif est présque celui de l'acide *trans*-caronique et le point de fusion de l'acide térébinique racémique est celui de l'acide *cis*-caronique. Alors dans des études de terpènes, il y a probablement des travaux qu'il faudra examiner de nouveau.

Partie Expérimentale

(Les points de fusion ne sont pas corrigés.)

1) Le pyrocin[1][2] et le (±)-pyrocin,[2] (III).—On a obtenu ces corps de la façon décrite dans le rapport précédent.[1][2] C'est-à-dire, on chauffe l'acide (+)-chrysanthémique naturel ou l'acide (±)-*cis-trans*-chrysanthémique dans un tube vide jusqu'à 400° pendant 30 minutes. Le contenant est pris dans l'éther et lavé plusieurs fois à la solution de carbonate de sodium à 10% et après avoir distillé le solvent dans le bain-marie, le sirop résiduel est saponifié par la potasse alcoolique. De l'eau est ajoutée et l'alcool est débarrassé de la solution. La solution restante est extraite à l'éther et on abandonne les corps neutres. On acidule la solution alcaline en ajoutant l'acide sulfurique dilué et on l'extrait à l'éther. On lave la solution d'éther à l'eau deux ou trois fois et on chasse l'éther de la solution. Le pyrocin ou le (±)-pyrocin se cristallisent dans la glacière. On les recristallise dans de l'éther de pétrole. F. du pyrocin: 83.5-84.5°, et F. du (±)-pyrocin: 61-62°. Rendement ca. 10% de la théorie.

$[\alpha]_D^{25°}$ du pyrocin = −57.7° (C: 0.6163 dans l'alcool).

2) Ozonisation du pyrocin actif.—Un courant d'air ozonisé passe pendant 50 minutes au travers de la solution de 120 mg. du pyrocin dans 50 cc. de chloroforme que l'on maintient à 0°. On chasse le chloroforme dans le vide et le résidu est bouilli avec de l'eau pendant une heure. On débarrasse une petite quantité de résine par passage sur une couche de norite. Après évaporation à sec dans le bain-marie, le résidu se cristallise. On recristallise les cristaux dans l'eau. Le point de fusion de ces cristaux (30 mg) est 200°.

$C_7H_{10}O_4$	calculé	C%	53.16	H%	6.33
	trouvé		52.93		6.77

Le point de fusion en mélange avec l'acide (+)-térébinique (F; 201-204°) est 200-201°, et le point de fusion en mélange avec l'acide (−)-térébinique (point de fusion 200°) est 175°. Il est sans aucun doute l'acide (+)-térébinique.

3) Résolution de l'acide térébinique.

a) L'acide (±)-térébinique, (VII).

Ce corps est obtenu par la méthode de Bruno Frost[6], mais la préparation est un peu modifiée: on ajoute 108 g. de méthylate de sodium dans 400 cc. d'éther anhydre et en réfroidissant à la glace on ajoute goutte à goutte un mélange de 120 g. d'acétone et 145 g. de succinate de méthyl. Après avoir laissé reposer deux jours, on y ajoute un mélange de 350 cc. d'acide hydrochlorique concentré et 350 cc. d'eau. Après évaporation de l'éther sur le bain-marie, on chauffe à reflux la solution pendant 12 heures. On ajoute 500 cc. d'eau chaude et on débarrasse la résine par passage sur une couche de norite et on laisse reposer une nuit. On sépare les cristaux et on lave deux fois à l'eau refroidie. Après recristallisation dans 200 cc. d'eau, on obtient 60 g. d'acide (±)-térébinique qui fond à 175°. On peut obtenir encore une petite quantitié de ce produit par évaporation des liqueurs-mères.

$C_7H_{10}O_4$	calculé	C%	53.16	H%	6.33
	trouvé		53.13		6.57

(6) Bruno Frost, *Ann.*, **226**, 363 (1884).

b) **Sel de cinchonine de l'acide (+)-térébinique.**

Six grammes et demi d'acide (±)-térébinique (F. 175°) dans 50 cc. d'alcool sont mêlés avec 12.5 g. de cinchonine dans 50 cc. d'alcool. On laisse reposer la solution résultante une nuit. Les cristaux séparés sont recristallisés dans 80 cc. d'alcool bouillant. Le produit (5 g.) fond à 222°. $C_{29}H_{32}O_3N_2$ calculé C% 68.35 H% 6.64 N% 6.68

trouvé 68.96 6.74 6.45

$[\alpha]_D^{25°} = +151°$ (c: 1.0 dans l'alcool à 12%).

c) **L'acide (+)-térébinique.**

Neuf grammes de cristaux de sel en haut sont dissous dans 160 cc. d'eau, on ajoute 10 cc. d'ammoniaque à 25%. Après refroidissement, la cinchonine qui est précipitée, est séparée et lavée à 100 cc. d'eau. La solution est évaporée à 25 cc. et acidulée en ajoutant 15 cc. d'acide hydrochlorique à 35%. Les cristaux se précipitent sous la forme de fragments carrés très jolis. Après recristallisation dans 30 cc. d'eau, l'acide (2 g.) fond à 201-204°.

$C_7H_{10}O_4$ calculé C% 53.16 H% 6.33

trouvé 52.84 6.00

$[\alpha]_D^{25°} = +9.0°$ (c: 4.0 dans l'alcool).

d) **L'acide (−)-térébinique.**

On laisse reposer 3 jours les liqueurs-mères du sel de cinchonine de l'acide (+)-térébinique et on débarrasse tous les cristaux séparés. Après l'évaporation d'alcool à sec, le résidu est repris dans 120 cc. d'eau et on ajoute 40 cc. d'ammoniaque à 25%. La cinchonine précipitée est débarrassée par filtration et la solution filtrée est évaporée à 40 cc. sur le bain-marie et on y ajoute 30 cc. d'acide chlorhydrique concentré. L'acide (−)-térébinique se sépare premièrement sous la forme de fragments carrés très jolis qui fondent à 198°. Après recristallisation dans 50 cc. d'eau, on obtient 1.5 g. du produit fondant à 200°.

$C_7H_{10}O_4$ calculé C% 53.16 H% 6.33

trouvé 52.60 6.54

$[\alpha_D]^{26.5°} = -7.95°$ (C; 3,333 dans l'alcool).

4) **Ozonisation du (±)-pyrocin.**—Un courant d'air ozonisé passe pendant deux heures à travers de la solution de 750 mg. du (±)-pyrocin dans 50 cc. de chloroforme que l'on maintient à 0°. Après évaporation à sec du chloroforme dans le vide à la température ordinaire, on décompose l'ozonide résiduel en chauffant avec de l'eau. Après avoir débarrassé une petite quantité de resine par passage sur une couche de norite, on évapore à sec la solution aqueuse. Il se sépare lentement des cristaux. Ils sont recristallisés dans de l'acide chlorhydrique dilué. On obtient ca. 300 mg. de produit fondant à 173° (pas encore tout-à-fait pur). En mélange avec l'acide (±)-térébinique fondant à 175° on trouve F. 174°.

$C_7H_{10}O_4$ calculé C% 53.16 H% 6.33

trouvé 52.93 6.47

5) **Traitement du (±)-pyrocin par l'acide sulfurique dilué.**—On chauffe à 100° dans un tube fermé 750 mg. du (±)-pyrocin et 50 cc. d'acide sulfurique à 5% pendant 12 heures et puis on laisse reposer une nuit dans une glacière. Les cristaux se séparent. Par recristallisation dans de l'eau on obtient 0.4 g. de cristaux fondant à 159°.

$C_{10}H_{16}O_3$ calculé C% 64.52 H% 9.69

trouvé 64.44 9.46

6) **Le (±)-pyrocin, (III).**—D'abord, on chauffe à reflux 45 g. d'acide (±)-térébinique, 200 cc. de benzène anhydre et 75 cc. de chlorure de thionyl pendant 20 heures sur le bain-marie. Après la distillation de benzène et excès de chlorure de thionyl on distille dans le vide. On obtient ainsi 45 g. de chlorure d'acide qui distille à 123° sous 10 mm.

On chauffe dans un ballon 55 g. d'iodure d'isopropyl, 30 cc. d'éther de pétrole et 65 g. de l'alliage éffacé de zinc et cuivre (10 : 1). Après que la réaction se produit on chauffe à reflux le mélange pendant deux heures. On ajoute 100 cc. de benzène anhydre. Les boues sont décantées et la solution versée dans un autre ballon muni d'une ampoule à brome contenant le chlorure d'acide (45 g.) susdit en solution dans 100 cc. de benzène anhydre. Le ballon est refroidi à 0° au moyen d'un mélange réfrigérant glace-sel et l'on introduit goutte à goutte le chlorure d'acide en agitant constamment. On laisse reposer une nuit, puis le produit de condensation est versé sur de la glace, extrait à l'ether, lavé à fond à l'acide sulfurique à 10%, au carbonate et enfin à l'eau.

On sépare ainsi 10 g. de parties neutres. Elles sont distillées dans le vide, on obtient 7 g. de produit distillant à 138-139° sous 35 mm. Il se cristallise dans une glacière. On sépare les cristaux et on recristallise dans de l'éther de pétrole. Ainsi on obtient 2 g. de cristaux qui fond à 61-62°. En mélange avec le (±)-pyrocin de 1) on observe F, 61-62°.

$C_{10}H_{16}O_2$ calculé C% 71.43 H% 9.52

trouvé 71.55 9.55

Il se cristallise lentement des liqueure-mères encore plus de cristaux.

7) **Traitement du (±)-pyrocin de[6] par l'acide sulfurique dilué.**—On chauffe dans un tube fermé 300 mg. du lactone derivé de l'acide (±)-térébinique et 23 cc. de l'acide sulfurique à 5% pendant 12 heures à 100°, et puis on laisse reposer dans une glacière une nuit. On sépare les cristaux et on recristallise dans de l'eau, F. 159°. En mélange avec le corps[5] dérivé de l'acide chrysanthémique, on observe F. 159°.

$C_{10}H_{16}O_3$ calculé C% 64.52 H% 9.68

trouvé 64.80 9.64

8) **Le pyrocin, (III).**—Comme pour la préparation du (±)-pyrocin, d'abord on prépare le chlorure de l'acide (+)-térébinique (6 g.) partant 6 g. d'acide, 40 cc. de benzène anhydre et 15 cc. de chlorure de thionyl par chauffage à reflux pendant

5 heures. Eb. 10 mm. 123°. Et puis on prépare la solution d'iodure de zinc isopropyl de la même façon que pour le cas[5] partant de 16 g. d'iodure d'isopropyl, 7 g. d'alliage éffacé de zinc et cuivre et 10 cc. d'éther de pétrole. Et, traitant de la même façon qu'au cas du (±)-pyrocin,[6] on obtient 0.8 g. du produit qui fond à 83-84° après recristallisation dans de l'éther de pétrole. Le point de fusion en mélange avec le lactone derivé de l'acide (+)-chrysanthémique naturel qui fond à 83.5-84.5° est 83-84°.

$C_{10}H_{16}O_2$ calulé C% 71.43 H% 9.52
trouvé 71.20 9.74
$(\alpha)_D^{25°} = -56.5°$ (C : 0.7512 dans l'alcool)
$-54.8°$ (C : 0.2993 dans l'alcool).

Résumé

A la pyrolyse des acides chrysanthémiques quelques lactones se produisent. Le pyrocin et le (±)-pyrocin sont les deux qu'on obtient sous la forme cristalline. Nous avons fait de nouvelles recherches et par des synthèses totales nous avons confirmé ces formules constitutionelles. Le pyrocin est le lactone lévogyre de l'acide 3-isocrotyl-4-méthyl-4-hydroxy-valérianique et le (±)-pyrocin est le corps racémique.

Nous tenons à remercier ici M. le Docteur Ryo Yamamoto et M. le Professeur Ryuzaburo Nodzu de précieux conseils qu'ils nous ont prodigués.

Laboratoire de la Compagnie Chimique de Nissin

On the Hydrazinolysis of Proteins and Peptides: A Method for the Characterization of Carboxyl-terminal Amino Acids in Proteins

By Shiro Akabori, Ko Ohno and Kozo Narita

(Received January 21, 1952)

The problem of determining the amino acid sequence in proteins has attracted the interest of many investigators because of its bearing on protein structures. Although several chemical methods[1-5] have been published heretofore for the characterization of carboxyl-terminal amino acids in peptides, most of them are not entirely suitable to be applied for proteins practically. C. Fromageot *et al.*[6] have reported the most eminent method, in which insulin was treated with lithium aluminium hydride and only carboxyl-terminal amino acids were reduced to amino alcohols. However, it seems to be worth-while to study some other methods, because the applicability of the methods cited is for practical reasons restricted.

The present authors have investigated the hydrazinolysis of peptides for the purpose of finding a simple method of the characterization of carboxyl-terminal amino acids in proteins. It is well known that acylamino compounds are easily decomposed by hydrazine to acylhydrazines and amines. But, so far as the present authors are aware of hydrazinolysis of protein has never been studied, except that A. Stoll *et al.*[7] have studied the degradation of ergot alkaloids which contain peptide linkages.

When proteins are treated with anhydrous hydrazine under certain conditions, only carboxyl-terminal amino acids are liberated as free amino acids and other amino acid residues are converted to amino acid hydrazides. On treating with benzaldehyde the latter residues condense with it to form water-insoluble dibenzal compounds while the former remain in solution and can be identified by paper chromatography as amino acids. The reactions are shown in the following scheme:

(1) P. Schlack and W. Kumpf, *Z. physiol. Chem.*, **154**, 125 (1926).
(2) F. Bettzieche, *Z. physiol. Chem.*, **161**, 178 (1926).
(3) E. Abderhalden and H. Brockmann, *Biochem. Z.*, **225**, 366 (1930).
(4) M. Bergmann and L. Zervas., *J. Biol. Chem.*, **113**, 331 (1936).
(5) N. Lichtenstein, *J. Am. Chem. Soc.*, **60**, 560 (1938).
(6) C. Fromageot, N. Jutisz D. Meyer and L. Penasse, *Biochim. Biophys. Acta*, **6**, 238 (1950); *Compt. rend.*, **230**, 1905 (1950).
(7) A. Stoll, T. petrzilka and B. Becker, *Helv. Chim. Acta.*, **33**, 57 (1950).

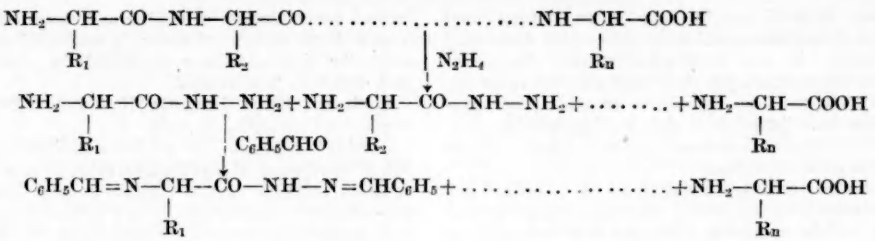

Amino acid hydrazides can also be detected on a paper chromatogram by their reducing power against ammoniacal silver nitrate solution as described in the experimental part.

Experimental

(I) Syntheses of Amino Acid Hydrazides and Their Dibenzal Compounds.—Amino acid hydrazides have not yet been synthesized except glycine-,[8] aspartic acid-[9] and tyrosine-hydrazides.[10] The authors synthesized, therefore, several new hydrazides as described below:

DL-Valine Hydrazide.—To DL-valine ethyl ester, which had been prepared as usual, a small excess of anhydrous hydrazine was added and heated in a water-bath for 10 minutes. On storing the reaction mixture *in vacuo* over sulfuric acid overnight, fine white needle valine hydrazide crystallized out. This was dissolved in hot chloroform and precipitated by addition of 3–4 volumes of ether. Thus, white crystalline DL-valine hydrazide, m. p. 96–7°C. (uncorrected), was obtained. This is very soluble in cold water (somewhat hygroscopic), ethanol and hot chloroform but insoluble in ether.

Analysis (Micro Dumas): N found, 31.06 %;* calcd. for $C_5H_{13}ON_3$, 32.05 %.

DL-Phenylalanine Hydrazide.—This was synthesized in the same manner as DL-valine hydrazide from DL-phenylalanine ethyl ester. After recrystallization from ethanol it melted at 123–4°C. (uncorrected).

Analysis: N found, 22.53%;* calcd. for $C_9H_{13}ON_3$, 23.45 %.

L-Leucine Hydrazide Dihydrochloride.—L-Leucine ethyl ester was treated with anhydrous hydrazine as usual and white plate crystals were obtained. But free hydrazide was so hygroscopic that conc. hydrochloric acid was added to it and heated for a few minutes. Leucine hydrazide dihydrochloride thus crystallized out, which, after evaporation of excess hydrochloric acid *in vacuo* over potassium hydroxide, was recrystallized from absolute ethanol, m.p. 275°C. (uncorrected), fine needles.

$$[\alpha]_D^{15} = +30.6°. \text{ (5\% in distil. water).}$$

Analysis: N found, 19.16%; calcd. for $C_6H_{17}ON_3Cl_2$ (as 2 HCl), 19.26%.

Other amino acid hydrazides synthesized in the same manner are cited in Table 1. Glycine-, alanine- and tryptophan-hydrazides were obtained not in crystalline but in syrupy forms, although these were sufficiently pure for paper chromatography. L-Tyrosine hydrazide[10] and L-glutamic acid-γ-hydrazide[11] were obtained in crystalline forms.

Amino acid hydrazides react with ninhydrin to give reddish purple color, with ammoniacal silver nitrate solution to give dark brown color, and reduce iodine and permaganate solutions. For the color reagent for paper chromatography, n-butanol solution saturated with ammoniacal silver nitrate aqueous solution is preferable. The chromatograms

Table 1

R_F Values of Several Amino Acid Hydrazides and Corresponding Amino Acids. Solvent for Paper Chromatography is Pyridine Base-aniline-water (9 : 1 : 4)

Amino acid hydrazides	R_F	Amino acids	R_F
Glycine hydrazide	0.26	Glycine	0.17
L-Alanine hydrazide	0.36	L-Alanine	0.24
DL-Valine hydrazide	0.56	DL-Valine	0.40
L-Leucine hydrazide	0.65	L-Leucine	0.51
DL-Phenylalanine hydrazide	0.71	DL-Phenylalnine	0.52
L-Tyrosine hydrazide	0.71	L-Tyrosine	0.55
L-Tryptophan hydrazide	0.70	L-Tryptophan	0.50
L-Glutamic acid-γ-hydrazide	0.15	L-Glutamic acid	0.11

(8) T. Curtius, *J. prakt. Chem.*, (2) **76**, 102 (1904).
(9) T. Curtius, *ibid.*, (2) **95**, 354 (1917).
(10) T. Curtius, *ibid.*, (2) **95**, 330 (1917).
* As there is a long time lag between the syntheses and analyses of these hydrazides, low values of found nitrogen must be due to their decomposition during their storage.
(11) S. Akabori and K. Narita, to be published shortly.

thus obtained can be stored after dipping them into thiosulfate solution, washing with water and drying. As the developing solvent for paper chromatography, pyridine base-aniline-water (9 : 1 : 4 : by volume) is found to be best. The "pyridine base" used is a high boiling fraction (b.p. 130–150°C.) of pyridines, *i. e.* a mixture of picolines and lutidines.

Amino acid hydrazides can be quantitatively estimated by oxidative titration using bromate or iodine standard solution. For example, we carried out the titration of leucine hydrazide dihydrochloride according to I. M. Kolthoff's analytical method for hydrazine.[12]

(1) Potassium bromate method.—Leucine hydrazide dihydrochloride (49 mg.) was dissolved in 2 ml. distilled water, added 2 ml. conc. hydrochloric acid and titrated with 0.100 N $KBrO_3$ using indigo as indicator. The sample required 2.22 ml. of the bromate. The calculated value for the next equation is 2.20 ml.: $RCH(NH_2)CONHNH_2 + 2/3KBrO_3 \rightarrow RCH(NH_2)COOH + N_2 + H_2O + 2/3KBr$

(2) Iodine method.—Leucine hydrazide dihydrochloride (18.8 mg.) was dissolved in 10 ml. distilled water containing 0.4 g. sodium bicarbonate and titrated with 0.1057 N iodine solution. The sample required 3.20 ml. of the iodine solution. The calculated value for the next equation is 3.25 ml.: $RCH(NH_2)CONHNH_2 + 2I_2 + H_2O \rightarrow RCH(NH_2)COOH + N_2 + 4HI$

In both cases the solution after titration was found to contain only free leucine by paper chromatography.

Dibenzal Compounds of Amino Acid Hydrazides.—Amino acid hydrazides condense with benzaldehyde in neutral aqueous solution to form white cold-water-insoluble dibenzal compounds, which develop no color by either ninhydrin or silver nitrate reagents. These benzal compounds, however, decompose to hydrazides and benzaldehyde in strong acidic solution. We synthesized dibenzal compounds of L-leucine- and L-alanine-hydrazides.

Dibenzal L-Leucine Hydrazide.—Crystalline L-leucine hydrazide dihydrochloride was dissolved in a small amount of water and an excess of benzaldehyde was added under cooling and stirring. As no precipitation occurred, the solution was neutralized with dil. NaOH until the precipitate separated out (*p*H 7.5). After standing over night in an ice box, the precipitate was collected on a filter and recrystallized from absolute ethanol. Thus white needle crystals, m.p. 149–50°C. (uncorrected), were obtained.

Analysis (Micro Dumas): N found, 13.20%; calcd. for $C_{20}H_{23}ON_3$, 13.10%.

Dibenzal Alanine Hydrazide.—Syrupy alanine hydrazide was dissolved in a small portion of water and an excess of benzaldehyde was added under cooling and stirring. On standing over night in an ice box, the white precipitate formed was collected on a filter and recrystallized from a large amount of water, whereby dibenzal L-alanine hydrazide was deposited in needles, m.p. 110–1°C. (uncorrected)

Analysis (Micro Dumas): N found, 15.06%; calcd. for $C_{17}H_{17}ON_3$, 15.05%.

Curtius[8] reported that he had obtained monobenzal compound of glycine hydrazide from acidic aqueous solution of the hydrazide, and that it was soluble in water, but for the present purpose it is preferable to precipitate hydrazides as dibenzal compounds. To accomplish this precipitation care must be taken not to shift the *p*H of the solution to acidic.

(II) Hydrazinolyses of Peptides.—As preliminary experiments we carried out the hydrazinolysis of several synthetic di- and tri-peptides. Peptides examined were as follows:

Dipeptides: glycyl-L-leucine, glycyl-L-tyrosine, glycyl-L-aspartic acid and L-leucyl-glycine.

Tripeptides: glycyl-glycyl-L-leucine and glutathione (SH form). All of these experiments gave successful results with ease. For example, two of them are described below.

Hydrazinolysis of Glycyl-L-Leucine.—Glycyl-L-leucine (73 mg.) was dissolved in 1 g. anhydrous hydrazine and heated under reflux at 125°C. (oil bath) for 1 hour. All glass apparatus was preferred in this treatment. After cooling the hydrazinolysate was poured into a watch glass and excess hydrazine was evaporated as perfectly as possible *in vacuo* over conc. sulfuric acid. The residue was dissolved in water and examined by paper chromatography. Using ammoniacal silver nitrate solution as color reagent, only glycine hydrazide developed the black spot, whereas on spraying ninhydrin solution two spots corresponding to glycine hydrazide and free leucine appeared. Therefore the carboxyl-terminal amino acid in this peptide was confirmed to be leucine.

Hydrazinolysis of Glutathione.—Glutathione (reduced form) (26 mg.) was dissolved in 1 g. anhydrous hydrazine and treated in the same manner. The paper chromatogram of the hydrazinolysate showed four spots indicating hydrazine, glutamic acid-γ-hydrazide, cysteine hydrazide and free glycine. The terminal amino acid, glycine, was confirmed further by treating as follows: The hydrazinolysate was dissolved in 1 cc. water and an excess of benzaldehyde was dropped into it under cooling and stirring, whereupon hydrazides condensed with benzaldehyde to form pale yellow amorphous precipitate (the yellow color is due to the formation of benzalazine from remaining hydrazine), and free glycine remained in the solution. After filtering the precipitate off, the colorless filtrate was examined by paper chromatography. Only one spot corresponding to glycine was found on the chromatogram, and no spot which reduced the silver nitrate solution was found. Fig. 1 shows the chromatograms of the hydrazinolysate and benzaldehyde-treated hydrazinolysate.

(III) Hydrazinolyses of Proteins.—In the case

(12) I. M. Kolthoff, *J. Am. Chem. Soc.*, **46**, 2009 (1924).

Fig. 1—a-Hydrazinolysate and b-benzaldehyde -treated hydrazinolysate of glutathione. Black spots, silver nitrate positive; white spots, ninhydrin positive. 1, cysteine hydrazide, 2, glutamic acid-γ-hydrazide; 3, glycine, and 4, hydrazine.

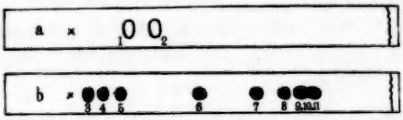

Fig. 2—a-Terminal amino acids of insulin: 1, glycine; 2, alanine. b-Hydrazinolysate of tyrocidin. Spots are hydrazides of ornithine (3), aspartic acid (4), glutamic acid (5), prolin (6), valine (7), leucine (8), tryptophan (9), tyrosine (10) and phenylalanine (11).

of lower peptides, the hydrazinolysis was completed in 1 hour, but in the case of proteins it was suspected that the time was not enough to hydrazinolyse proteins completely, and it was proved to be the case in a preliminary experiment. Hereby we hydrazinolysed glycyl-L-leucine for 10 hours and confirmed the fact that the other by-reaction such as hydrazidation of free amino acids did not occur in such a time. Therefore we decided to treat proteins with anhydrous hydrazine for 10 hours. This time of hydrazinolysis was enough to degrade proteins into amino acid hydrazides and free amino acids.

Hydrazinolysis of Insulin.—C. Fromageot *et al.*[6] reported by lithium aluminium hydride method that the carboxyl-terminal amino acids in beef insulin are glycine and alanine. On the other hand A. C. Chibnall and M. W. Rees[13] showed recently by means of the lithium boron hydride method that they are two alanines, one glycine and one as yet undetermined amino acid. We applied the hydrazinolysis to beef insulin, kindly supplied by Dr. J. Lens, N. V. Organon, Oss (the Netherlands), to compare its result with those of investigators mentioned above.

Crystalline insulin (55 mg.) was dissolved in 1 g. anhydrous hydrazine, heated to 125°C. for 10 hours, and after cooling, the excess hydrazine was evaporated *in vacuo* over sulfuric acid. The residue was taken up in water, an excess of benzaldehyde was added in small portions, and precipitates thus formed were filtered off. If hydrazides could not be completely precipitated, the *p*H of the solution was to be adjusted and made neutral by addition of dilute alkali. The mother liquor was concentrated *in vacuo* and free amino acids in it were identified by paper chromatography. Only glycine and alanine were detected on chromatogram (Fig. 2 a) showing good agreement with the result of Fromageot *et al.* Although we did not determine the result quantitatively, the intensity of the color and the area of the spots indicated that both amino acids existed in the protein in equal portions. From this result we reconfirmed the validity of this hydrazine treatment.

Hydrazinolysis of Tyrocidin.—Tyrocidin hydrochloride (200 mg.), which was kindly provided by Prof. Ohtani, Osaka Municipal University, was treated with 2 g. hydrazine for 9 hours. The hydrazinolysate gave, after evaporation of excess hydrazine, silver nitrate- and ninhydrin-positive 8 spots on paper chromatogram (Fig. 2 b), which corresponded to the hydrazides of amino acids composing tyrocidin. The chromatogram of the benzaldehyde-treated mother liquor gave no spots by spraying either ninhydrin or silver nitrate solutions. Therefore, tyrocidin was proved to be a cyclic peptide as reported heretofore.

Discussion

The present method has two excellent points: one of which is that anhydrous hydrazine is a good solvent for proteins. All proteins and peptides can be dissolved even at room temperature. The other point is that, being identified as amino acids themselves in respect to the terminal amino acids, there is no need to synthesize authentic amino acid derivatives and, if necessary, the quantitative estimations can be made by some suitable methods for microdetermination of amino acids published heretofore. Further, this method is very simple and can be carried out easily.

Besides the above mentioned experiments, the completion of the hydrazinolysis of proteins in 10 hours, on which we shall report elsewhere with details, was confirmed, in the following way: the benzaldehyde treated with mother liquor of protein hydrazinolysate was found to undergo no change in its amino acid either by further treatment with anhydrous hydrazine for 10 hours or by hydrolysis with 6 N HCl.

The applications of the hydrazinolysis to several crystalline proteins shall be reported in near future.

Summary

(1) A brief method for the characterization of carboxyl-terminal amino acids in peptides and proteins was investigated.

(2) Several new amino acid hydrazides were synthesized.

(3) Soveral di- and tri-peptides were hydrazinolyzed and identified their carboxyl-

(13) A. C. Chibnall and M. W. Rees, *Biochem. J.*, **48**, xlvii (1951).

terminal amino acid.

(4) The method was applied to beef insulin and tyrocidin for the demonstration of its applicability.

The authors wish to express their thanks to Dr. J. Lens, Organon, Oss (the Netherlands) for the supply of pure beef insulin, to Prof. Ohtani, Osaka Municipal University, for tyrocidin, and to Messrs. Fujii and Toki for the technical assistance offered in the syntheses of amino acid hydrazides. Hydrazine hydrate and sulfate were obtained through the courtesy of Mr. S. Yasuda of Mitsui Co. Ltd. and Messrs. Kumamoto and Harada of Ajinomoto Co. Inc.

Department of Chemistry, Faculty of Science, Osaka University

Fungus and Enzyme Preparation of Aspergillus Oryzae Amylase and its Use

By Taichi HARADA

(Received September 26, 1951)

Introduction

In 1934, the author[1] discussed the relation between various chemicals and fungi, and pointed out that thiourea exhibits a definite toxic value for fungi combined with neutral and harmless properties for human tissue. Application of this finding on the preparation or food and its value to fruits has aroused great interest which has appeared in recent literatures.[2], [3], [4]

The present paper of this series of investigations deals chiefly with a practical application of fungal amylase to the textile industry.

The fungal amylase taka-diastase[5] is a group of a great many enzymes among which protease, invertase and a few others are important ones. The mixture of such enzyme gives an undesirable result in one case but in an other case it gives a much better result than when used as a relatively pure amylase. The former case is seen in bread making[6] and the latter in desizing textiles in which the starch for sizing is not always pure.

Therefore, it is desirable to know how much of these enzymes are present in the amylase preparation before they are used in practice.

1) Hydrolysis of starch.—Saccharogenic hydrolysis of Lintner's starch by taka-diastase is found roughly to be a zero order of reaction since the value of n in the equation $\frac{dx}{dt} = K(a-x)^n$ is found to be -0.34.[7]

2) Estimation of Invertase.—To estimate this enzyme the author described the method[8] in which the amount of glucose is present and convenient for its calculation in accordance with the number of titer cc. which is not exactly reciprocally proportional to the true amount of produced sugar. This amount can now be calculated by the following equation with a fairly experimental agreement.

$$X = \left(0.5000 \div \frac{Y}{5}\right) + \frac{0.5000(Y-5)}{1000}$$

X = glucose % in the case of 0.1-0.5% titer solution, Y = titer cc.

3) Use in Banana Powder Making.—In bread making, from two to three percent of sucrose is usually added to the flour for baking bread leavened with yeast which contains a considerable amount of invertase compared with that in the amylase preparation. Therefore, when a relatively small amount of the preparation is added to the dough, the invertase itself might not affect the

(1) T. Harada, This Bulletin, **9**, 186 (1934).
(2) Denny, *Contrib. Boyce Thompson Inst.*, **7**, 55 (1935); *C. A.*, **29**, 6966 (1935).
(3) Childs and Siegler, *Science*, **102**, 68 (1945); *Ind. Eng. Chem.*, **38**, 82 (1946).
(4) Hartzell, *Contrib. Boyce Thompson Inst.*, **12**, 472 (1942); also refer Reineke and Turner, *Poultry Sc.*, **24**, 340 (1945); *C. A.*, **39**, 4968 (1945).
(5) The amylase preparation from pure culture on bran does not show the presence of alcohol oxidizing enzyme.
(6) T. Harada, This Bulletin, **24**, 105 (1951); *J. S. R. I.*, **44**, 189 (1950).
(7) This value was formally represented by the author as 2.34 and it was, therefore, thought that the reaction is to be a bimolecular one *Ind. Eng. Chem.*, **22**, 1424 (1931).
(8) T. Harada, *Ind. Eng. Chem., Anal. Ed.*, **3**, 1 (1931).

Table 1

Titer cc. and Glucose %

No.	Titer, cc.	Glucose % obtained	Glucose % calculated	Error
1	5.00	0.5000	0.5000	0
2	6.25	0.4000	0.4000	0
3	7.50	0.3380	0.3346	0.1
4	8.50	0.3000	0.2959	0.1
5	10.00	0.2550	0.2525	1.4
6	13.00	0.2000	0.1986	1.0
7	17.50	0.1500	0.1492	0.5
8	21.75	0.1250	0.1234	1.5
9	29.00	0.1000	0.0982	1.8

bread compared with the control. However, in the banana powder making industry, the preparation helps a great deal to give a more digestive and nutritious product since a considerable amount of sucrose and the amylase preparation are both used. The analytical result was made by the author for one of the samples prepared by North-John's company, U. S. A. It is given in Table 2.

Table 2

Analysis of the banana powder obtained by treating with amylase and the control

	Untreated, %	Treated, %
Reducing sugar as glucose	28.14	43.84
Sucrose	52.00	41.23
Starch	7.68	3.53
Total carbohydrate	90.96	90.96

4) Effect of Electrolyte upon the Liquefaction of Starch Paste by Amylase.—The action of fungal amylase upon a swollen starch or starch paste is presumed to take three steps; that is to say, the starch is first transferred into soluble starch, then to dextrine and finally to sugar. The ratio of liquefying power to saccharogenic power differs depending on the origin of amylase and the process of the preparation and the condition.

The viscosity of starch paste in enzyme treatment is greatly influenced by the addition of an electrolyte. Among the electrolytes, ammonium, sodium and potassium chlorides, ammonium sulphate, potassium bromide and iodide, have the greatest effect, and these are followed in order by ammonium sulphate, potassium chloride, potassium bromide and iodide respectively when they are used by percent in weight; that is $NaCl \fallingdotseq NH_4Cl > (NH_4)_2SO_4 > KCl > KBr > KI$.

The activating power of the enzyme as measured by the liquefaction of starch is quickly established with a trace of the electrolyte NaCl in the case of pancreatic amylase, the maximum being obtained with a concentration of approximately 0.0025-0.0100 percent in the buffered starch solution (200 cc. with 50 cc. of 0.2 M H_2KPO_4 and 17.80 cc. of 0.2 M NaOH) to *p*H 6.6, and then is slowly decreased as the concentration increases. This buffer istelf decreases the viscosity of starch paste solution about 8.56 percent. The experimental results are shown in Tables 4, 5, 6, 7 and 8.

It appears that a trace of NaCl is essential for the liquefaction of starch by pancreatic amylase; in other words, the enzyme can not be liquefied without NaCl. The small decreases (0.010) in the viscosity is due probable to an experimental error in this type of experiment. In this, it differs from malt and fungal amylases. The last named two enzymes are not essential for liquefying action but are greatly activated by the salt.

The decrease of viscosity of starch paste by electrolyte alone is cosiderable. The action of electrolyte on starch is not clearly known. There is a lack of information regarding the effect of electrolyte on the viscosity of solution or paste of starch. In this connection, Boutaric and Chapeaux's report[9] appeared recently in the chemical abstract; however, unfortunately neither the details nor the original paper of the above authors are available to the author at present in Japan.

As the result of experiment, it was found that the viscosity is not alone due to the degree of acidity of the solution, since the chloride of the alkaline earth metal $CaCl_2$ liquefies much more than that of $AlCl_3$. Among phosphates, the acid one gives a greater effect than that of the alkaline one. Moreover (addition of 5 cc. of 0.2 M) sodium hydroxide in many experiments gives only a little change on the liquefaction of starch paste on standing at room temperatures.

5) Viscosity of Native Starch Solution and Time of Heating at 50°C.—The viscosity of the solution of starch paste, relative to that of water is calculated by means of the formula:

$$\eta\,(\text{starch solution}) = \frac{(\text{time} \times \text{density})_{\text{starch}}}{(\text{time} \times \text{density})_{\text{water}}}$$

The viscosity of 0.5 percent native potato starch solution was little influenced (not more than 5 percent) by heating at 50°C. for more than one hour.

As experiment, five grams of native potato starch were introduced into a large beaker with a small amount of water (about 30 cc.) to which about

Table 3

Relation between the Viscosity of 0.5 percent Native Starch Solution and Time of Incubation at 50°C. (viscosity relative to that of water at 25°C.)

No.	1	2	3	4
Time in min.	0	5	10	15
η change	2.4375	2.5000	2.4375	2.5000

No.	5	6	7
Time in min.	20	25	30
η change	2.4375	2.4375	2.4375

(9) Boutaric and Chapeaux, *Compt. rend.* **214**, 949 (1942); *C. A.*, **39**, 236 (1945).

Table 4

Influence of NaCl on Starch Liquefying Action of Fungal Amylase (Viscosity relative to that of water at 25°C.) with 0.0050% Solution

No.	A		B	C	D	E	F
	NaCl %	*p*H	η controls water +NaCl +NaOH +enzy.	η controls starch soln. +NaCl +NaOH +enzy.	η starch soln. +NaCl +enzy. then add. NaOH	η reduced, due to NaCl (C_1–C_n)	η actively reduced by enzy. (C_1–D_n)
1	—	6.2	1.0002	2.3134	2.0004	—	0.3130
2	0.0050	6.2	1.0002	2.2509	1.6257	0.0625	0.6877
3	0.0100	6.2	1.0315	2.1884	1.4378	0.1250	0.8756
4	0.0200	6.2	1.0327	1.9383	1.3755	0.3751	0.9379
5	0.2000	6.2	1.0628	1.6884	1.1882	0.6250	1.1252
6	0.5000	6.2	1.0632	1.5012	1.1259	0.8122	1.1875

No.	G	H	I	J	K	L
	η reduced, due to enzy. (C–D)	η starch soln. (C–B)	η reduced, due to NaCl and enzy. combined (D_1–D_n)	η starch soln. alone by enzy. (D–B)	η reduced, due to enzy. activation by NaCl (H_1–H_n)	η corresp. soluble starch soln. (0.5%)
1	0.3130	1.3132	—	1.0002	—	1.0627
2	0.6252	1.2507	0.3747	0.6255	0.0625	1.0627
3	0.7506	1.1569	0.5626	0.4063	0.1563	1.0627
4	0.5628	0.9056	0.8754	0.3428	0.4076	1.0638
5	0.5002	0.6252	1.0627	0.1254	0.6880	1.0630
6	0.3753	0.4380	1.1250	0.0627	0.8752	1.0634

Table 5

Influence of NaCl on Starch Liquefying Action of four different Amylase Preparations (viscosity relative to that of water at 25°C.) with 0.0050% Solution

P. D. = pancreatic diastase, T. D. = taka-diastase, M. D. = malt diastase, B. D. = bacterial diastase (Minagawa's commercial, is mixed with salt ?).

No.		P. D.	T. D. No. 1	T. D. No. 2	M. D.	B. D.*
	NaCl %	η decreased, due to enzy.	η decreased, due to enzy. (L. V. 3000)	η decreased, due to enzy. (L. V. 2030)	η decreased, due to enzy. (L. V. 780)	η decreased, due to enzy. (L. V. 570)
1	—	0.010	0.313	0.188	0.063	0.813
2	0.0025	1.576	—	—	—	—
3	0.0050	1.675	0.625	0.625	0.438	0.813
4	0.0100	1.513	0.751	0.751	0.469	0.743
5	0.0200	—	0.563	0.563	0.375	0.532
6	0.1000	1.274	—	—	—	—
7	0.2000	—	0.500	0.500	0.250	0.313
8	0.2500	1.183	—	—	—	—
9	0.5000	0.978	0.375	0.375	0.156	0.219

* The author thanks Dr. T. Minagawa for his bacterial amylase which was kindly given for this experiment.

300 cc. of boiling distilled water was added with a moderate constant stirring by means of a glass rod. The solution was boiled by heating for about ten minutes or over, cooled, then transferred to a 500 cc. volumetric flask and then diluted to the mark with freshly boiled and cooled distilled water.

A series of glass-stoppered Erlenmeyer's flasks containing 50 cc. of the solution of starch were incubated in a 50°C. thermostat for about 30 minutes until the internal temperature reached the temperature of the thermostat.

Each of the seven solutions was treated further for zero, 5, 10, 15, 20, 25 and 30 minutes respectively, and exactly at the end of the time of incubation, the solutions were treated with 5 cc. of 0.2 N NaOH and of water and mixed.

The rate of flow and the density of the respective solutions were determined by means of an Ostwald's viscosimeter and a picnometer at 25°C. respectively.

6) Method of Measuring the Liquefaction of

Starch Paste by Amylase.—150 cc. of the 0.5 percent starch solution prepared as above in (5) was transferred by means of a pipette very carefully free from saliva into several 250 cc. glass-stoppered Erlenmeyer's flasks containing respectively 0.0038, 0.0075, 0.0150, 0.1500, 0.3750 and 0.7500 g. of sodium chloride so as to give the solutions of 0.0025, 0.0050, 0.0100, 0.2500 and 0.5000 percent as the examples.

Two series of 100 cc. capacity of Erlenmeyer's flasks with glass stoppers, each containing 50 cc. of starch solution as above described, were prepared by means of a thoroughly cleaned 50 cc. pipette. The series of flasks were placed in a 50°C. thermostat for about 30 minutes and then they were treated as follows: Five cc. of a clear enzyme solution (0.005 percent) was added by means of a 5 cc. pipette to each solution and allowed to stand for exactly 5 or 7 minutes according to the strength of the enzyme preparation. At the end of this time 5 cc. of 0.2 M NaOH solution was added to destroy the activity of the enzyme. However, for the controls the NaOH solution was first added and then the enzyme solution followed. The viscosity of the each solution was determined as described above.

In the experiment, the substrate starch solution for liquefying power test of amylase was not buffered except in the case of pancreatic enzyme, since it has little meaning in the textile desizing factory, or is rather a contamination. The results are given in the following tables which are the average values of at least three experiments.

7) **Desizing of Cotton.**—The wetting agent Nekal BX, as the example, gives great help for desizing of cotton cloth when it is added to the enzyme solution. However, when the cotton material is, previously, treated with boiling water, the agent gives little help for the purpose of desizing. In practiec in the factory, it is suggested that the sized material be first passed through a boiling NaCl or other salt solution and then through the enzyme solution containing NaCl or other salt at the temperature of 45-50°C. This is the conclusion of many desizing experiments.

The order of salts with respect to decreasing the viscosity of starch solution was $CaCl_2 > NaCl > AlCl_3 \fallingdotseq KH_2PO_4 \fallingdotseq KCl > Na_2HPO_4$.

8) **Making of "Ame".**—Fungal amylase preparation gave a slightly colored product, to "ame", a favorite kind of Japanese candy, when potato starch paste was treated with the amylase in the usual process; while malt amylase preparation gave a much better white product.

Summary

The liquefaction of starch by means of electrolytes and of amylase preparations of various origins has been studied by the viscosity method. It appears that the presence of NaCl is necessary for the liquefaction of starch paste by pancreatic one. Nevertheless, for other enzymes, NaCl is not essential for the liquefaction but the presence of NaCl accelerates greatly the enzymatic action.

The maximum activation appears at about 0.01 percent cocentration. The relation between various salts and viscosity of starch solution has been also studied.

The Scientific Research Institute, Komagome, Bunkyo, Tokyo

Table 6

Influence of NaCl on Starch Liquefying Action of Two different Amylase Preparations (viscosity relative to that of water at 25°C.) with 0.0100% Solution.

No.	NaCl %	T.D. No. 1 η decreased, due to enzy. G (C–D)		η decreased, due to enzy. M. D. G (C–D)	
1	—	0.3755	opaque	0.2505	opaque
2	0.0050	0.8131		0.5631	
3	0.0100	1.0632	trans-parent	0.6250	
4	0.0200	0.8755		0.5004	
5	0.2000	0.6254		0.3127	
6	0.5000	0.4378		0.2502	

Table 7

Influence of various Salts on Starch Liquefying Action of Taka-diastase Preparation (viscosity relative to that of water at 25°C.)

No.	Salt 0.0100%	η obs.	η reduced by enzy.	order of salts
1	NaCl	1.4065	0.9069	$NaCl \fallingdotseq NH_4Cl$
2	NH_4Cl	1.4065	0.9069	$(NH_4)_2SO_4 > KCl >$
3	$(NH_4)_2SO_4$	1.4375	0.8759	$KBr > KI$
4	KCl	1.4692	0.8442	
5	KBr	1.5945	0.7189	
6	KI	1.7201	0.5933	

Table 8

Relation between Salt and Viscosity of Starch Solution at 25°C.

No.	Salt 0.2000%	*p*H	η obs.	η reduced by salt
1	NaCl	6.2	1.5764	0.7882
2	$CaCl_2$	6.4	1.5461	0.8185
3	$AlCl_3$	4.8	1.6067	0.7579
4	KH_2PO_4	5.0	1.6067	0.7579
5	KCl	6.2	1.6067	0.7579
6	Na_2HPO_4	7.8	1.6370	0.7276

The Bitter Substance, Produced in Black-rotten Sweet Potato. II. On the Constitution of Ipomoeamarone. Part 1

By Takashi OHNO

(Received December 21, 1951)

In a previous report,[1] some properties of ipomoeamarone, the main constituent of the bitter subtance obtained from black-rotten sweet potato, have been reported. Now I report more findings about its functional groups and degradation products.

Crude ipomoeamarone was isolated as the fraction, b.p. 140–155°/7 mm., from neutral part of the ethereal extract of sweet potato which was inoculated with *Ceratostomella fimbriata*. The semicarbazone, $C_{16}H_{25}O_3N_3$, m.p. 131–2°, and oxim, $C_{15}H_{23}O_3N$, b.p. 153–6°/6mm., were obtained from this fraction. Pure ipomoeamarone was regenerated from the semicarbazone by hydrolysis with oxalic acid, and it accorded with formula $C_{15}H_{22}O_3$; b.p. 146–9°/5 mm., d_4^{20} 1.0290, n_D^{20} 1.4808, $[\alpha]_D^{20}$ +10.0°.

It is obvious by its attitude to potassium permanganate and bromine that ipomoeamarone is an unsaturated compound. By catalytic reductions, free ipomoeamarone absorbed 2 or 3 mols of hydrogen according to conditions, but the products could not lead to the crystalline derivatives. If the semicarbazone was hydrogenated, it gave tetrahydroipomoeamarone semicarbazone, $C_{16}H_{29}O_3N_3$, m.p. 95°, taking 2 mols of hydrogen. The hydrogenated compounds did not absorb bromine, but decolorised potassium permanganate after some minutes. Under some condition, the semicarbazone absorbed 3 mols of hydrogen, but the products did not crystallise, and hydrolysed ketone was tetrahydroipomoeamarone, $C_{15}H_{26}O_3$, b.p. 180° (bath)/5 mm. The ketone did not absorb bromine, but decolorised potassium permanganate after some minutes. The fact that dihydrocompound could not be obtained by stopping reduction when it absorbed one mol of hydrogen, shows two ethylenic linkages having same resistance to hydrogen.

With sodium and alcohol, ipomoeamarone formed an alcohol, ipomoeamarol, b.p. 162°/9 mm., which gave no ketonic reactions, and was derived to 3, 5-dinitrobenzoyl ester which, although liquid, gave the crystalline additional product with α-naphthylamine, m.p. 107–9°.

By catalytic reduction, ipomoeamarol absorbed 3 mols of hydrogen, but the product could not be made into crystalline derivatives. This fact leads to the conclusion that two ethylenic linkages cannot be in the $\alpha\beta$-position to the carbonyl group, nor conjugated with each other.

Of three oxygen atoms, one was confirmed to be ketone. The other two were probably oxide types, since all the reactions about hydroxyl groups, including Zerewitinoff-Fraschenträger method, were negative. In spite of the presence of three oxygen atoms, ipomoeamarone is liquid and it is difficult to obtain crystalline compounds from its derivatives; these facts, also, prove the absence of hydroxyl group in the molecule.

Although I cannot yet give evidences of whether two oxydic oxygens are aliphatic ether, cyclic ether, peroxide, or methylene-dioxide, it is rational to suppose that ipomoeamarone is a derivative of sesquiterpene and is an open-chain diolefinic ketone containg two oxide rings.

By oxidation of ipomoeamarone with potassium permanganate at room temperature, oxalic acid and a liquid keto-acid (supposed to be $C_{12}H_{20}O_4$) were obtained. For the latter, we propose the name ceratonic acid after the genus name of the fungus, *Ceratostomella fimbriata*.

This acid will be discussed in my next report.

By oxidation of ipomoeamarone semicarbazone at 100°, acetone, acetic acid, oxalic acid and a liquid acid were obtained. Production of acetone shows the presence of an isopropyl group in the molecule, and this suggests that it is a terpenic substance.

When a drop of ipomoeamarone or ipomoeamarol was added to a solution of vanillin in concentrated hydrochloric acid, pink color was produced and it turned gradually to dark red, then violet. Ipomoeamarone gave, also, color reactions by acetic anhydride and sulfuric acid (turning from blue-violet to brown), and glacial acetic acid and sulfuric acid (turning from dark red to brown). It is interesting that all of these color reactions are common through many terpenic compounds which contain oxide groups.

(1) T. Ohno and T. Takeuchi, *Botyu-Kagaku (Scientific Insect Control)* **12**, 26-9 (1949).

F. H. McDowall has been isolated ngaione[2] (pronounced "ny-one") which resembles to ipomoeamarone, from the essential oil of the leaves and terminal branchlets of *Myoporum laetum* of New Zealand. He has reported; ngaione, $C_{15}H_{22}O_3$, the main fraction of the essential oil, was a lemon-yellow oil with faint odour, b.p. 182–3°/27 mm., d_{20}^{20} 1.0276, $[\alpha]_D$ -26.20°, n_D^{20} 1.4804, the semicarbazone, m.p. 120–2° (decomp.), *p*-nitrophenylhydrazone, m.p. 103°, and was an open-chain compound with two non-conjugated double bonds, one ketonic group, and two separated oxide rings. Although his work has been interrupted and the results of his research have taken no definite form, many resemblances of the properties of both subtances and their derivatives suggest that these are mutually optical isomers, or, at least, analogous substances.

Recently, H. Watanabe and H. Iwata[3] reported nearly the same recognitions about ipomoeamarone.

Experimental

Ipomoeamarone.—Sweet potato (518 kg.) was treated as reported in a previous paper, and 125 kg. of dry black-rotten sweet potato was extracted with ether by a large scale Soxhlet extraction apparatus in batches of about 20 kg. About 6 kg. of extract was obtained. Its neutral part, obtained by treatment with aqueous alkali, was a reddish-brown, extremely bitter oil. The oil was fractionated.

B.p.	up to 141°/7 mm.	799 g.
	141–147°/7 mm.	686 g.
	147–160°/7 mm.	237 g.
	over 160°/7 mm.	93 g.
Total		1,815 g.

Residue *ca.* 1 kg.

Repeated distillation of these fractions gave the following fractions:

Lower fraction	b.p.	up to 140°/7 mm.	
Fraction 1.	b.p.	140–145°/7 mm.	467 g.
Fraction 2.	b.p.	145–150°/7 mm.	517 g.
Fraction 3.	b.p.	150–155°/7 mm.	262 g.
Higher fraction	b.p.	over 155°/7 mm.	

The physical constants and the analytical values of these main fractions were as follows:

Fraction 1,	d_4^{15} 1.0353,	n_D^{15} 1.4869,	$[\alpha]_D^{17}$ 13.3° (*c*, 17.5 in benzene)
Fraction 2,	1.0351,	1.4859,	15.2° (*c*, 18.4 in benzene)
Fraction 3,	1.0346,	1.4880,	13.5° (*c*. 19.2 in benzene)

Anal-Found: Fraction 1, C, 71.24; H, 7.17%. Fraction 2, C, 73.23; H, 8.30%. Fraction 3, C, 71.09; H, 9.04%. Calcurated for $C_{15}H_{22}O_3$: C, 72.00; H, 8.80%.

Ipomoeamarone Semicarbazone.—A mixture of 100 g. of crude bitter oil (above-mentioned fractions), 46 g. of semicarbazide hydrochloride, 40 cc. of pyridin, 200 cc. of alcohol and 100 cc. of water was allowed to stand at room temperature. After a few days the crystals of the semicarbazone were deposited. It was filtered, once dissolved in alcohol for the isolation of disemicarbazide, concentrated and recrystallised with dilute ethyl alcohol repeatedly. M.p. 131–2°, $[\alpha]_D^{19}$+85.0° (*c*, 2.0 in benene). The pyridine method gave better yield in shorter time than sodium acetate method.

Hydrolysis of the Semicarbazone.—A mixture of 6 g. of the semicarbazone and 6 g. of oxalic acid in 100 cc. of water was distilled with steam. From the distillate, pure ipomoeamarone was isolated with ether. B.p. 145–9°/5 mm., $[\alpha]_D^{27}$+10.0° (*c*. 2.5 in benzene), d_4^{20} 1.0290, n_D^{20} 1.4808, $[R]_D$ 69.0 (calc. for $C_{15}H_{22}O_3$, F_2: 69.43). (*Anal.* Found: C, 71.89; H, 9.02%. Calc. for $C_{15}H_{22}O_3$: C, 72.00; H, 8.80%.)

It gave the same semicarbazone again, but the yield was low; probably it was accompanied by a certain amount of racemisation.

Ipomoeamarone Oxim.—A mixture of 50 g. of the crude bitter oil (fraction 1), 14 g. of hydroxylamine hydrochloride, 11.5 g. of sodium carbonate, 40 cc. of water and 100 cc. of alcohol was refluxed on the water bath. After fifteen hours, alcohol was distilled off, ether was added, and this was followed by washing with dilute acid and alkali, and an ethereal layer was dried and concentrated. The residue was fractionated.

b.p.	118–133°/6 mm.	30 g.
b.p.	153–156°/6 mm.	11 g.

The first fraction, non-oximable oil was a pale yellow, mobile liquid, giving negative color reaction with sodium nitroprusside; d_4^{15} 1.0087, $[\alpha]_D^{15}$ +12.8° (*c*, 12.5 in benzene), n_D^{15} 1.4850. (Found: C, 75.44; H, 9.21)

The second fraction, ipomoeamarone oxim, was a pale yellow, very viscous liquid; d_4^{15} 1.0633, $[\alpha]_D^{15}$ +23.3° (*c*, 6.0 in benzene), n_D^{15} 1.5032. $[R]_D$ 73.7 (calc. for $C_{15}H_{23}O_3N$, F_2: 73.91). (*Anal.* Found: C, 67, 39; H, 8.38; N, 5.24%. Calc. for $C_{15}H_{23}O_3N$: C, 67.90; H, 8.68; N, 5.28%.)

Hydrogenation of the Crude Bitter Oil.—One gram of crude bitter oil in presence of 0.5 g. of Pd-$BaSO_4$ and 10 cc. of alcohol absorbed 225 cc. (2.5 mols) of hydrogen during nine hours. The resulting oil was a pale yellow oil of sweet odour

(2) F. H. McDowall, *J. Chem. Soc.*, **1925**, 220; **1927**, 731; **1928**, 1324.

(3) H. Watanabe and H. Iwata, Lecture at the meeting of Agricultural Chemical Society of Japan, 3rd Nov. 1951.

and decolorised $KMnO_4$ only after a few minutes. But it did not give any crystalline derivatives.

Hydrogenation of Ipomoeamarone Semicarbazone.—1) The semicarbazone (3.07 g.) in 55 cc. of ethyl acetate was treated with a stream of hydrogen and 2.00 g. of Pd-$BaSO_4$. During nine hours, 492 cc. (2.2 mols) of hydrogen were absorbed. The reduced product crystallised by treatment with dilute alcohol.

Tetrahydroipomoeamarone semicarbazone, m.p. 95–6°, was soluble in common organic solvents except petroleum ether, did not absorb bromine and decolorised $KMnO_4$ only slowly. (*Anal.* Found: C, 61.70; H, 9.25; N, 13.58%. Calc. for $C_{16}H_{29}O_3N_3$: C, 61.73; H, 9.33; N, 13.51%.)

The oil, obtained by treatment of the hydrogenated semicarbazone with dilute mineral acid or aqueous oxalic acid, gave color reaction with sodium nitroprusside.

Other experiments of hydrogenation derived to the same tetrahydroipomoeamarone semicarbazone as follows;

a) Semicarbazone 0.45 g., acetone 16 cc., Pd-$BaSO_4$ 0.45 g. Absorbed H_2 60 cc. (1.8 mols), during 2 hrs.

b) Semicarbazone 0.92 g., alcohol 15 cc., Pd-$BaSO_4$ 1.0 g. Absorbed H_2 186 cc. (2.8 mols), during 12 hrs.

c) Semicarbazone 0.92 g., alcohol 20 cc., PtO_2 0.05 g. Absorbed H_2 183 cc. (2.7 mols), during 6.5 hrs.

2) One gram of the semicarbazone in presence of 0.50 g. of Pd-$BaSO_4$ and 25 cc. of ethyl alcohol absorbed 232 cc. (3.12 mols) of hydrogen during thirteen hours. The product was a very viscous oil which did not crystallised for a long period. This was treated with aqueous oxalic acid. The resulting pale yellow oil (720 mg.), which gave color reaction with sodium nitroprusside, was distilled twice under 5 mm. (bath temp. 180°), yielding 410 mg. It did not absorb bromine, decolorised $KMnO_4$ after a few minutes, kept colorless for long time, and was shown to be tetrahydroipomoeamarone by analysis. (*Anal.* Found: C, 71.13, 70.82; H, 10.13, 10.39%. Calc. for $C_{15}H_{24}O_3$: C, 71.43; H, 9.52%. Calc. for $C_{15}H_{24}O_3$: C, 70.87; H, 10.24%. Calc. for $C_{15}H_{28}O_3$: C, 70.31; H, 10.94%)

Half-Hydrogenation of Ipomoeamarone Semicarbazone.—Five grams of the semicarbazone in 50 cc. of ether was shaken with 2.5 g. of Pd-$BaSO_4$ in the stream of hydrogen. Reaction was interrupted at the absorption of one molecule of hydrogen. Repeated crystallisation of the resulting product yielded ipomoeamarone semicarbazone (m.p. 128°, and there was no depression of melting point with the specimens which melt at 131°). After the decolorisation of total half-hydrogenated products with active carbon, reduction was continued and tetrahydroipomoeamarone semicarbazone was obtained after the absorption of another molecule of hydrogen.

Reduction of Ipomoeamarone with Sodium and Alcohol; Ipomoeamarol.—Five grams of crude ipomoeamarone was reduced with 5 g. of sodium and 100 cc. of alcohol. The product, which boiled at 162°/9 mm. (3.33 g.), was a pale yellow oil, having a bitter taste, hardly ever colorised with sodium nitroprusside, and decolorised $KMnO_4$ at once.

A 0.3 g. portion of the substance in 10 cc of benzene was refluxed with 0.5 g. of 3, 5-dinitrobenzoyl chloride and a few drops of pyridine on the water bath for half an hour. 3, 5-Dinitrobenzoyl ester (0.44 g.), thus obtained, was a very viscous oil and did not crystallise.

To 0.4 g. of the liquid ester, a solution of 0.2 g. of α-naphthylamine in 80% alcohol was added. Addition products of α-naphthylamine were separated, m.p. 107–9°, dark-red crystals, but could not be purified because of their unstability.

Ipomoeamarol (0.85 g.) in alcohol was hydrogenated with 0.50 g. of Pd-$BaSO_4$. About 3 mols (228 cc.) of hydrogen was absorbed during ten hours. The pale yellow oil obtained, did not produce any crystalline derivatives.

Analysis of the Active Hydrogen by Zerewitinoff-Fraschenträger Method.—By the analysis, ipomoeamarone, regenerated from the semicarbazone, showed absence of active hydrogen.

111.6 mg. of substance; 0.02 cc. of CH_4 (15°, 759 mm.). Calcurated for one active hydrogen; 10.00 cc.

Oxidation of Ipomoeamarone with Potassium Permanganate at Room Temperature.—A 1.8 g. portion of ipomoeamarone, which was regenerated from the semicarbazone, was suspended in 50 cc. of water. Small portions of powdered $KMnO_4$ were added to the mixture successively under shaking and occassional cooling with water. Four and a quarter grams (8.55 atoms of oxygen) of $KMnO_4$ were required. Manganese dioxide was removed by filtration and washed with hot water. There were no neutral substances in the oxidised solution. Then, after this solution was concentrated, it was acidified with dilute sulfuric acid, and was distilled with steam. The distillate required only a small amount of aqueous alkali by titration. The non-volatile part was, then, extracted with ether. The extract (1.06 g.) was a brown viscous oil, and gave ketonic reaction with sodium nitroprusside. By distillation under 4.5 mm. (bath temp. 145–190°), 0.45 g. of the oil was obtained, which gave neither semicarbazone, nor 2, 4-dinitrophenylhydrazone, showed negative iodoform reaction, and was with difficulty soluble in cold water. Three months later, the crystals grew in the oil. After five months, large crystals were picked up and washed with ether. This was proved to be oxalic acid (m.p. 98°) by mixed melting point determination and analysis. (*Anal.* Found: C, 20.17; 19.95; H, 5.21, 5.12%. Calc. for $C_2H_2O_4 \cdot 2H_2O$: C, 19.05; H, 4.76%.)

The liquid acid, separated from oxalic acid, was redistilled under 5 mm. (167–180° bath temp.). It gave ketonic reaction with sodium nitroprusside. For this liquid keto-acid, I suggest the name ceratonic acid. This will be discussed in my next report.

Oxidation of Ipomoeamarone Semicarbazone with Potassium Permanganate at 100°.—Five grams of the semicarbazone was suspended in 100 cc. of boiling water. Small portions of powdered $KMnO_4$ were added successively. During the operation, vapor from the top of the reflux condenser was lead to the solution of 2, 4-dinitrophenylhydrazine (mixture of 0.5 g. of 2, 4-dinitrophenylhydrazine, 2.0 cc. of H_2SO_4, and 20 cc. of alcohol). About 43 g. (25 atoms of oxygen) of $KMnO_4$ were required. From the solution of 2, 4-dinitrophenylhydrazine orange-yellow crystals were isolated. This, after several recrystallisations from alcohol, was proved to be acetone 2, 4-dinitrophenylhydrazone (m.p. 127°) through mixed melting point determination and analysis. (*Anal.* Found: C, 45.76, 45.70; H, 4.08, 4.39; N, 23.57, 23.75%. Calc. for $C_9H_{10}O_4N_4$: C, 45.38; H, 4.20; N, 23.53%.)

From the oxidised solution, no other neutral product was isolated except a small amount of the recovered semicarbazone (m.p. 129°). As to volatile acid, acetic acid was caught as the *p*-bromophenacyl ester (m.p. 82°) and proved by mixed melting point determination and analysis. (*Anal.* Found: C, 46.73, 46.41; H, 3.68, 3.41%. Calc. for $C_{10}H_9O_3Br$: C, 46.69; H, 3.50%.) As to non-volatile acid, crystalline and liquid acids were obtained by ether extraction. The former was proved to be oxalic acid through mixed melting point determination and analysis. (*Anal.* Found: C, 19.59, 19.47; H, 4.87, 5.39%. Calc. for $C_2H_2O_4 \cdot 2H_2O$: C, 19.05; H, 4.76%.) The latter was distilled under 6 mm. (bath temp. 170–200°). The pale yellow oil gave negative reaction with sodium nitroprusside.

Summary

Ipomoeamarone is an open-chain ketone with two oxide rings and two ethylenic linkages. It gives a liquid keto-acid and oxalic acid by oxidation with potassium permanganate at room temperature, and acetone, acetic acid, oxalic acid and a liquid acid by oxidation with the same reagent at 100°.

I wish to express my sincere gratitude to Dr. M. Ohno for his guidance and to Dr. M. Matsui for his helpful advice given to me during the research. I also express my hearty thanks to Mr. T. Takeuchi, Miss M. Toyao and other members of Osaka Factory of Nisshin Chemical Co. for their helpfulness and friendship which facilitated my work.

Takei Laboratory, Institute for Chemical Research, Kyoto University, and Osaka Factory of Nisshin Chemical Co.

LETTER

X-Ray Investigation of Trimethylacetic Acid Crystal

By Yoshiyuki NAMBA and Tsutom ODA

(Received April 30, 1952)

Timmermans[1] elucidated that trimethylacetic acid (pivalic acid) crystal possesses a very small entropy of fusion, 2.6 e. u./mole, and is an example of the organic plastic crystals so called by him. Hence, we have now carried out an X-ray investigation of this crystal in order to amplify our knowledge on the structures of such plastic crystals as cubic pentaerythritol,[2] tetranitromethane,[3] cyclohexane,[4] cyclohexanol[5] and hexachloroethane.[6]

The present material was prepared by the method of Puntambeker and Zoellner[7] and the product was subjected to fractional recrystallization and distillation, m. p. 33—34°. Samples of this compound were sealed in thin-walled glass capillary tubes and the single crystals were grown from the liquid by slow cooling of the tubes previously warmed to 40°. Rotation and oscillation photographs were obtained with these crystals using Cu

(1) J. Timmermans, *J. chim. phys.*, **35**, 331 (1938).
(2) I. Nitta and T. Watanabé, This Bulletin, **13**, 28 (1938).
(3) T. Oda, T. Iida and I. Nitta, *J. Chem. Soc. Japan*, **64**, 616 (1943); T. Oda and T. Watanabé, *ibid.*, **65**, 154 (1944); T. Oda and I. Nitta, *ibid.*, **65**, 621 (1944); T. Oda and T. Matsubara, *X-Rays*, **6**, 27 (1950).
(4) T Oda, *ibid.*, **5**, 26 (1948).
(5) T. Oda, *ibid.*, **4**, No. 4, 2 (1945); *ibid.*, **5**, 95 (1949).
(6) M. Atoji, T. Oda and T. Watanabe, The 2nd Congress of the International Union of Crystallography (1951).
(7) S. V. Puntambeker and E. A. Zoellner, "Organic Syntheses", Coll. Vol. I, A. H. Blatt, Ed., John Wiley and Sons, Inc., New York, N. Y., 1947, p. 524.

radiations. From the results it was found that the crystal conforms to a face-centered cubic lattice, containing four molecules of $(CH_3)_3CCO_2H$ in the unit cell with the edge $a=8.82$ A. The calculated density is 0.98, which is reasonable in comparison with values extraporated from the known[8] densities of the liquid. The space group is T^2–$F23$, T^3_h–$Fm3$, T^2_d–$F\bar{4}3m$, O^5–$F43$ or most probably O^5_h–$Fm3m$. From the symmetry consideration it is shown that the molecules arranged at 0, 0, 0; 0, 1/2, 1/2; 1/2, 0, 1/2; 1/2, 1/2, 0 take either orientational or rotational disorder.

Such structure is seen to be in harmony with the extraordinarily rapid decrease of the intensities for increasing angle of scattering. On the other side, on several Laue photographs there appeared intense diffuse spots such as accompanied by {111} and {200}. These results are quite in resemblance to certain cases[3],[4],[5] of the above examples and those of *t*-butyl chloride, *t*-butyl bromide and neohexane recently published by Schwartz, Post and Fankuchen.[9]

It may be added that we have confirmed optically that the isotropic[8] crystals transform at about −2° to small birefringent needles. The transition may be due to cessation of the molecular rotation.

This investigation is aided by the Scientific Research Encouragement Grant from the Ministry of Education to which the authors' thanks are due. We are also indebted to the interest and helpful suggestions of Professors Isamu Nitta and Tokunosuké Watanabé of Osaka University.

Chemical Laboratory Osaka Liberal Arts University, Osaka

(8) A. Butlerow, *Ann.*, **173**, 355 (1874).

(9) R. S. Schwartz, B. Post and I. Fankuchen, *J. Am. Chem. Soc.*, **73**, 4490 (1951); *ibid.*, **73**, 5113 (1951). See also *ibid.*, **69**, 2502 (1947).

New Colorimetric Determination of Chloride using Mercuric Thiocyanate and Ferric Ion[1]

By Iwaji IWASAKI, Satori UTSUMI and Takejiro OZAWA

(Received April 22, 1952)

A new colorimetric method for the determination of low concentrations of chloride using slightly dissociating mercuric thiocyanate and ferric ion is mainly based on the following reactions:

$$2Cl^- + Hg(CNS)_2 \rightleftharpoons HgCl_2 + 2CNS^-$$
$$4Cl^- + Hg(CNS)_2 \rightleftharpoons HgCl_4^{--} + 2CNS^-$$
$$CNS^- + Fe^{+++} \rightleftharpoons Fe(CNS)^{++}$$

The orange color of ferric thiocyanate formed in the solution is determined colorimetrically.

Reagents:

A series of standard potassium chloride solutions containing 0.2, 0.5 ppm., 1 to 10 ppm. with differences of 1 ppm. and 10 to 20 ppm. with differences of 2 ppm., of chloride is prepared.

Mercuric thiocyanate solution is prepared by dissolving 0.3 g. of mercuric thiocyanate in 100 cc. of 95% ethyl alcohol.

Ferric alum solution is prepared by dissolving 6 g. of ferric ammonium sulfate in 100 cc. of 6 N nitric acid.

Procedure:

Ten cc. of the sample solution and 10 cc. of standard chloride solution are poured into the matched test tubes with stopper. Then 1.0 cc. of mercuric thiocyanate solution and 2.0 cc. of ferric alum solution are added to each solution. Comparisons are carried out after ten minutes from mixing. It is better to observe the colors from above against a white background.

Interfering substances are: bromide, iodide, cyanide, thiosulfate, and nitrite.

Results:

The lowest concentration of the standard solution whose color can be easily distinguished from that of the blank test, is 0.05 ppm. Cl^-. Therefore this is the minimum determinable concentration. However this colorimetric method is applied with best results in the concentration range of 0.1-20 ppm. of chloride. The colored solution has an absorption maximum at 460 mμ and its orange color is stable for several hours. The colored substance is not extracted with organic solvents such as ether or amyl alcohol.[2]

Table 1

Present. Cl^-	0.3	0.5	1.0	5.0	10.0	15.0 ppm.
Found. Cl^-	0.3	0.5	1.1	5.0	10.0	15.5 ppm.

There are excellent agreements.

This rapid and simple colorimetric method for the determination of low concentrations of chloride can be widely applied to the detrmination of chloride in water, rocks etc.

Laboratory of Analytical Chemistry and Geochemistry, Tokyo Institute of Technology, Tokyo

(1) This report was presented at the 5th annual Meeting of the Chem. Soc. Japan, April, 1952.

(2) Reported by I. Iwasaki and H. Shimojima at the 5th annual Meeting of the Chem. Soc. Japan, April, 1952.